MARIA S. MERIAN-Berichte

Coastal Upwelling System in a Changing Ocean - Trophic Transfer Efficiency of the Humboldt Current Upwelling System off Peru

Cruise No. MSM80

20.12.2018 – 31.01.2019,
Bahia Las Minas (Panama) – Valparaiso (Chile)
CUSCO-1

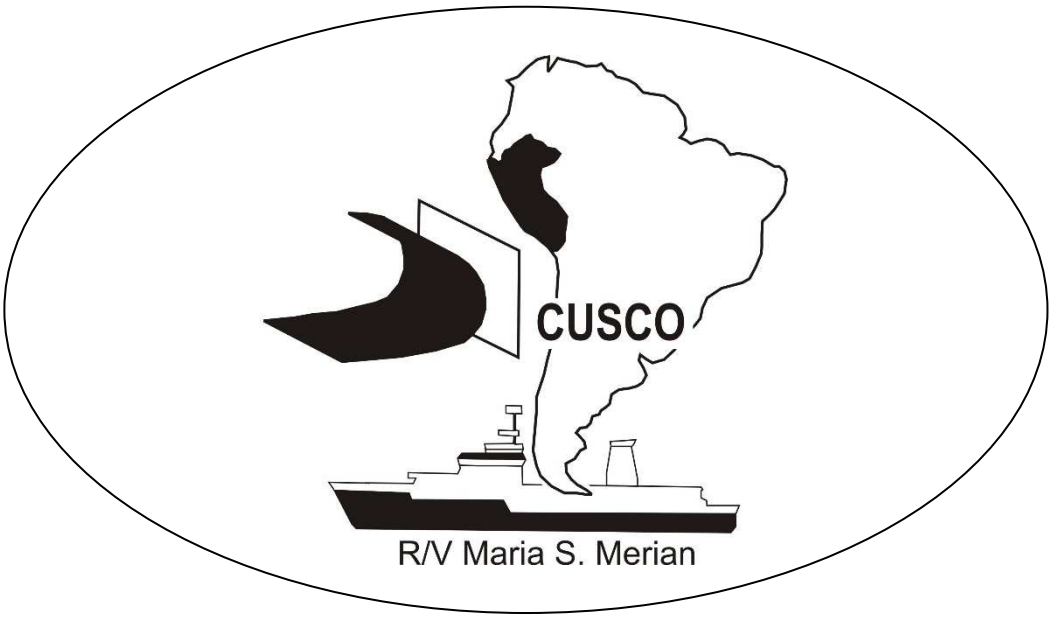

HOLGER AUEL
with contributions from the cruise participants

PD Dr. Holger Auel
Universität Bremen (FB02)
BreMarE - Bremen Marine Ecology

2019

Table of Contents

1 Cruise Summary

1.1 Summary in English

The MSM80 research cruise with R/V Maria S. Merian to the Humboldt Current upwelling system off Peru was the essential field campaign of the BMBF-funded project CUSCO - Coastal Upwelling System in a Changing Ocean in cooperation with IMARPE Peru. We focused on carbon and energy fluxes in the marine foodweb to solve the enigma of why the Humboldt upwelling system provides eight-to ten-times higher fisheries yield than other upwelling systems at similar primary production rates. In total, 106 stations were sampled, covering the continental shelf (200 m) and continental rise (1000 m) along the Peruvian coastline with different upwelling intensity. Process studies were conducted from the coast line offshore, following aging upwelling plumes and filaments. CTD casts, zooplankton nets, and optical profilers were deployed to establish abundance, biomass, and biodiversity of the pelagic community. Dietary spectra and trophic levels of key species were studied with trophic biomarkers. Respiration measurements were conducted on board to establish energy budgets and trophic transfer efficiencies of dominant predator-prey interactions.

1.2 Zusammenfassung

Die Forschungsreise MSM80 mit FS Maria S. Merian in das Küstenauftriebsgebiet des Humboldtstroms vor Peru diente dem vom BMBF geförderten Verbundvorhaben CUSCO - Coastal Upwelling System in a Changing Ocean in enger Kooperation mit IMARPE Peru. Das wissenschaftliche Interesse galt der Quantifizierung der Kohlenstoff- und Energieflüsse im marinen Nahrungsnetz, um das Rätsel zu lösen, warum das Humboldt-System acht- bis zehnfach höhere Fischereierträge liefert als andere Auftriebsgebiete trotz ähnlicher Primärproduktionsraten. Insgesamt wurden 106 Stationen beprobt auf dem Schelf (200 m) und am Kontinentalhang (1000 m) entlang der peruanischen Küste bei unterschiedlichen Auftriebsintensitäten. Prozessstudien konzentrierten sich auf die Sukzession in einer Auftriebsfahne von der Küste nach draußen. CTD-Profile, Zooplanktonnetze und optische Profiler erfassten Abundanz, Biomasse und Biodiversität der pelagischen Gemeinschaft. Nahrungsspektren und Trophiestufen von Schlüsselarten wurden mittels trophischer Biomarker untersucht. Respirationsmessungen an Bord erfassten Energiebudgets und trophische Transfereffizienzen wichtiger Räuber-Beute-Beziehungen.

2 Participants

2.1 Principal Investigators

Name	Institution
Auel, Holger, PD Dr.	Universität Bremen, BreMarE
Mohrholz, Volker, Dr.	IOW Warnemünde
Koppelmann, Rolf, Dr.	Universität Hamburg, IMF
Riebesell, Ulf, Prof. Dr.	GEOMAR Kiel

2.2 Scientific Party

Name	Discipline	Institution
Auel, Holger, PD Dr.	Plankton Ecology / Chief Scientist	Uni HB
Hagen, Wilhelm, Prof. Dr.	Zooplankton Ecophysiology	Uni HB
Schukat, Anna, Dr.	Zooplankton Ecology	Uni HB
Massing, Jana	Zooplankton Ecology	Uni HB
Auch, Dominik	Gelatinous Zooplankton	Uni HH
Janssen, Silke	MOCNESS & IKMT Deployment	Uni HH
Kurbjuweit, Stefanie	Ichthyology	Uni HH
Martin, Bettina, Dr.	MOCNESS & IKMT Deployment	Uni HH
Welker, Annelie	Ichthyology	Uni HH
Heene, Toralf	Physical Oceanography	IOW
Beier, Sebastian	Physical Oceanography	IOW
Mohrholz, Volker, Dr.	Physical Oceanography	IOW
Fernández Méndez, Maria del Mar, Dr.	Phytoplankton	GEOMAR
Kiko, Reiner, Dr.	Underwater Vision Profiler	GEOMAR
Kittu, Leila	Nitrogen Fixation	GEOMAR
Meyerhöfer, Michael, Dr.	Biogeochemistry	GEOMAR
Ortiz, Joaquin	Phytoplankton	GEOMAR
Paul, Allanah Joy, Dr.	Nitrogen Fixation	GEOMAR
Qelaj, Kastriot	Biogeochemistry	GEOMAR
Pinedo Arteaga, Elda Luz	Zooplankton Ecology	IMARPE
Correa Acosta, Jonathan Angello	Ichthyoplankton Ecology	IMARPE

2.3 Participating Institutions

Uni HB	Universität Bremen (FB02), BreMarE - Bremen Marine Ecology
Uni HH	Universität Hamburg, IMF - Institut für marine Ökosystem- und Fischereiwissenschaften
IOW	Leibniz-Institut für Ostseeforschung Warnemünde
GEOMAR	Helmholtz-Zentrum für Ozeanforschung Kiel
IMARPE	Instituto del Mar del Perú

2.4 Crew

Name	Rank
Maaß, Björn	Kapitän / Master
Peters, Ralf	Ltd. Offizier / Chief Officer
Schilling, Sandra	1. Offizier / 1st Officer
Angelis, Wilhelm	2. Offizier / 2nd Officer
Rogers, Benjamin	Ltd. Ingenieur / Chief Engineer

Boy, Manfred	2. Ingenieur / 2nd Engineer
Zerbin, Sebastian	3. Ingenieur / 3rd Engineer
Reize, Emmo	System Operator
Herrmann, Jens	Elektroniker / Electronics
Beyer, Thomas	Elektriker / Electrician
Wiechert, Olaf	Deckschlosser / Fitter
Bosselmann, Norbert	Bootsmann / Bosun
Wolff, Andreas	Schiffsmechaniker / SM
Werner, Andre	Schiffsmechaniker / SM
Peschkes, Peter	Schiffsmechaniker / SM
Plink, Sebastian	Schiffsmechaniker / SM
Altmann, Detlef	Schiffsmechaniker / SM
Peschel, Jens	Schiffsmechaniker / SM
Nebe, Tom	Schiffsmechaniker / SM
Sauer, Jürgen	Motormann / Oiler
Matter, Sebastian	1. Koch / 1st Cook
Streifling, Stefan	2. Koch / 2nd Cook
Seidel, Iris	Stewardess
Wolters, Gabriele, Dr.	Bordärztin / Ship's Doctor

3 Research Program

3.1 Aims of the Cruise

In the framework of the BMBF-funded joint research project CUSCO - "Coastal Upwelling System in a Changing Ocean", during the cruise MSM80, productivity and trophic interactions were studied in the Humboldt Current Upwelling System off Peru in order to elucidate the reasons for the extremely high fisheries yield compared to other coastal upwelling regions and to answer the question how the system will respond to global climate change.

Eastern Boundary Upwelling Systems (EBUS) are among the most productive marine ecosystems, providing 7% of total marine primary production and 20% of global marine fish landings, but accounting for <2% of the ocean area. Although the four major EBUS have similar upwelling intensities and similar primary productivity per unit area, the Humboldt Upwelling System (HUS) provides eight to ten times higher fisheries yields per unit area than the other systems. To elucidate the reasons for this extremely high productivity at upper trophic levels and how the mechanisms will respond to global climate change is the overarching objective of the BMBF-funded joint research project CUSCO - "Coastal Upwelling System in a Changing Ocean - Trophic Transfer Efficiency of the Humboldt Current Upwelling System off Peru". The CUSCO research cruise MSM80 was its first fieldwork campaign. Biological and physical oceanographers cooperated with marine ecologists, biogeochemists, and fisheries scientists in order to trace carbon and energy fluxes through the marine food web and to study how different upwelling intensities affect overall trophic transfer efficiency (TTE).

Major aim of the cruise was to establish which processes and mechanisms determine TTE and, hence, affect food-web structure, community composition and trophic pathways, and to study

potential regional differences within the Peruvian upwelling system related to differences in upwelling intensity and water mass distribution. Major trophic pathways were quantified by covering the following topics:
(i) Phytoplankton composition and primary production under different upwelling regimes.
(ii) Length of the food chain between primary producers and harvested species via trophic biomarkers (stable isotopes, fatty acids).
(iii) Role of filter feeders (e.g. krill). Since filter feeders efficiently consume a wide range of prey sizes, they form less complex food webs with a higher overall TTE.
(iv) Gelatinous zooplankton, since they are often "dead ends" of the food chain and predators and competitors for small pelagic fish.
(v) Abundance, distribution and prey spectra of pelagic and mesopelagic fishes.
(vi) Effects of physical-biological boundaries (meso-scale eddies, upwelling filaments, margins of the oxygen minimum zone) on zooplankton dynamics.

3.2 Agenda of the Cruise

The cruise MSM80 started on 20th December 2018 in Bahia Las Minas, Panama, and ended on 31st January 2019 in Valparaiso, Chile. A total of 106 stations was sampled along the Peruvian coastline, concentrated along six sections perpendicular to the coast (Fig. 3.3.1).

3.3 Description of the Work Area

Scientific investigations were performed on the Peruvian shelf between 8°30’S and 16°30’S. The hydrographic stations were mainly organized in six cross-shelf transects, with 9 to 13 stations each (Fig. 3.3.1).
The first and second transects covered the wide and shallow shelf area off northern Peru. The central shelf was sampled with the third transect off Callao. The transects four, five and six were carried out on the narrow southern shelf between 14.5°S and 16°S, the main working area during the cruise. Between those transects, a number of stations were sampled near the shelf edge to gather additional information on water mass distribution. An overview of the location of CTD stations, ScanFish transects, Drifter paths, and the cruise track is given in Figure 3.3.1.

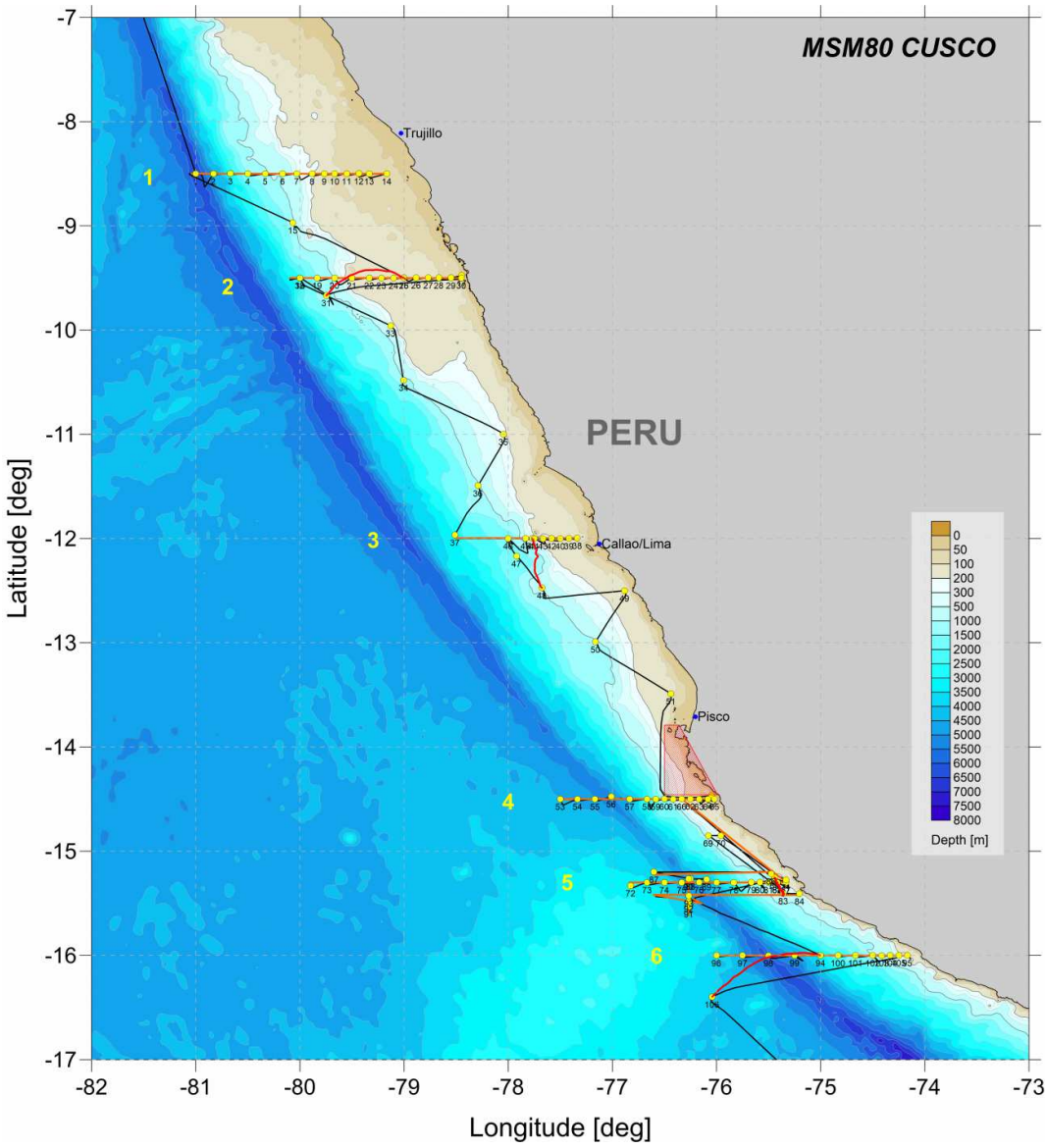

Fig. 3.3.1 Station map and cruise track of MSM80 from 20th Dec. 2018 to 31th Jan. 2019. Yellow dots and black labels indicate the positions and names of CTD/MSS stations. The orange lines depict the ScanFish transects. The red lines indicate the deployments and pathways of the drifting surface mooring. The thin black line is the ship track (provided by IOW team).

4 Narrative of the Cruise

On 20th December 2018, an interdisciplinary and international research team including 19 scientists with four different nationalities from three German universities and two marine research institutions boarded R/V Maria S. Merian in Bahia Las Minas, Panama, for the start of the MSM80 expedition. Two days later, two scientists from the Peruvian fisheries research institute IMARPE joined the cruise.

During the first few days on board, we unpacked our expedition equipment from the freight containers, assembled measuring devices and plankton nets, and established ourselves in the labs. We benefited from the fact that the ship was still moored in port on the first day and after that anchored on roads off the Caribbean coast of Panama with very calm conditions.

In the late afternoon of 23.12.2018 we entered the locks on the Caribbean side of the Panama Canal. The passage through the canal took eight hours, until we finally reached the Pacific Ocean at midnight. On the evening of Christmas Day we crossed the equator.

On 27.12.2018 at 2 p.m. we reached our study area in the coastal upwelling system of the Humboldt Current off Peru and started with station work at 8°30‘S 081°00’W. Standard stations always began with CTD/rosette casts for physical measurements of water temperature, salinity, oxygen concentration, light intensity and turbulence in relation to water depth. We also collected water samples from different depths in order to study inorganic nutrients, suspended matter, particulate organic carbon, nitrogen and phosphorus (POC, PON, POP), biogenic silica (BSi) as well as phytoplankton abundance and composition (using flow cytometry, microscopy, HPLC pigment analysis). Water samples were incubated on board for determination of primary production and nitrogen fixation.

After that, we deployed different kinds of nets to catch zooplankton. This included a stratified vertical haul with a HydroBios Multinet Midi in order to catch mesozooplankton, two successive double-oblique tows with another HydroBios Multinet Midi in order to catch fish larvae and gelatinous zooplankton and the deployment of an Isaacs Kidd Midwater Trawl (IKMT, 10 m2 mouth opening) for larger macrozooplankton and micronekton. At the deepest offshore stations, a 1 m2 Double-MOCNESS was deployed with 18 separate nets to provide high vertical resolution. Specimens of zooplankton key species were used for respiration measurements on board to establish their individual energy demands (Winkler titration, optode respirometry). For the quantitative determination of dietary spectra, specimens were sorted from the catches and deep-frozen at -80°C for trophic biomarker analysis (fatty acids and stable isotopes). Predator-prey relationships and food-web structure of the pelagic ecosystem were studied by stable isotope ratios of nitrogen and carbon (δ15N, δ13C). This approach provides information on the dietary source and trophic levels in order to trace energy flows through the pelagic food web and to establish trophic transfer efficiencies for major predator-prey interactions.

During the following days, we sampled a total of 14 stations, along a section at 8°30’S towards the Peruvian coast. In between standard stations, the physical oceanographers often added short stations with microstructure profiles only in order to increase the spatial resolution of the hydrographic measurements. The final station on this transect was completed at 65 m water depth in sighting distance to the coast. Thereafter, we deployed the ScanFish, a towed undulating CTD, and returned along the entire section at 8°30‘S back to the first station and completed our first transect after about 2.5 days in the study area.

A second section perpendicular to the Peruvian coast was sampled at 9°30’S. This time, we first deployed the ScanFish and steamed along the transect in order to assess the water mass distribution and upwelling activity. Thereafter, we sampled a total of 13 stations along the transect with CTD/rosette, optical profilers, microstructure profiler and different plankton nets. In spite of the relatively short distance between the first section at 8°30’S and the second at 9°30’S, the high temporal and spatial variability was responsible for strong differences in water mass structure. Surprisingly, phytoplankton concentration was rather low close to the coast, where stronger phytoplankton growth was to be expected during periods of active upwelling. On this section, we also deployed a surface drifter for the first time during this cruise. This device is drifting with the surface currents, independent from the vessel, and provides hydrographic data on changes in the upper 50 m of the water column in high temporal resolution. After three days,

the drifter was recovered successfully on 03.01.2019. Thereafter, we headed south and steamed to a series of stations alternating between 200 m water depth on the shelf and 1.000 m bottom depth above the continental rise in order to identify large-scale differences in the upwelling pattern along the Peruvian coastline.

In the evening of 05.01.2019 we reached 12°S, where we sampled along a third transect perpendicular to the coast, since this is also one of the regular monitoring lines of our Peruvian partners from the national fisheries research institute IMARPE. At 07:20 p.m. we deployed the ScanFish again and towed it for 12 hours along the transect from a position at 2.800 m bottom depth to close to the coast in front of the Peruvian capital Lima and its port Callao. Station work along the 12°S section also included a full-day 24 h-station at 12°S 78°W in order to study diel vertical migrations (DVM) by zooplankton (mainly krill) and mesopelagic fish.

On 07 January, immediately before the 24 hours-station, five out of seven of our regular sampling gears showed malfunctions, all at the same station. Thanks to the efforts of the technicians on board, in particular, the members of the scientific-technical service (WTD), all technical problems could be solved within a few hours and gears were repaired in time for the 24 h-station. The 24 h-station Stn. 46 was located over the continental rise at 1.600 m water depth. Four times during the day, we deployed the CTD and a multiple opening/closing net, both at daylight and during darkness. In addition, we developed a special sampling scheme for the hours of sunset and sunrise. Exactly half an hour before sunset, the krill species Euphausia mucronata began to migrate from its daytime distribution at 300 m depth to the sea surface, where it spent the night. The interdisciplinary co-operation of biologists, biogeochemists and physical oceanographers on board allowed us to gather a comprehensive data set to study DVM of krill in the Humboldt Current and its effects on the carbon flux to the deep sea.

Between 11.01. and 14.01.2019 we sampled along the fourth section at 14°30’S with a similar sampling strategy. During the fifth week of the expedition, we focussed on small- to meso-scale processes and differences in water mass distribution and upwelling intensity. For that purpose, we deployed the ScanFish along three sections, which were separated by only a few miles in geographic latitude at 15°12’S, 15°18’S and 15°25’S and extended from the coast far into the open ocean. The spatial analysis of the data revealed certain areas with colder, less saline or warmer, saltier water, respectively. There were also differences in biological parameters. Almost 70 miles off the coast, we found a spot with a typical coastal zooplankton community, dominated by small copepod species. At another location, also far away from the coast, we encountered an intense algal bloom of dinoflagellates and small diatoms, which one would usually expect closer to shore in a coastal upwelling region, but not 65 miles offshore above 5.000 m water depth. The section at 15°18'S also included another 24 h-station over the continental rise, Stn. 80 on 17. to 18.01.2019.

On 21st January 2019, we completed the sampling campaign for small- to mesoscale processes and gradients in water mass distribution and upwelling intensity. During the remaining days in the study area from 22. till 26.01.2019, sampling concentrated on the southernmost section at 16°S. Routine sampling included steaming to a position about one third of the total section length away from the coast to deploy the drifter as the first procedure in order to allow the drifter the maximum time in the water and the longest measurement period. Thereafter, we moved to the easternmost station, closest to the coast, and deployed the ScanFish. With the ScanFish in tow, we steamed about 120 nm westwards along the entire section from the station

closest to the coast to the one most distant from the coastline. Along that track, water depth increased from 120 m to more than 5.000 m. On our way back to the coast, we took water samples in regular intervals, conducted hydrographic measurements and sampled zooplankton with different nets. The entire scientific programme for this section required about three days. At the end, we still had to recover the drifter.

During its four deployments, the drifter always headed in a different direction. At the last deployment, it moved westwards relatively fast with almost one nautical mile per hour. Therefore, we had to steam again for ca. 100 nm at the end of the cruise to pick up the drifter. We completed the final station work of the expedition MSM80 at the drifter's position on 26.01.2019 at 02:00 a.m.

On 30th January 2019, we reached Valparaiso in Chile, from where most of the cruise participants flew back to Germany. The research cruise MSM80 was very successful. We sampled 106 stations, far more than originally planned.

5 Preliminary Results

5.1 Hydrography and Water Mass Distribution

Objectives

The cruise MSM80 CUSCO aims to investigate the relation between physical and trophic transfer efficiency in the Peruvian Upwelling System. The cruise is the main field expedition of the collaborative project CUSCO "Coastal Upwelling System in a Changing Ocean". The work package 1 analyses the impact of variability of physical forcing on upwelling dynamics and water mass distribution on the Peruvian shelf. Using field and remote sensing data the following questions will be attributed:

1. How do spatial pattern and temporal variability of wind forcing control the dynamics and intensity of upwelling on the Peruvian shelf?
2. How do the spatial pattern of curl driven and coastal upwelling correlate with the pattern of primary production?
3. What is the impact of subsurface distribution of central water on the upwelling related nutrient transports into the mixed layer?
4. What is the impact of climate change related shifts in wind field on the upwelling intensity and water mass distribution in the Humboldt Current upwelling system?

The main objective of the hydrography group of the Baltic Sea Research Institute during the FS Merian MSM80 cruise was gathering field data for the investigation of horizontal and vertical distributions of hydrographic and optical water properties along the Peruvian shelf in relation to atmospheric forcing. This covers

- the identification, characterization and classification of water masses by hydrographic as well as inherent and apparent optical water properties,
- observations of current patterns on the Peruvian shelf,
- the investigation of turbulent mixing in the upper water column for the estimation of vertical turbulent matter fluxes at the base of the surface mixed layer,

- the observation of mesoscale and sub mesoscale patterns with high resolution measurements performed with an undulating CTD (ScanFish) and a drifting surface mooring.

Work at Sea

Data acquisition for the hydrographic investigations was carried out using the following devices and measuring platforms.

At stations and transects:

- CTD SBE 911+ with rosette water sampler
- Lowered ADCP
- Optical profiler AC-S
- Microstructure profiler MSS
- ScanFish undulating CTD
- Oceanographic drifter (drifting surface mooring)

Continuous measurements:

- Vessel mounted ADCP 75kHz Ocean Surveyor
- Vessel mounted ADCP 38kHz Ocean Surveyor
- Trios spectrometer system

The CTD-system "SBE 911plus", SN-09P66504-1072, (SEABIRD-ELECTRONICS, USA) was used to measure the variables:

- Pressure
- Temperature (2x SBE 3)
- Conductivity (2x SBE 4)
- Oxygen concentration (2x SBE 43)
- Chlorophyll-a fluorescence (683nm)
- Turbidity
- PAR
- SPAR

To minimize salinity spiking, temperature- (SBE 3), conductivity (SBE 4) and oxygen sensors (SBE 43) are arranged within a tube system, where seawater is pumped through with constant velocity. The CTD was equipped with a redundant sensor system sensor system for temperature, conductivity and oxygen. The temperature is given in ITS-90 temperature scale. Salinity is calculated from the Practical Salinity Scale (1978) equations. Fluorescence and turbidity are measured with a downward looking WET Labs fluorimeter. Pressure is determined with a Paroscientific Digiquartz pressure sensor.

Data were monitored during the casts and stored on hard disk with SeaSave Version 7. For each station a configuration file was written which contains the complete parameter set, especially sensor coefficients used for the conversion of raw data (frequencies) to standard output format.

Additionally, the CTD-probe was equipped with a Rosette water sampler with 21 Free Flow bottles of 10l volume each. This design allows for closing of bottles automatically at predefined

depths during down-casts. Closing depth and sensor values are aligned by appropriate choice of parameters of the CTD software generating the "bottle files". The CTD was attached to a single conductor winch 2.

Sampling

A CTD cast was started below the sea surface with the pressure sensor usually at about 3 to 5m depth to prevent a contamination of the CTD pumping system with air bubbles. Data were collected down to 1000m or 3m above the bottom at shallow stations. An attached altimeter was used to determine the bottom distance. Sampling rate of the CTD probe was 24Hz. Data were displayed online to determine appropriate sampling depth and stored on a PC hard drive.
The probe sheds water in its wake over a long distance. Hence, only downcast registration was reliable. Upcast registration was used only for water sampling, if the closing depth was determined during the downcast. At downcast bottles were closed while fiering in an auto-fire mode. For sampling during upcast, the CTD was stopped and bottles closed manually after a 30 second adjustment period. When the device was back on deck oxygen samples were taken first, followed by water samples for nutrients and water for several biological and geochemical techniques.

Sensor check

The CTD sensors were checked during the cruise by comparison measurements. Temperature and conductivity sensors of sensor package 1 and were compared to each other to discover sensor failures. In well mixed layers the observed differences amount to 0.002K and 0.004mS/cm between the particular temperature and conductivity sensors. These deviations are in the usual range of uncertainty of the measuring method. The stability of the digiquarz of the CTD has been checked by an external frequency source. During the entire cruise no drift was observed. Thus, no correction of the recorded temperature and conductivity data will be applied during the post processing.

Slope and offset of the oxygen sensors SBE 43 will be determined by help of water samples taken at each station. Oxygen content of the samples was determined with a titration set (Winkler method, accuracy of 0.02ml/l). Oxygen concentration is calculated using Seasoft, oxygen formula "1",

$$ox = Soc * (V + V_{offset}) * (1 + A*T + B*T^2 + C*T^3) * OXSAT * \exp(E*P/k)$$

The pressure sensor was checked by measuring pressure on deck before and after the casts. After applying the actual air pressure, the deviation from normal surface pressure was about +0.90dbar. This offset will be applied during post processing of the CTD data.

Calibration measurements for the fluorescence sensor have not been done so far. However, after the quantitative phytoplankton data will be available, a post calibration will be performed for the chlorophyll-a fluorescence.

During the cruise an LADCP-2 system was used to obtain full depth velocity profiles of currents at each CTD-station, where the water depth exceeds 200m. Two ADCP WH-300s were mounted in the frame of the CTD-probe. The LADCP-system was equipped with an external battery case for elimination of magnetic disturbances by battery packs. One LADCP was used in upward looking mode (serial number: 15230) and one in downward looking mode (serial number: 1129) in order to get a large range as possible.
The Workhorse LADCP produces profiles of velocity and echo intensity. Additionally, temperature inside the ADCP's case is recorded. The downward looking device is equipped with a pressure sensor.

Post-processing of LADCP data were carried out with MATLAB LADCP-2 software Version 7 by Martin Visbeck. First the velocity profiles were differentiated with respect to depth to eliminate the CTD-package's motion. Then a depth record was obtained by integrating the vertical velocity over time. Subsequently the shear profiles were averaged together within depth bins. The average shear profile was then integrated vertically to obtain a baroclinic velocity profile. The barotropic correction was calculated with start and end position from a GPS, which were recorded if the CTD-probe pass the 30dbar depth level. The software package was extended by a routine for calculating the acoustic backscatter cross section and a data export in BluePrint formatted file. The correction of magnetic deviation was applied during the data post-processing.

The microstructure-turbulence profiler MSS 90-S (Serial number 077) is an instrument for simultaneous microstructure and precision measurements of physical parameters in marine waters. The MSS profiler was equipped with 2 velocity microstructure shear sensors (for turbulence measurements), a microstructure temperature sensor, standard CTD sensors for precision measurements, an oxygen sensor, a turbidity sensor, and a vibration control sensor.

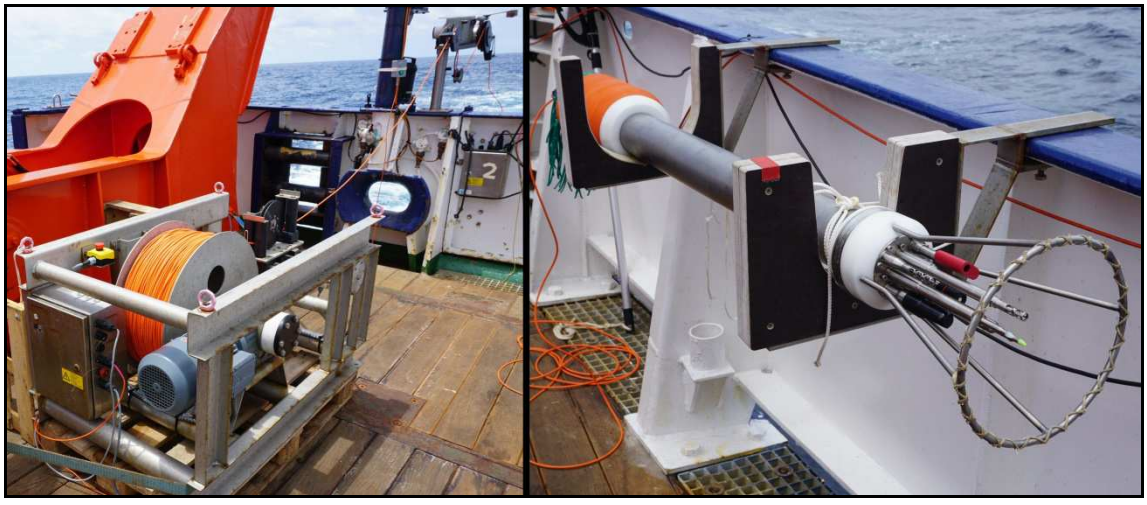

Fig. 5.1.1 MSS Powerblock-Winch and MSS90L profiler used during the cruise (right).

All sensors are mounted at the measuring head of the profiler, the microstructure ones being placed about 150 mm in front of the CTD sensors. The sampling rate for all sensors was 1024

samples per second. At each station a set of 2 to 6 subsequent profiles was gathered. The profile to profile interval depends on water depth and ranges from 4 min in 60 m to 20 min in 500 m water depth respectively. The profiler was balanced with negative buoyancy, which gave it a sinking velocity of about 0.6 m/s. It was operated via a power block winch from the stern of FS Meteor. Disturbing effects caused by cable tension (vibrations) and the ship's movement were excluded by a slack in the cable. After each deployment the sensors were flushed with pure water to prevent fouling. The dissipation rate of turbulent kinetic energy was calculated by fitting the shear spectrum to the theoretical Nasmyth spectrum in a variable wave number range from 2 to maximum 15 cycles per meter (cpm). The low wave number cut off at 2 cpm is to eliminate contributions from low frequent tumbling motions of the profiler.

Sensor calibration

The temperature and conductivity sensor of probe MSS055 and spare probe MSS038 were calibrated prior the cruise in IOW calibration lab. Thus, temperature and conductivity were not calibrated during the cruise.

Pressure: The probe MSS077 consists of two pressure sensors p-100 and p-20 for a pressure range of 1000dBar and 250dBar, respectively. When profiling was carried out down to 550m the pressure sensor p-100 was used, and the pressure sensor p-20 was sealed with a screw. For profiles in shallow water (< 200m depth) both sensors were used. A number of measurements on deck (with air pressure) were performed to obtain the offsets of both sensors. The pressure offsets applied during post processing were in the range of -0.07 to 0.1 dbar.

NTC sensor: The NTC sensor did not show any significant deviation from the temperature sensor. Thus, no correction was applied.

Turbidity sensor: The used sensor range was 0-25 NTU. The turbidity sensor is extremely sensitive to the position of the sensor protecting frame of the probe. Thus, there is no single zero point offset for the entire data set. On air the sensor depicts a blind value of -0.19 NTU.

Oxygen sensor: The MSS was equipped with a PyroSens oxygen sensor. This is an oxygen optode with a response time of 2-3 seconds. Since the sensor was used for the first time, after the cruise a qualification of the Sensor will be performed by cross checking the data with CTD sensors and Winkler titration data from water samples. On the first impression the gathered data are highly comparable with the SBE 43 oxygen sensor, used at the CTD.

During the cruise more than 500 MSS profiles were performed. A major technical problem during the deployments was a strong drill in the cable, most probably due to a fast rotation of the probe during the free fall phase. The reason for the rotation could not be detected.

The Wetlabs AC-S is an in-situ spectrophotometer to measure the total absorption coefficient $\boldsymbol{a}$ and the beam attenuation coefficient $\boldsymbol{c}$ at 84 wavelengths in the spectral range from 400 to 730 nm in about 4 nm steps with half-widths of 10-18 nm. The device system consisting of the AC-S, data logger and battery pack is installed with a pump and a pressure sensor in a frame and

operates autonomously. The water is pumped through a flow-through system by two 25 cm cuvettes. The light source is a Wolfram lamp. The device start-up takes place just prior to exposure through the connection with the battery pack. The device is programmed with a delay time of 2 min, to reach the water before the warm up phase starts. During the warm up phase water is pumped through the systems "a" and "c" tubes to ensure bubble-free measurements, which then leaves the pump. The AC-S System was lowered by a crane with a velocity of 0.3 m/s to the maximum measuring depth of 105 m depending on the stratification.
The background absorption and beam attenuation were measured by filling the system with deionized water in the lab. For calculation of the final absorption and beam attenuation coefficients the background values were applied to the *in-situ* observations, as well as a temperature correction.
During MSM80 the AC-S was deployed at 68 stations and usually lowered down to maximum depths of 105 m.
The offset of the pressure sensor at the surface was about -0.13dbar. This was corrected during the post processing. At some profiles disturbances of the profile measurements occurred. The reason may be the contamination of the device with jelly fish tentacles. At profiles 23 to 25 communication errors between the AC-S and the data logger DH-4 cause a partial loss of profile data. The AC-S device was checked, and the communication problem could be fixed finally.

The ScanFish towed CTD (SF) was used along twelve transects during the cruise. The platform consists of a Seabird 911+ CTD mounted on a wing shaped body undulating between sea surface and about 130m depth when towed behind the ship. Additionally, to the usual CTD sensors, the probe was equipped with sensors for dissolved oxygen concentration, chlorophyll-a fluorescence and turbidity. Hydrographic data were transmitted via a multi-conductor cable and stored in the lab on a computer disc. The instrument was deployed over the stern of the ship. The cable was operated from a separate winch mounted at the aft deck. The cable was guided by a pulley block mounted below the A-crane. The A-crane was used for deployment and recovery.
The device was towed with about six knots, the undulation depth is controlled from the lab. Commands are transmitted via the cable.

The device worked properly during all deployments. Only the altimeter was temporarily not working. However, since the bottom depth was mostly much deeper than the maximal deployment depth, this did not caused any measuring limitation.

A 75kHz Acoustic Doppler Current Profiler (VMADCP) Ocean Surveyor (frequency 76kHz, beam angle 30deg), manufactured by RD-Instruments, was mounted downward looking at the ship hull. The data output of the ADCP was merged online with the corresponding navigation data and stored on the hard disc using the program VMDAS. Pitch, roll and heading data are converted from NMEA. Current data should be collected in beam coordinates to apply all corrections during post processing. For unknown reason the VMDAS seemed to store the raw data in earth coordinates, although the configuration was set to beam coordinates. This will be corrected during the post processing. The VMADCP was operated continuously in the EEZ and territorial waters of Peru between the 26th December 2018 and the 26th January 2019. The following configuration was used for data acquisition.

Post-processing of the VMADCP data was carried out using the Matlab® ADCP toolbox of IOW. The final profiles are 60s and 300s averages of the single ping profiles. The heading bias of the instrument and the magnetic deviation were applied during post processing. The ships Doppler log caused interferences during the first 3.5 hours of the deployment 1. Later the Doppler log was switched off. Due to a failure of the control PC no data were gathered with the 75Khz VMADCP between 06.01. 10:00 UTC and 07.01.2019 14:50 UTC.
No tilt and heading data were collected in the ADCP raw data files before 18.01.2019 03:00 UTC. These data were extracted from the DSHIP database and will be included in the ADCP data during post processing.
Due to the lack of appropriate scatters in the pronounced oxygen minimum zone between 50 and 600m the performance of the device was low. Only in regions with Krill accumulations reliable data were gathered in the OMZ.

Another 38kHz Acoustic Doppler Current Profiler (VMADCP) Ocean Surveyor (frequency 38kHz, beam angle 30deg), manufactured by RD-Instruments, was mounted downward looking at the moon pool. The data output of the ADCP was merged online with the corresponding navigation data and stored on the hard disc using the program VMDAS. Pitch, roll and heading data are converted from TCPTIP to UDP protocol with an own program, running on the VMADCP control PC. Current data should be collected in beam coordinates to apply all corrections during post processing. For unknown reason also the VMDAS of the 38kHz PC seemed to store the raw data in earth coordinates, although the configuration was set to beam coordinates. This will be corrected during the post processing. The VMADCP was operated continuously in the EEZ and territorial waters of Peru between the 26th December 2018 and the 26th January 2019. The following configuration was used for data acquisition.

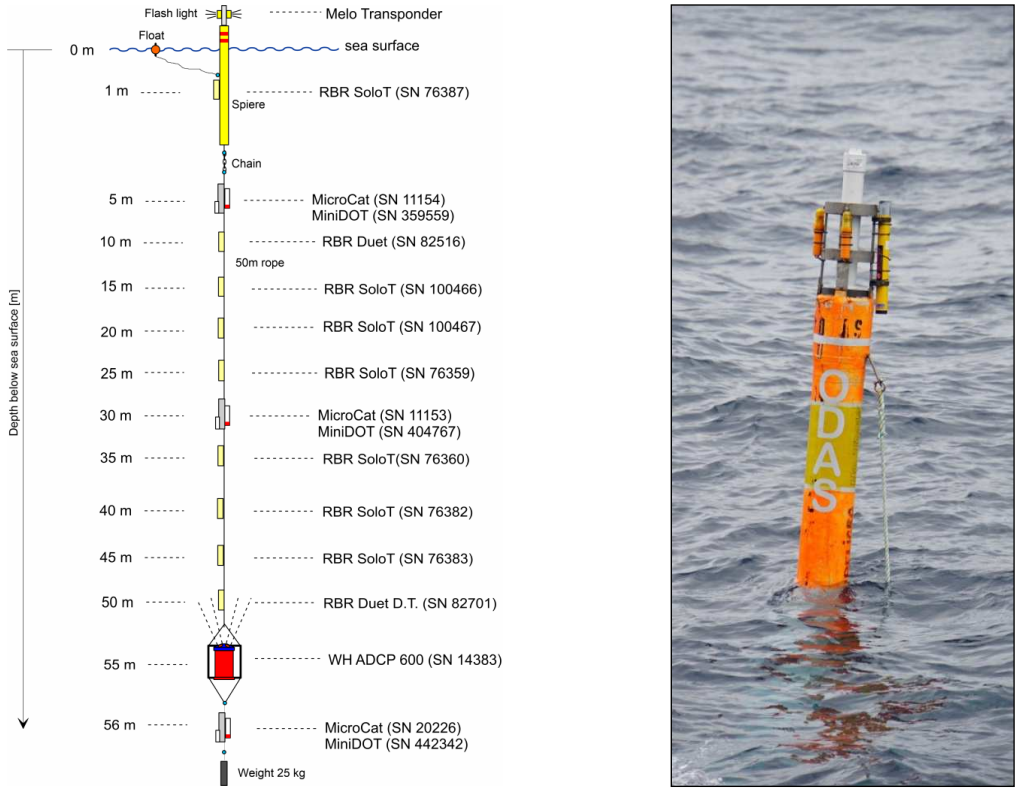

Fig. 5.1.2 Sketch and picture of the Drifter mooring deployed during MSM80.

Post-processing of the VMADCP data was carried out using the Matlab® ADCP toolbox of IOW. The final profiles are 180s averages of the single ping profiles. The heading bias of the instrument and the magnetic deviation were applied during post processing.
No tilt and heading data were collected in the ADCP raw data files before 18.01.2019 03:00 UTC. These data were extracted from the DSHIP database and will be included in the ADCP data during post processing.
Due to the lack of appropriate scatters in the pronounced oxygen minimum zone between 50 and 600m the performance of the device was low. Only in regions with Krill accumulations reliable data were gathered in the OMZ. Due to a failure of the control PC no data were gathered with the 38Khz VMADCP between 19.01.2019 06:00 UTC and 20.01.2019 00:36 UTC.

For the investigation of the upper mixed layer and its transition to the subsurface waters a drifting surface mooring was used. Four deployments were performed during the cruise at different latitudes. Figure 5.1.2 depict a principle sketch of the drifting mooring, and a picture of the surface buoyancy float in water. The drifter was equipped with an upward looking ADCP at the lower end of the sensor string, three MicroCat thermosalinometer SBE37, three PME oxygen optode sensors and a seven RBR temperature logger. All devices were configured with the fastest possible sampling interval. That was 1s for the ADCP and the temperature loggers, and 60s for the MicroCats and the Oxygen optodes.

During the entire cruise a TRIOS radiation measurement system was used to gather reflectance data. The system was mounted at the bow of the ship. It consists of three spectrometers measuring the incoming global radiation, the forward incoming radiation and the reflectance of the sea surface. The data are stored in an ACCESS data base. No additional validation or preprocessing was performed during the cruise.

Preliminary results
The results presented in the following section are preliminary and not comprehensive, since they are based in most cases on unevaluated raw data! The aim of this section is to give a first impression on the collected data set. An advanced data analysis will follow after all validated data sets are available.

Meteorological conditions
The general meteorological conditions during the cruise were characterized by steadily blowing southeast trade winds (SET). During the work on the northern Peruvian shelf wind velocities between 6 and 10 ms^{-1} were observed till the 3rd January. On the next day the wind decreased to weak and later to calm strength, when the ship crossed 11°S. The transect off Callao was worked in this period of weak winds. After passing the latitude of 14°S the wind velocity increased again to 8 to 10 ms^{-1} (5.1.3). This period of moderate wind speed last till the 18th January. Later the wind decreased again to 3 to 8ms^{-1} and remained at this level till the end of scientific program on 27th January.

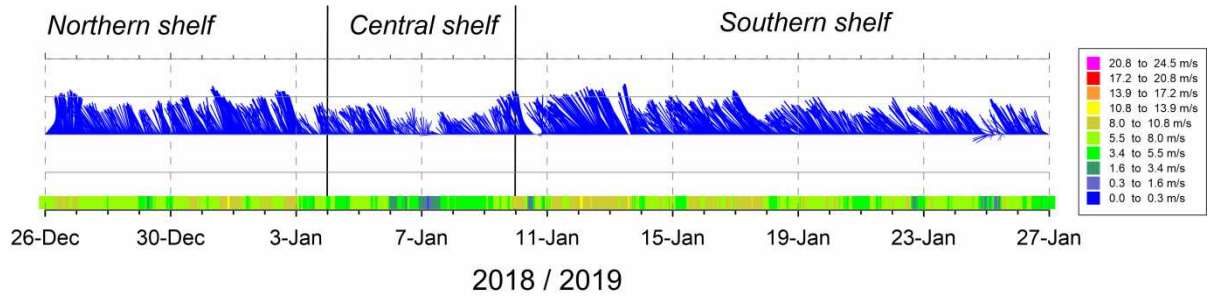

Fig. 5.1.3 Stick plot of wind vector measured by the ship weather station of FS Merian.

The air temperature of the Peruvian shelf was normal for the early summer season of the southern hemisphere. It was on average about 23°C till the 13th January. On that day the air temperature dropped by two degree shortly after the onset of moderate winds when the ship reached the southern shelf area. During the second part of the cruise the air temperature depicted a small positive trend and reached again 23°C at the end of the cruise (Fig. 5Fig. 5.1..1.4). During the entire cruise the air temperature depicted a weak daily cycle. The difference between daily minimum and maximum temperatures was about 2°C. The few larger drops in air temperature indicate the times when the ship worked close to the coast.

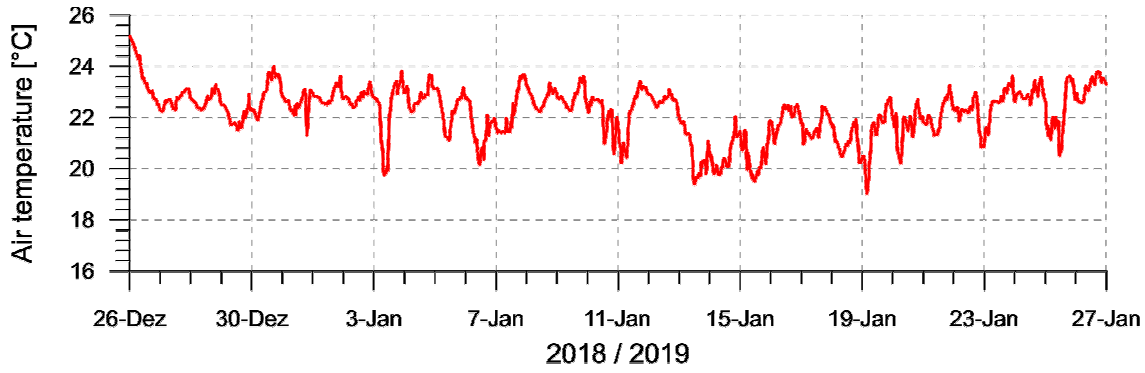

Fig. 5.1.4 Air temperature measured by the ship weather station of FS Merian (30 min averaged values).

The air pressure variations during the cruise show the typical short-term variation with a dominating 12 h period. This signal with amplitude of about 3mbar is caused by the tides of the atmosphere. The overall variations in air pressure were small. During the entire cruise the air pressure remained at a level of 1010 to 1015 mbar (Fig. 5.1.5).

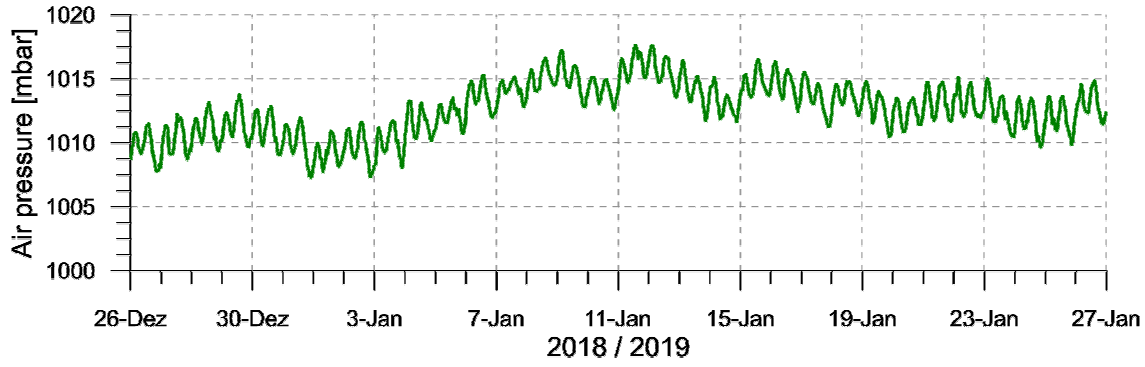

Fig. 5.1.5 Air pressure measured by the ship weather station of FS Merian (30 min averaged values).

The humidity was relatively high, but typical for the summer season in the equatorial Southeast Pacific. It was varying between 80 and nearly 100%, with a minor daily variation of about 10 to 15 (Fig. 5.1.6). However, no significant rain fall was observed during the entire cruise.

The cruise started with some days of cloud free sky. Traveling south the cloud coverage increased slightly. The global radiation was strongly related to the cloud coverage. Maximum values, at noon on sunny days, were about 1000 Wm^{-2} at the northern shelf. Towards south the maximum values of global radiation increased to about 1100 Wm^{-2} due to the increasing inclination angle of the sun. On 10th and 18th January the dense cloud coverage caused low values of global radiation which were at noon at about 800 Wm^{-2} (Fig. 5.1.7). The longwave radiation was at about 400 Wm^{-2} with only minor fluctuations.

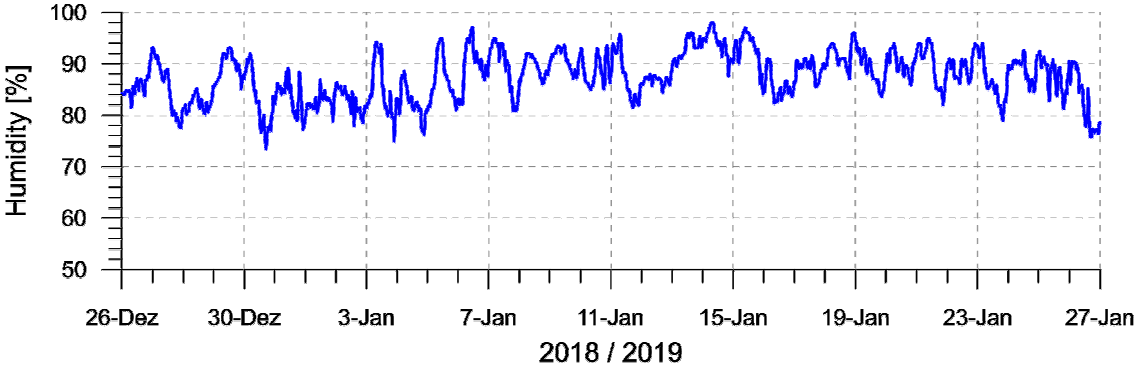

Fig. 5.1.6 Air humidity measured by the ship weather station of FS Merian (30 min averaged values).

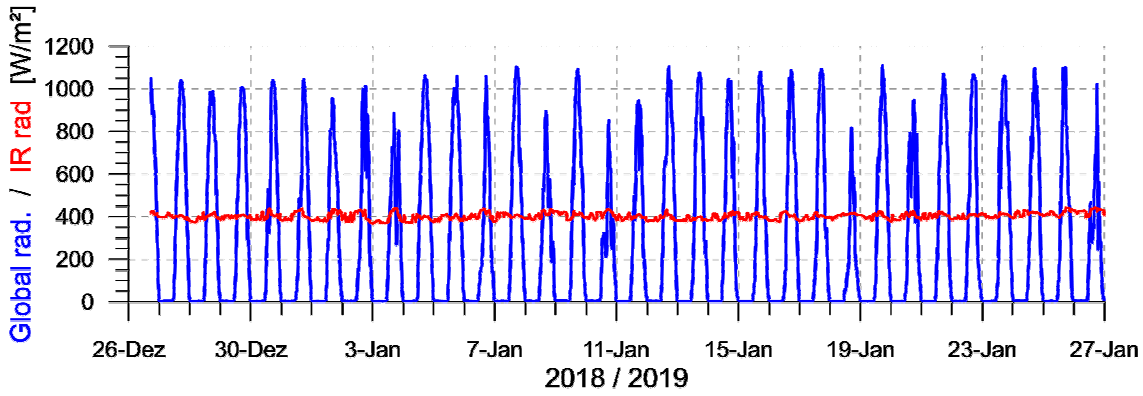

Fig. 5.1.7 Global and infrared radiation measured by the ship weather station of FS Merian (30 min averaged values).

Properties of sea surface water

Sea surface temperature, salinity, chlorophyll-a concentration and turbidity distributions in the investigation area were compiled from data gathered with the two underway measurement systems of RV Merian, which worked alternating with a period of 12 hours. The distributions shown in Fig to Fig are based on unvalidated data. Beside some outliers both systems depicted comparable values during the entire measuring period. The light (system 1) and dark color (system 2) in the particular plots indicate the source of the data.

The surface water temperature on the Peruvian shelf ranged between 17°C close to the coast near 15°S and 24°C in the northern oceanic part of the investigation area (Fig. 5.1.8). Upwelling was weak during the entire cruise due to the moderate to weak wind velocities. Thus, only between 14°S and 16°S a larger area of cool temperatures was found. Usually the sea surface temperature ranged between 22°C and 24°C on the northern shelf, and between 20°C and 22°C on the southern shelf.

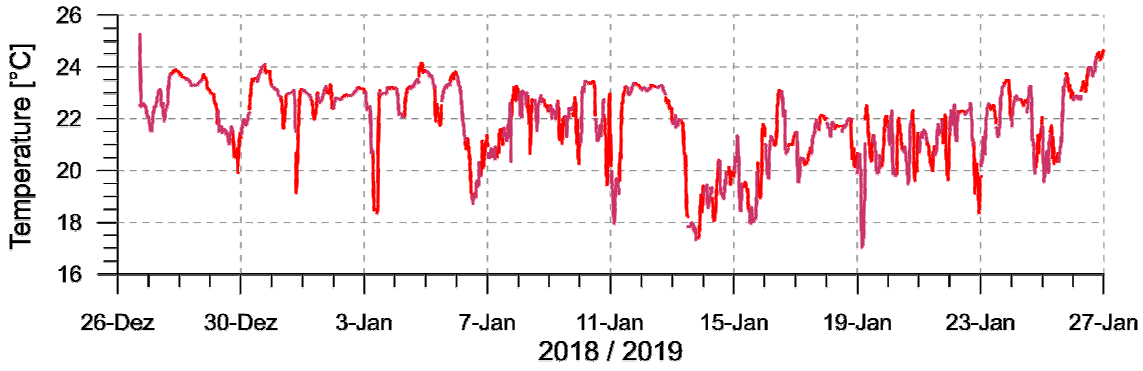

Fig. 5.1.8 Surface temperature measured with the ship thermosalinograph of FS Merian (unvalidated 30 min averaged values).

In the entire area the sea surface salinity was on average at about 35.2 gkg^{-1}. On the northern and central shelf some patches of water with higher salinity of 35.4 gkg^{-1} were observed at the

offshore parts of the transects. In the southern part of the investigation area the sea surface salinity remained nearly constant.

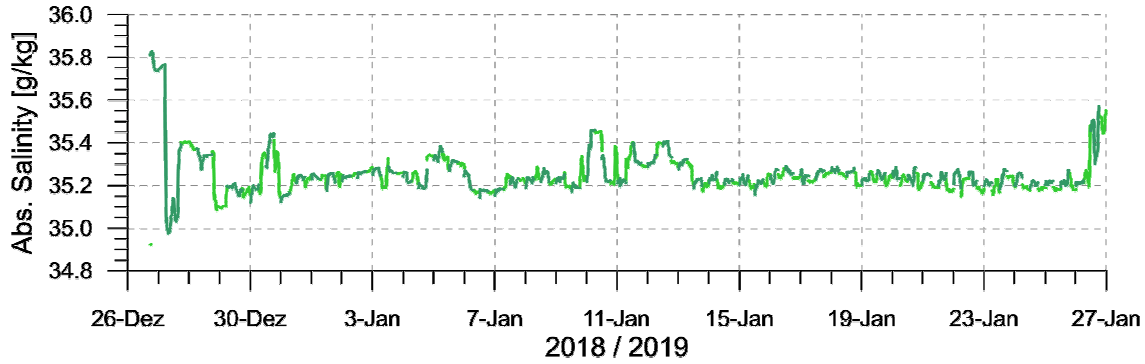

Fig. 5.1.9 Surface salinity measured with the ship thermosalinograph of FS Merian (unvalidated 30 min averaged values).

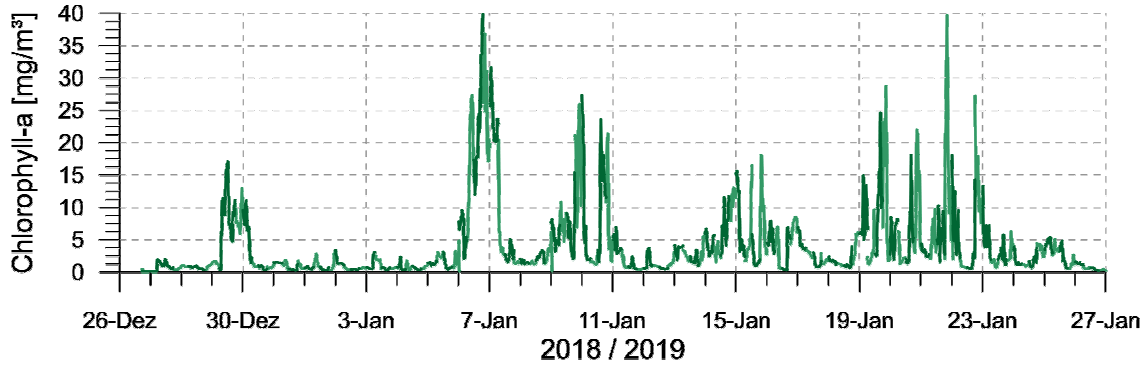

Fig. 5.1.10 Surface Chlorophyll-a concentration measured with the ship thermosalinograph of FS Merian (unvalidated 30 min averaged values).

The surface chlorophyll-a concentration and the turbidity revealed the patchy distribution of areas with high primary productivity. The range of the observed chlorophyll-a concentration was quite large. Maximum values of about 40 mgm^{-3} were observed off Callao and on the southern shelf. This was also supported by the data of the vertical CTD.

The surface turbidity distribution was strongly correlated with the chlorophyll-a concentration. However, the underway measurement system 2 depicted a number of outliers which has to be threated during the post processing of the underway data.

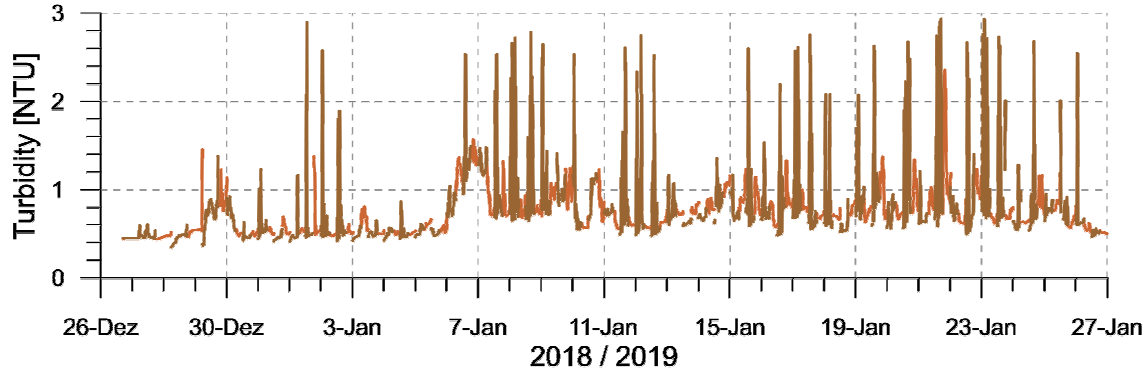

Fig. 5.1.11 Surface turbidity measured with the ship thermosalinograph of FS Merian (unvalidated 30 min averaged values).

Northern Peruvian shelf area

The northern Peruvian shelf was covered with two cross shelf transects at 8.5°S and 9.5°S. In this are the shelf is relatively wide. Each transect consists of 5 to 6 full CTD stations. In between additional MSS stations were performed to increase the spatial resolution of the hydrographic observations. The ScanFish was used along both transects to get a high-resolution picture in the upper 130 m. The transect was worked with upwelling favorable wind conditions. However, the active upwelling at the coast was weak.

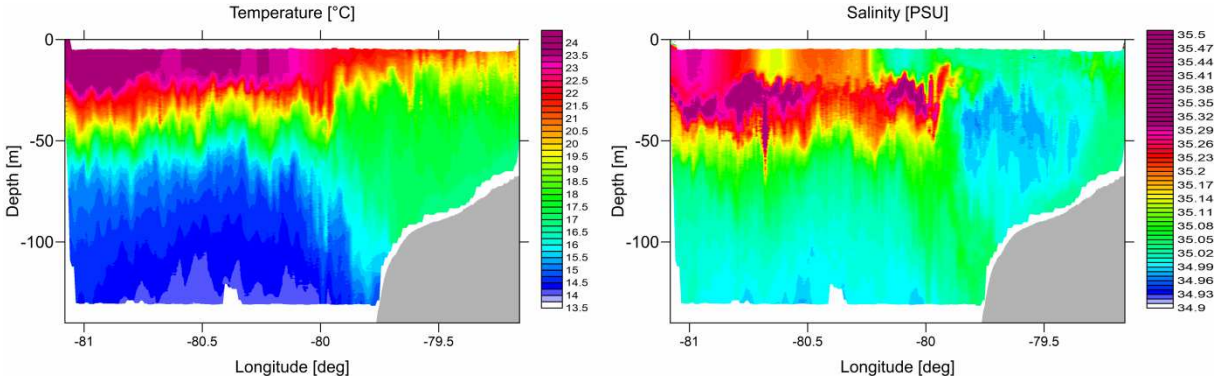

Fig. 5.1.12 Distribution of temperature and salinity along the Northern Peruvian Shelf transect at 8°30'S. The figure is based on the preliminary ScanFish CTD data gathered on 29. - 30.12.2018.

The temperature and salinity distribution depicted a typical upwelling pattern (Fig. 5.1.13). The mixed layer depth decreased from about 40 m in the offshore area to only 15 to 20 m near the coast. Below the mixed layer the temperature and salinity depict the usual vertical profile for the central water layer. On the shelf the vertical temperature gradient was strongly reduced. One reason might be the enhanced mixing at the shelf edge. The salinity shows the typical subsurface salinity maximum, caused by the offshore drift of upwelled low saline water. The patch of lower salinity over the shelf may indicate the equatorward advection of lower saline water in the coastal branch of the Humboldt Current.

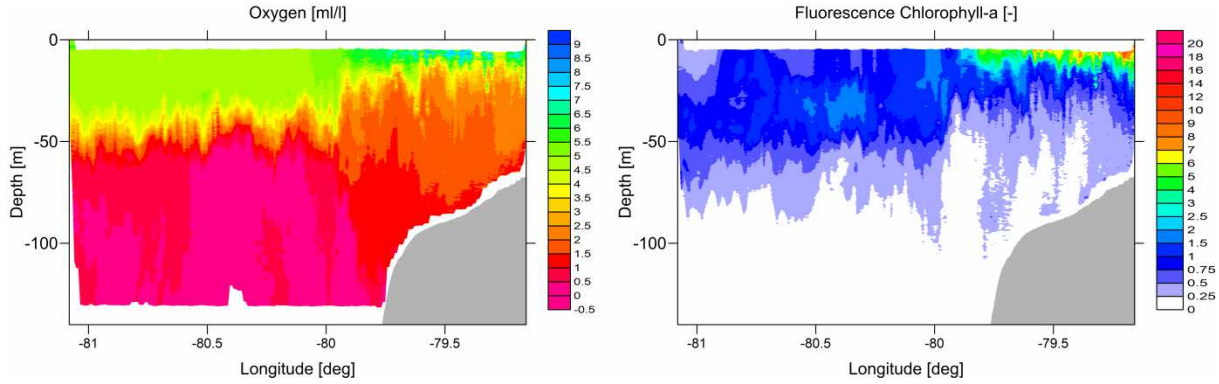

Fig. 5.1.13 Distribution of oxygen concentration and Chlorophyll-a fluorescence along the Northern Peruvian Shelf transect at 8°30'S. The figure is based on the preliminary ScanFish CTD data gathered on 29. - 30.12.2018.

The distribution of dissolved oxygen follows the shape of temperature patterns. The mixed layer was well ventilated on the entire transect. Below the thermocline the oxygen concentration dropped rapidly to zero in the offshore region (Fig. 5.1.14). On the shelf oxygen is also strongly reduced but well above zero, which indicate the impact of mixing and advection in the subsurface layer. Near coast the very thin surface layer was over saturated with oxygen, caused by the high primary production.

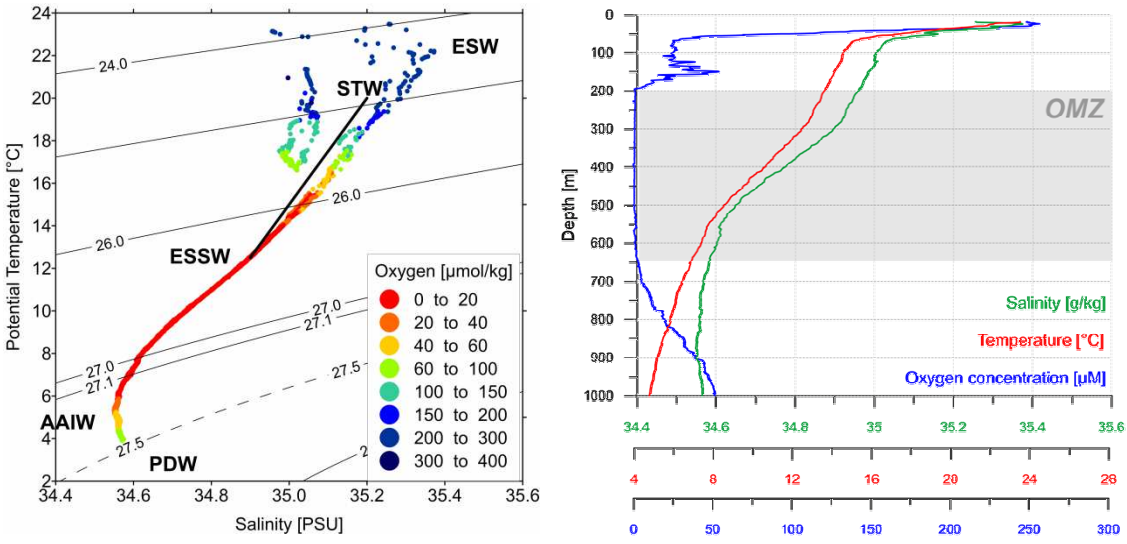

Fig. 5.1.14 TSO – diagram of all CTD stations performed on the 8.5°S transect (left) and the TSO profiles of the westernmost station of the transect (right).

The Chlorophyll-a fluorescence was at its maximum in the surface layer near the coast. The fluorescence decreased towards the open ocean. Near the shelf edge the transition from surface maximum to a subsurface chlorophyll-a maximum indicates the removal of nutrients in the surface layer by primary production.

The TSO diagram of the transect was constructed from all CTD measurements gathered along the transect. The surface and subsurface water is a mixture of Equatorial Surface Water (ESW) and Subtropical Water (STW) with ESW as dominating fraction. The central water layer was covered by Equatorial Subsurface Water (ESSW). Down to 300 m it contained also decreasing fractions of ESW and STW. The transition between ESSW and Pacific Deepwater (PDW) contained also a fraction of Antarctic Intermediate Water (AAIW). At the oceanic end of the transect the OMZ stretched from about 50m down to 650 m depth. Oxygen was depleted below 200 m depth.

Additional information about the distribution of phytoplankton, particulate matter and dissolved organic matter was gathered at the majority of the stations with an AC-S in-situ spectrophotometer. The observed profiles of absorption, attenuation and scattering coefficients were compared with the CTD measurements of Chlorophyll-a fluorescence and turbidity. At the coastal station of the 8.5°S transect the optical profiles are dominated by the Chlorophyll-a distribution and the high turbidity near the bottom. The absorption coefficient increases with decreasing wave length whereas the scattering coefficient seems to be independent of the wave length. That points to a high impact of particulate matter on the observed profiles (Fig. 5.1.15). The spectral distribution of the absorption coefficient for different depth is depicted in Fig. 5.1.16.

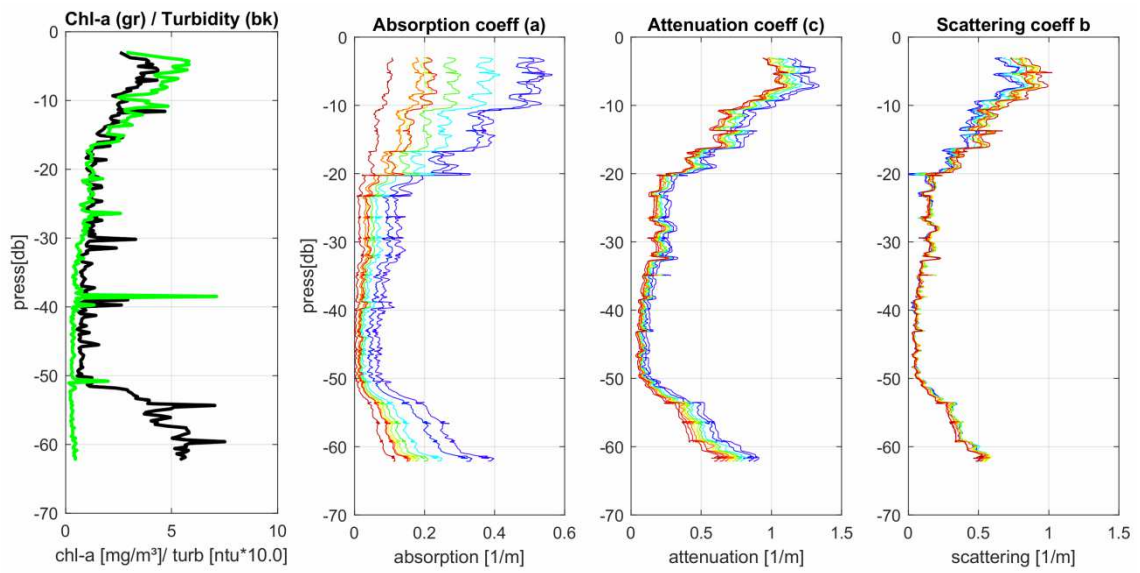

Fig. 5.1.15 Vertical profiles of chlorophyll-a fluorescence and turbidity observed with the CTD on station MSM80_14 near the coast (left). Preliminary data of absorption, attenuation and scattering coefficients gathered with the AC-S profiler (middle to right) for nine selected wave length in the visible light spectrum.

Here the absorption peak of chlorophyll a is visible near 670 nm at 8 m and 20 m depth. The light absorption below the surface mixed layer was dominated by Colored Dissolved Organic Carbon (CDOM), indicated by the exponential distribution of the absorption coefficient.

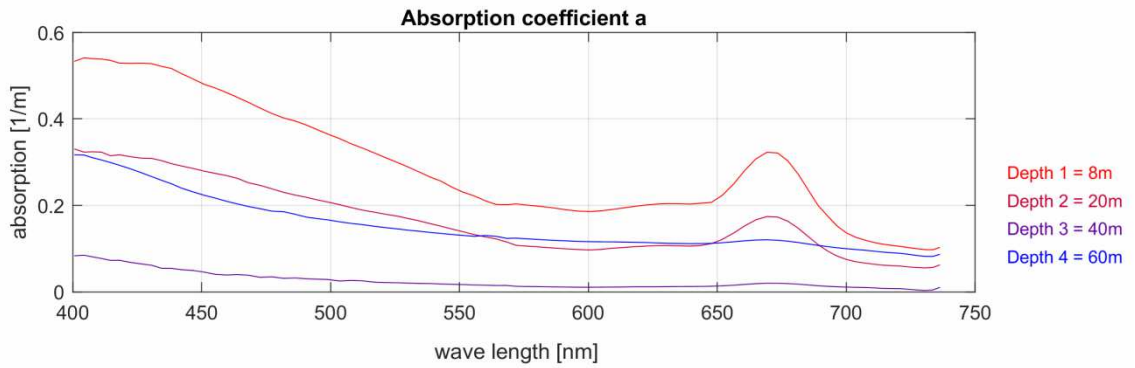

Fig. 5.1.16 Spectral distribution of the absorption coefficient for four different depth on station MSM80_14 near the coast. At about 670nm the absorption peak indicates the high chlorophyll-a concentration**.**

The second transect on the northern Peruvian shelf was performed at 9.5°S. Overall it reveals similar patterns as the transect at 9.5°S. Differences occurred mainly near the coast where the upwelling was more intensive. The chlorophyll-a fluorescence depicted a second surface maximum at the offshore end of the transect (not shown). At 9.5°S 79.0°W the drifter was deployed to gather information about the processes in the upper 50 m. After deployment the drifter was advected in offshore with a mean speed of 0.4 ms^{-1}. However, the true speed in the surface layer of 20 m thickness was about 0.6 ms^{-1} as proved by the current measurements. The lower speed in the subsurface layer decelerated the total speed of the drifting mooring (Fig. 5.1.17).

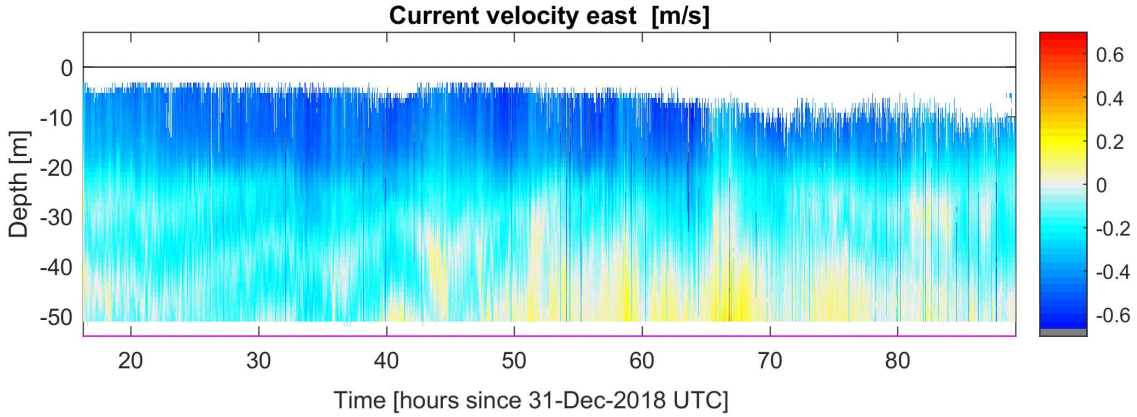

Fig: 5.1.17 Eastward current velocity along the drifter path at 9.5°S measured with the upward looking ADCP of the system.

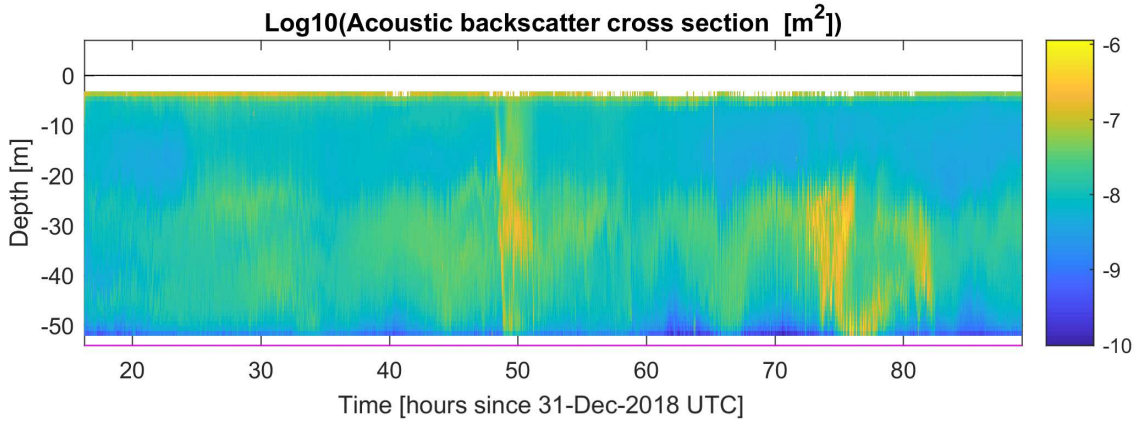

Fig. 5.1.18 Acoustic backscatter cross section along the drifter path at 9.5°S measured with the upward looking ADCP of the system.

The backscatter signal of the ADCP contains information about the spatial distribution of zooplankton in the surface layer (Fig. 5.1.18). The calculated acoustic backscatter cross section is approximately proportional to the biomass of the scatters. The major part of the drift path was on the shelf. Here no pronounced dial vertical migration was detected. The maximum concentration of scatter particles was found at the lower boundary of the mixed layer above the oxygen depleted water.

Central Peruvian shelf area

The third cross shelf transect of the cruise was performed in the central shelf area off Callao, after some CTD stations on the way from the northern shelf (Fig. 5.1.19). The transect was worked first with the ScanFish. On the way back towards the open ocean CTD and MSS stations were conducted.

At the coast active upwelling is indicated by the cool water at the surface. Here the thermocline almost vanished. Towards the open sea the depth of the mixed layer increased from 10 m over the shelf to 30 m at the oceanic edge of the transect.

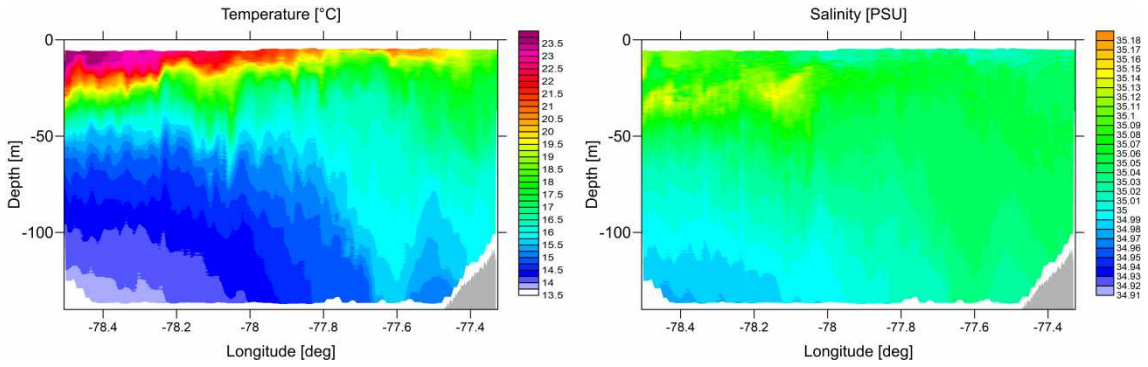

Fig. 5.1.19 Distribution of temperature and salinity along the Central Peruvian Shelf transect at 12°S. The figure is based on the preliminary ScanFish CTD data gathered on 06.01.2019.

Concurrently also the surface temperature increased from 19°C near the coast to 24°C in the open ocean. In contrast to the inner shelf the offshore region depicted a well pronounced vertical temperature gradient below the surface mixed layer. Here the temperature and salinity were decreasing with depth according the usual conditions in the central water layer. Over the shelf the vertical gradients of temperature and salinity are reduced. In contrast to the northern shelf the surface salinity was significantly lower. The subsurface salinity maximum was weakly developed.

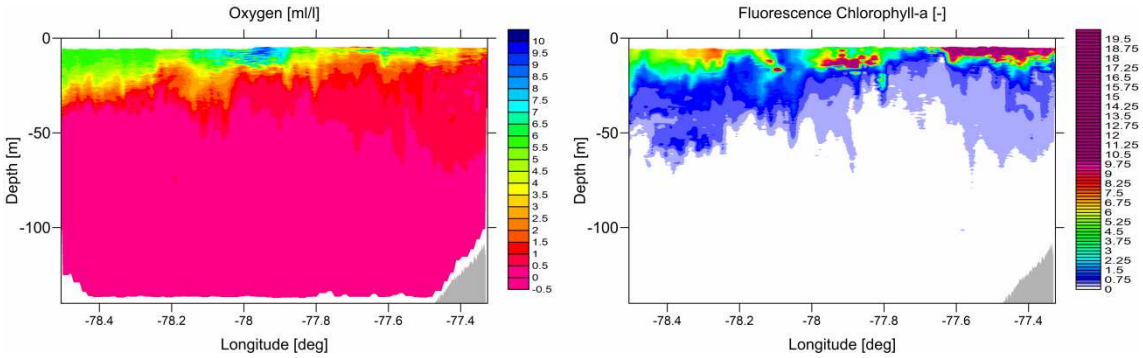

Fig. 5.1.20 Distribution of dissolved oxygen and chlorophyll-a fluorescence along the Central Peruvian Shelf transect at 12°S. The figure is based on the preliminary ScanFish CTD data gathered on 06.01.2019.

The oxygen concentrations at the coast were low due to the upwelling of low oxygen water (Fig. 5.1.20). Towards the open ocean the exchange with the atmosphere and the primary production led to increasing oxygen concentrations in the surface layer. Below the mixed layer the oxygen concentrations dropped to almost zero. The chlorophyll-a distribution showed a patchy structure. Directly at the coast, where the upwelling is active the heist chlorophyll-a fluorescence was observed. In the mixed layer of the offshore area the chlorophyll-a concentration was still high pointing to a high primary production. No pronounced subsurface chlorophyll maximum was detected. The high primary productivity caused a strong over saturation with oxygen in the middle part of the transect.

The water mass distribution along the transect is depicted in the TS0 diagram (Fig. 5.1.21). The observed water mass properties were almost similar to the northern shelf. However, the impact of ESW was decreased in the upper layer. The lower value of the salinity minimum between ESSW and PDW points to a slightly increased fraction of AAIW below the central water layer.

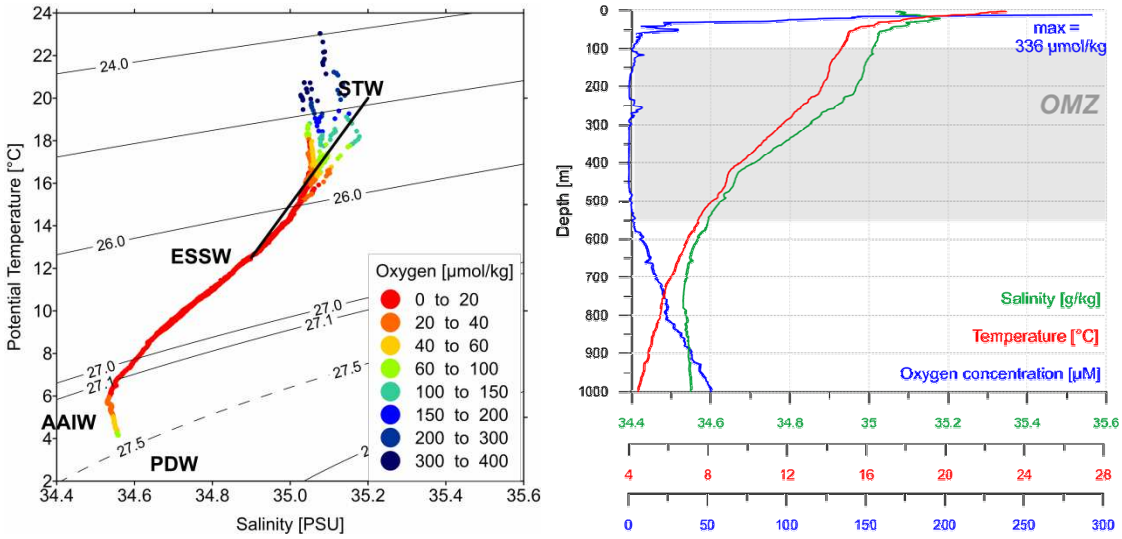

Fig. 5.1.21 TSO – diagram of all CTD stations performed on the 12°S transect (left) and the TSO profiles of the central station of the transect at 78°W (right).

The right panel of Fig. 5.1.21 depicts the vertical distribution of temperature, salinity and oxygen concentration in the central part of the transect. Approximately, at the position where the oxygen over saturation was detected with the ScanFish (compare Fig. 5.1.20). The maximum oxygen concentration amounted to 336µmol/kg in the surface layer. Below the shallow mixed layer of 20m thickness the oxygen concentration decreased rapidly and reached zero at about 100 m depth. The OMZ was shallower than on the northern shelf and stretched from 30 m to 550 m depth. Below that layer the oxygen concentration is increasing with depth. The core of AAIW was found at 750 m.

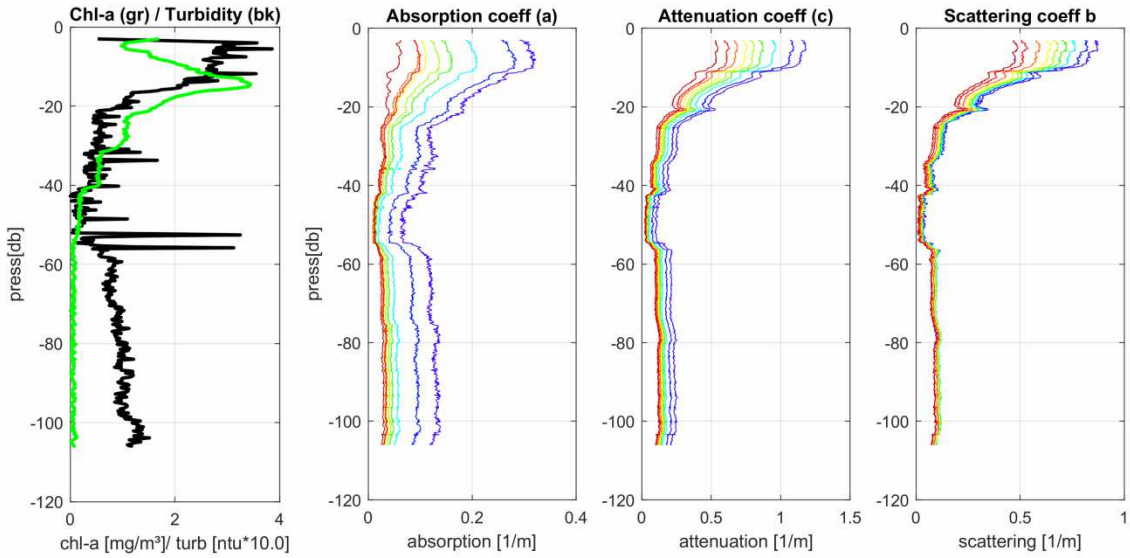

Fig. 5.1.22 Vertical profiles of chlorophyll-a fluorescence and turbidity observed with the CTD on station MSM80_26 (left). Preliminary data of absorption, attenuation and scattering coefficients gathered with the AC-S profiler (middle to right) for nine selected wave length in the visible light spectrum.

The vertical profiles of optical parameters revealed the shallow surface layer of high primary productivity at the central part of the transect (Fig. 5.1.22). The profiles of light absorption and scattering follow the CTD profiles of chlorophyll-a fluorescence and turbidity. However, the absolute value of absorption and scattering is significantly lower than at the coastal station of transect 1.

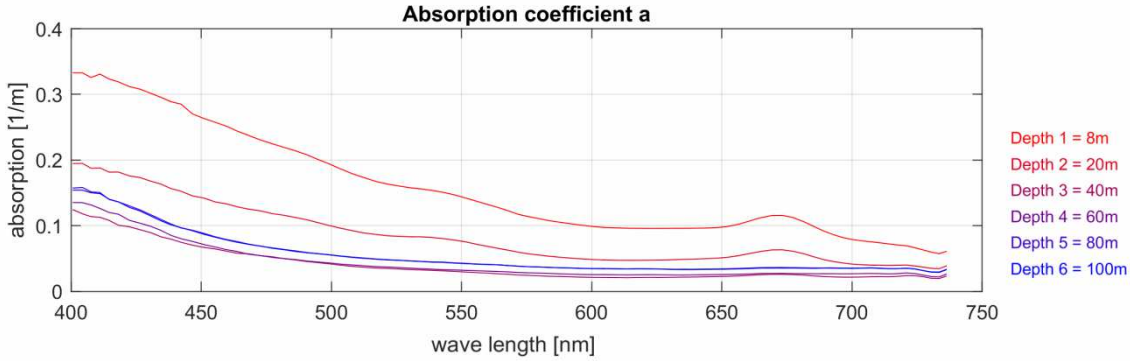

Fig. 5.1.23 Spectral distribution of the absorption coefficient for six different depths on station MSM80_26 near the coast. The chlorophyll-a absorption peak at 670nm is less pronounced than on station MSM80_14.

On the central transect the second drifter deployment was carried out. In contrast to the first deployment the drifter went strait southward against the main wind direction. The drifter followed the shelf edge with a drift velocity of 0.2 to 0.4 ms^{-1}. The current measurements in the upper 50 m showed a strong poleward directed current component which can be related either to the Peru-Chile counter current or the subsurface Gunther current. The vertical current shear was weak. There was weak indication that a very shallow layer at the surface follows the expected wind drift.

The acoustic back scatter cross section indicated a pronounced dial vertical migration at the shelf edge. That may be caused most probably by Krill, since it covers also the layer of very low oxygen between 30 m and 55 m depth (Fig. 5.1.26). The zooplankton stays at night in a very thin surface layer of about 15 to 20 m thickness.

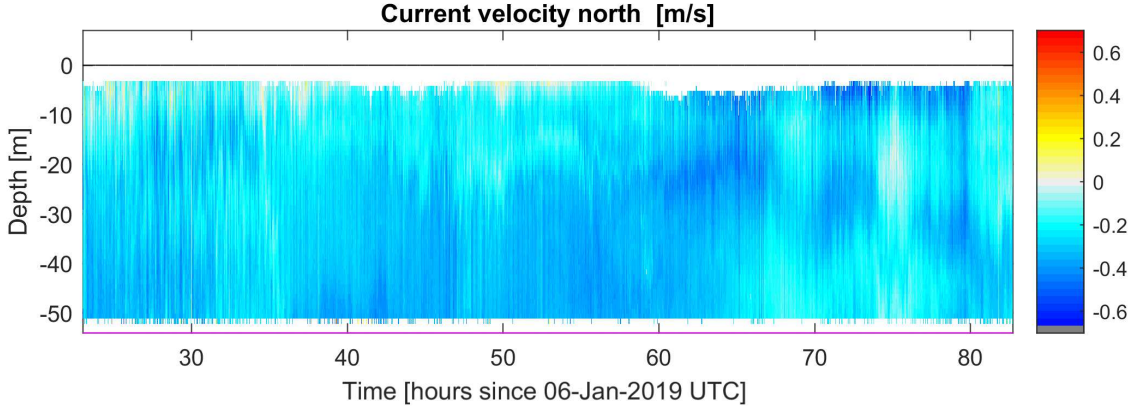

Fig. 5.1.24 Northward current velocity along the drifter path at 12°S measured with the upward looking ADCP of the drifter.

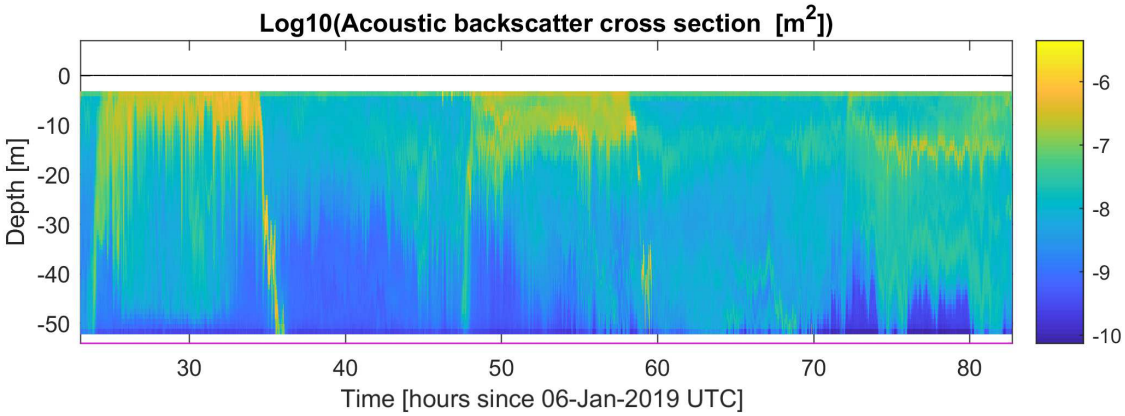

Fig. 5.1.25 Acoustic back scatter cross section along the drifter path at 12°S measured with the upward looking ADCP of the drifter.

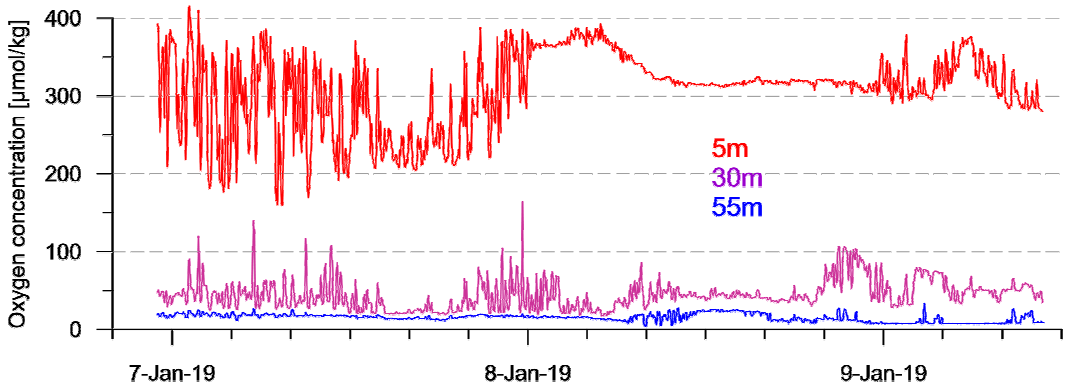

Fig: 5.1.26 Oxygen concentration at three depth levels along the drifter path at 12°S measured with PME optodes mounted on the drifter.

Southern Peruvian shelf area

The major part of the scientific work was carried out on the southern Peruvian shelf between 14.5°S and 16.5°S. At all 53 stations and five ScanFish transects were performed in the area, where the upwelling was most intensive. The presented results are only a subset of all gathered data and will illustrate the main hydrographic situation on the southern shelf. In contrast to the previous transects the upwelling pattern was not as obvious. Only the low surface temperature and the low oxygen concentration near the coast pointed to weak active upwelling. Generally, the spatial distribution of the main hydrographic parameters was very patchy, caused by mesoscale and sub mesoscale dynamics. However, the general trend of increasing mixed layer depth towards the open ocean was visible. Towards the offshore end of the transect the vertical temperature gradient at the thermocline increased together with the surface temperature. The temperature and salinity pattern below 20 m depth hints to an eddy like structure, centered at 75.7°W. There the subsurface salinity maximum vanished, and subsurface water seems to be pumped downward.

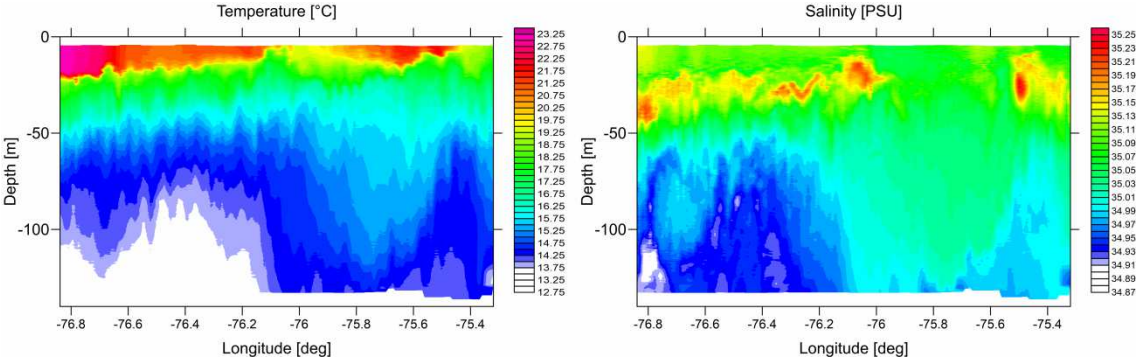

Fig. 5.1.27 Distribution of temperature and salinity along the Central Peruvian Shelf transect at 15.3°S. The figure is based on the preliminary ScanFish CTD data gathered on 15./16.01.2019.

The surface oxygen concentration followed the patchy distribution of temperature and salinity (Fig. 5.1.27). The well oxygenated layer was very shallow with about 20m thickness and strongly related to the warm surface water patches. Below 50 m oxygen was completely exhausted. The chlorophyll-a fluorescence was enhanced at the edges of the eddy like structure and in a third patch at 76.5°W. These areas correlate with the areas of high surface oxygen concentration (Fig. 5.1.28). A secondary chlorophyll-a accumulation was observed at the offshore part of the transect between 70 m and 100 m water depth. This indicated an enhanced downward export of particulate organic matter after phytoplankton bloom in the surface layer.

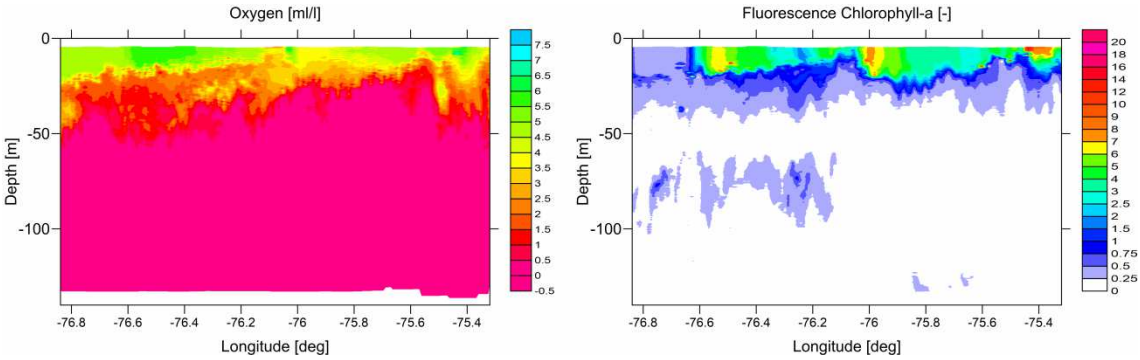

Fig. 5.1.28 Distribution of oxygen concentration and chlorophyll-a fluorescence along the Central Peruvian Shelf transect at 15.3°S. The figure is based on the preliminary ScanFish CTD data gathered on 15./16.01.2019.

On the southern shelf another three ScanFish transects were performed across the shelf. They depicted different structures of temperature, salinity and chlorophyll-a fluorescence, but a similar variability and patchiness. Thus, they are not shown here.

The TSO diagram and the vertical profiles at the off shore CTD station at 16°S are depicted in Fig. 5.1.29. In the upper layer, almost no impact of ESW was detected. The TS distribution followed the mixing path between STW and ESSW. The impact of AAIW is increased. Its core was observed at a depth of about 750 m. The OMZ starts very close to the thermocline at 20 m to

30 m depth and reaches down to about 450 m depth, compared to 650 m and 550 m depth in the northern and central area, respectively.

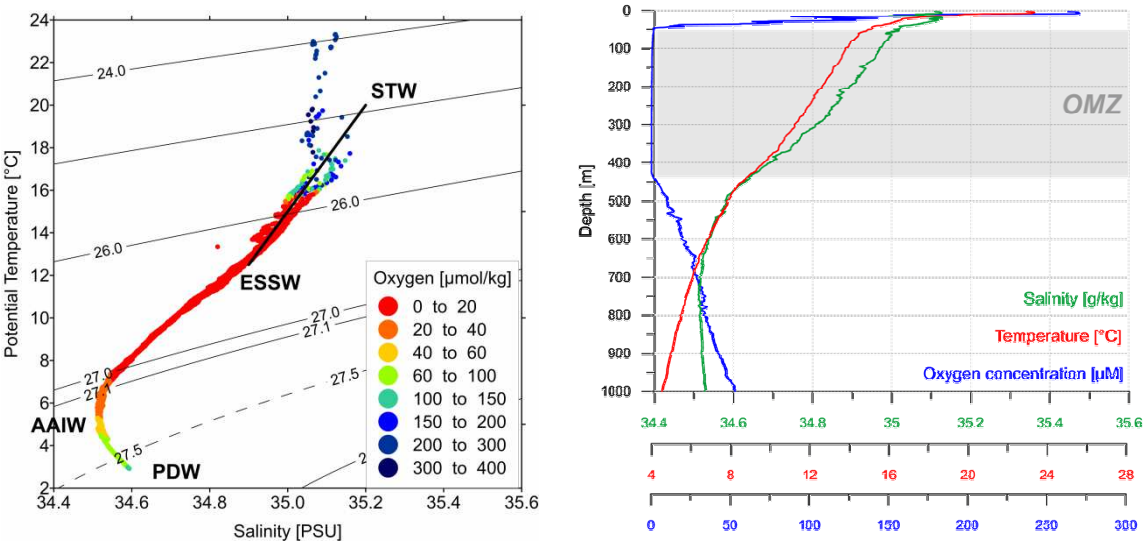

Fig. 5.1.29 TSO – diagram of all CTD stations performed on the 16°S transect (left) and the TSO profiles of the western most station of the transect at 76.5°W (right).

An unusual observation in the southern part of the investigation area was the detection of patches of extremely high chlorophyll-a fluorescence far offshore. The water color changed in these patches to a dirty brown color like river water. The estimated chlorophyll-a concentration reached maximum values of 35 mg/m^{-3} at some stations. The optical measurement with the AC-S profiler verified the CTD fluorescence measurements. An example is given for station MSM80_88 which was performed in a high chlorophyll a patch.

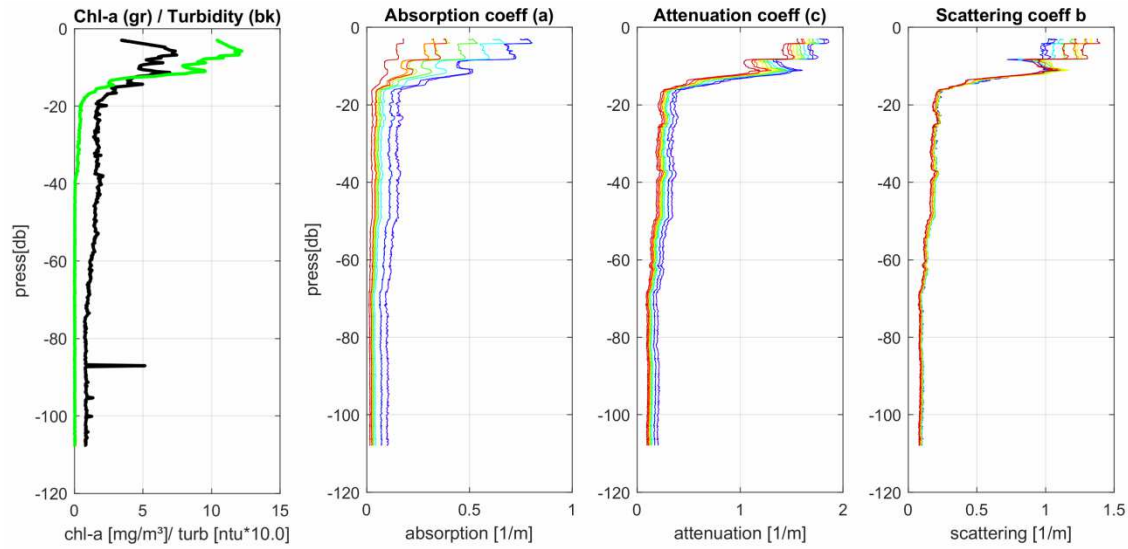

Fig. 5.1.30 Vertical profiles of chlorophyll-a fluorescence and turbidity observed with the CTD on station MSM80_88 (left). Preliminary data of absorption, attenuation and scattering coefficients gathered with the AC-S profiler (middle to right) for nine selected wave length in the visible light spectrum.

At this station the maximum chlorophyll-a concentration of 12 mg m^{-3} was observed in about 6 m depth. The high chlorophyll-a layer is limited to the SLM of 15 m thickness. Curl driven upwelling cannot be assumed as driver for this high productivity. In that case a deep chlorophyll-a maximum (DCM) would be expected. A fast off shore drift of newly upwelled coastal water seems to be the most probably reason for the patches. The extreme chlorophyll-a concentration is also reflected in the absorption at 8 m depth (Fig. 5.1.31). Both chlorophyll peaks at 670 nm and 430 nm were unusual high. In the subsurface layer, almost no chlorophyll absorption was detected. Here the absorption profile followed the exponential shape of CDOM absorption.

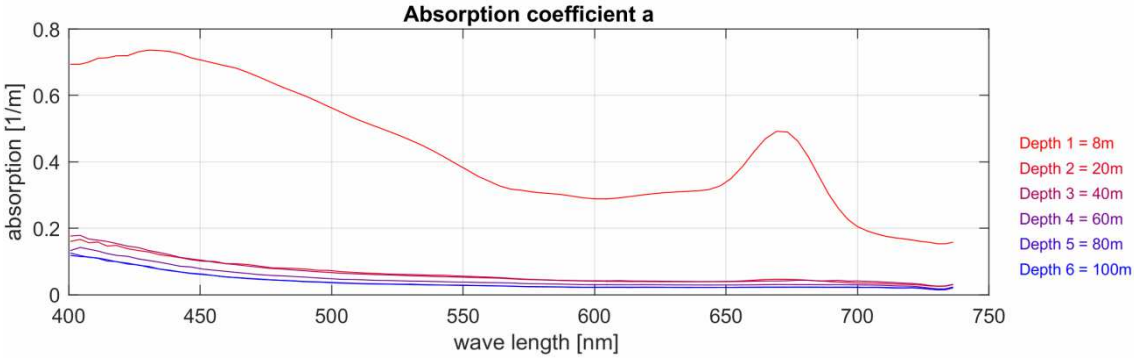

Fig. 5.1.31 Spectral distribution of the absorption coefficient for six different depths on the offshore station MSM80_88 at 15°16'S, 76°15'W. The chlorophyll-a absorption peak at 670 nm was extremely high, as also the chlorophyll absorption at short wave number near 430 nm.

During the repeated profiling with the MSS on several stations the action of internal waves was observed. Internal waves were seen particular near the shelf edge and on the shelf, where they might contribute to turbulent mixing. In order to investigate the mixing processes on the shelf edge in more detail a short cross shelf transect was worked with continuous profiling microstructure probe at 14°51'S. The transect covered the shelf edge between the 400 m and 200 m isobaths.

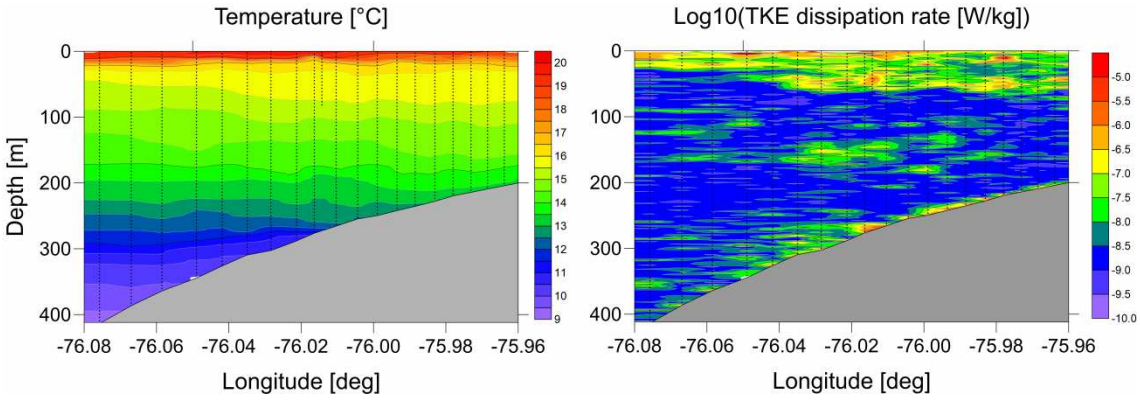

Fig. 5.1.32 Temperature (left) and TKE dissipation rate distribution (right) along the short shelf edge transect at 14.85°S, gathered with the MSS profiler on 15th January 2019.

The temperature distribution showed the very shallow but warm surface mixed layer (SML) with a thickness of about 20 m at the outer shelf edge. The temperature in the SML decreased eastward, as also the vertical temperature gradient between the SML and the sub surface water. Below the SML the vertical temperature gradient was relatively constant, as expected for the central water layer. However, local vertical displacements of the isotherms were observed throughout the water column. They seemed to be enhanced in the section with water depths between 300 to 250 m (Fig. 5.1.32). The dissipation rate of turbulent kinetic energy (TKE) is shown in the right panel of Fig. 5.1.32.

Generally, TKE dissipation was enhanced in the surface and upper layer, and close to the bottom. However, the maximum values of TKE dissipations were confined to the part of transect with water depths between 350 to 250 m. Here the TKE dissipation was high near the bottom and in a pronounced patch in mid water depth. The layer with high TKE dissipation at the surface increased from about 30m thickness to 80m thickness. West of this section the TKE dissipation was close to the noise level below the SML. Also towards the inner shelf the TKE dissipation rate was decreasing. No obvious effects of enhanced mixing were detected in the distribution of dissolved oxygen (Fig. 5.1.33). The well oxygenated surface layer was separated from the OMZ by the depth of the 17°C isotherm. Below this SML oxygen concentration decreased rapidly towards zero. At about 100 m to 120 m depth a layer with slightly enhanced oxygen concentration of up to 8 µmol kg^{-1} was visible. However, there was some indication in the turbidity distribution that the enhanced mixing at the shelf edge causes remobilization of fluffy material near the bottom. This material might be exported into the ocean, forming a nephloide layer at about 300 m depth.

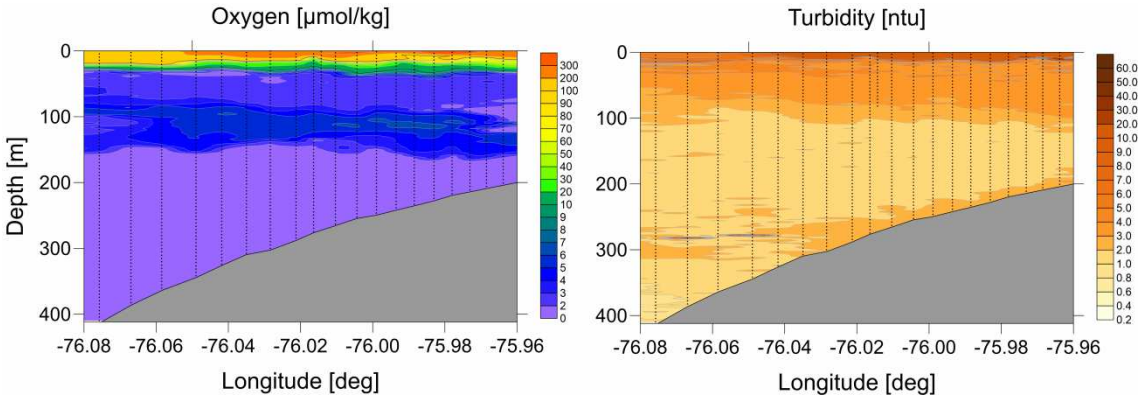

Fig. 5.1.33 Oxygen concentration (left) and turbidity distribution (right) along the short shelf edge transect at 14.85°S, gathered with the MSS profiler on 15th January 2019.

On the southernmost transect at 16°S the final drifter deployment of the cruise was conducted. The drifter was released over deep water at 75°W, west of the shelf edge. The drifter was fast moved offshore with velocities between 0.4 and 0.6 ms^{-1}. During the first part of the deployment a strong current shear was observed at the base of the SML near 15 m.

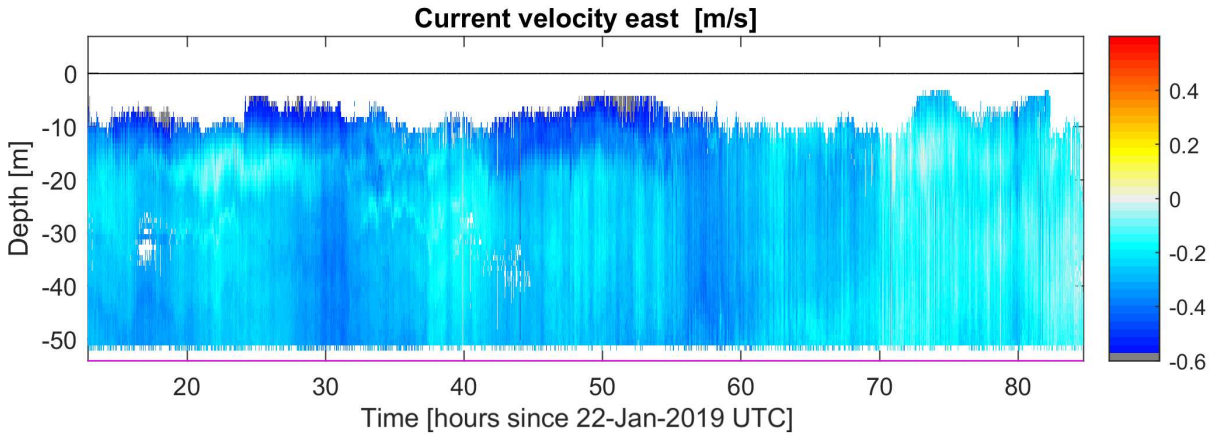

Fig. 5.1.34 Eastward current velocity along the drifter path at 15°S measured with the upward looking ADCP of the drifter.

The acoustic backscatter signal depicted different patterns of diurnal vertical migration (DVM) of zooplankton. During the first night the drifter was in waters with a very shallow upper edge of the OMZ. Thus, the DVM was limited to the upper 30 m of the surface water. Further offshore the usual DVM pattern was found, although the very surface layer depicted a relatively low backscatter signal. That was quite different to deployment two.

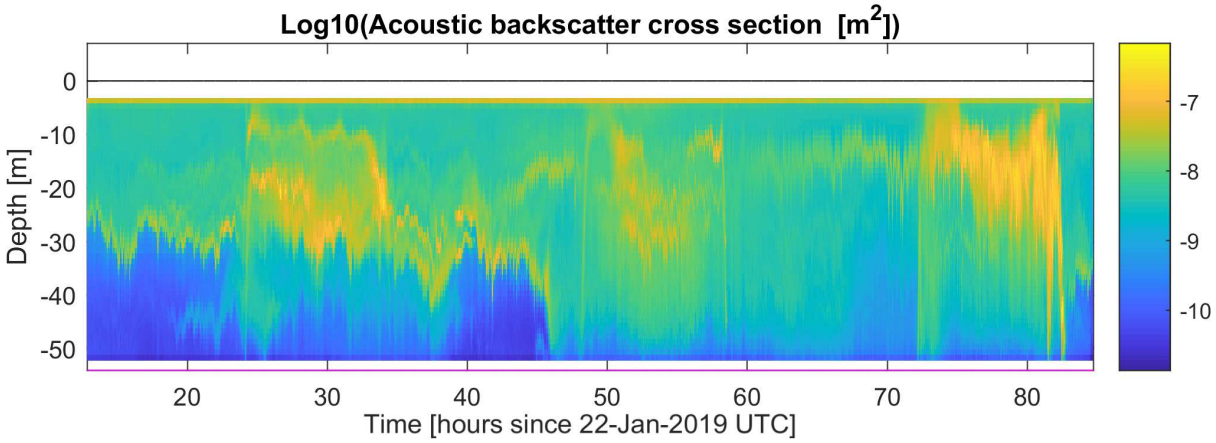

Fig. 5.1.35 Acoustic back scatter cross section along the drifter path at 16°S measured with the upward looking ADCP of the drifter.

Data Management

All data gathered by the hydrography group will be stored on a data repository in the IOW immediately after the cruise. The processed and validated data will be stored in the ODIN data base (https://odin2.io-warnemuende.de). According to the IOW data policy and to facilitate the international exchange of data, all metadata will be made available under the international ISO 19115 standards for georeferenced metadata.

The access to the data itself will be restricted for three years after data acquisition to protect the research process, including scientific analysis and publication. After that period the data becomes openly available to any person or any organization who requests them, under the international Creative Commons (CC) data license of type CC BY 4.0

5.2 Underwater Vision Profiler – In situ particle and zooplankton observations

(R. Kiko[1])
[1]GEOMAR

During all regular CTD casts, an Underwater Vision Profiler 5 HD (UVP5 HD; serial number 210) was operated on the CTD rosette. The instrument consists of one down-facing HD camera in a 6000 dbar pressure-proof case and two red LED lights which illuminate a 1.24 L-water volume. During the downcast, the UVP takes 20 pictures of the illuminated field per second. For each picture, the number and size of particles are counted and stored for later data analysis. Furthermore, images of particles with a size > 500 µm are saved as a separate "Vignettes" - small cut-outs of the original picture – which allow for later, computer-assisted identification of these particles and their grouping into different particle, phyto- and zooplankton classes. Since the UVP was integrated in the CTD rosette and interfaced with the CTD sensors, fine-scale vertical distribution of particles and major planktonic groups can be related to environmental data. In total 72 UVP5 profiles could be obtained. During five additional CTD casts so called yoyo's were performed from 1.5 hours before to 1.5 hours after sunrise. During this time the CTD-Rosette and the contained UVP5 HD were moved up and down continuously to observe changes in particle distribution at 150 to 450 m depth. ADCP-data indicated that Krill moves to about 225 m depth at dawn and the yoyo's were conducted to test the hypothesis that Krill defecates at this depth, which might also result in changes in nutrient concentrations. Accordingly, nutrient samples were taken approximately every hour at 200, 250, 300 and 350 m depth. Further, computer-assisted analysis of the approximately 600000 images taken with the UVP5 during normal and yoyo casts will be done in the home laboratory in order to reveal fine-scale distribution patterns of particles and zooplankton.

5.3 Scaling upwelling intensity with plankton community production, water column biogeochemistry and primary productivity

(M. Fernández-Méndez [1], A. J. Paul[1], L. Kittu[1], J. Ortiz[1], K. Qelaj[1], M. Meyerhöfer[1])
[1]GEOMAR

Objectives

Our aim was to quantify and characterize the phytoplankton community and the biogeochemical properties of the upper water column. We selected stations to cover regions of low, medium and high upwelling intensity from the coast to the mid-shelf and further offshore to determine the functional relationship between upwelling intensity and phytoplankton productivity.

Onboard sampling

Water samples were collected on board from the CTD casts. For the background biogeochemical data, such as inorganic nutrients (nitrate, nitrite, phosphate, silicate and ammonium), the water column down to maximum 100m was sampled at every CTD station. Particulate matter (particulate organic carbon, nitrogen and phosphate, and biogenic silica), dissolved organic

nutrients (dissolved organic nitrogen and phosphate) and phytoplankton community composition (samples for pigment composition, microscopy and flow cytometry) samples were collected at every station during the six onshore-offshore transects covering the upper 300 m.
Samples for phytoplankton pigment concentrations were collected by filtration of seawater through GF/F filters, and stored at -80°C immediately after filtration. These pigments will then be extracted and analysed in Kiel by High Performance Liquid Chromatography (HPLC). Seawater samples (4 mL) were collected for analyses of the phytoplankton and bacteria community and composition by flow cytometry to compliment phytoplankton pigment data, fixed and stored at -80°C. These samples will also be analysed in Kiel.
Carbon and nitrogen fixation rates were measured using stable isotope incubations (13C-DIC and 15N-N2 gas) were taken at 3-5 stations (4 to 6 depths) during each transect to enable the comparison between off-shore and on-shore conditions. Particulate matter samples for elemental and isotopic composition were collected from the CTD directly, as well as at the end of each incubation onto GF75 (0.3 µm pore size) filters. These samples will be analysed an elemental analyser (Flash EA) coupled to an Isotope Ratio Mass Spectrometry (IRMS) and the data will then be used to calculate estimated rates of dinitrogen fixation and inorganic carbon uptake. Additionally, subsamples for 15N-N2 gas isotope analysis were taken at the end of each incubation to determine isotopic enrichment of N2 gas. During the third transect (IMARPE Callao transect, 12°S) additional samples were taken to determine the fraction of nitrogen fixed that ends in the dissolved organic nitrogen pool. Samples for total iron concentrations and the genetic detection of nitrogen fixing organisms present were also collected from the same depths as each incubation directly from the CTD.
In addition, five photosynthesis vs. irradiance assays at six different light intensities were carried out at two on-shore, two off-shore and one high-chlorophyll station. In these assays, 15N-nitrate and 15N-ammonium were added with 13C-DIC to quantify the ratio between new and regenerated productivity. Furthermore, two bioassays were carried out over 4-5 days at one off-shore and one on-shore station to determine potential contrasting responses of phytoplankton communities to the addition of nutrient-rich deep water (150-300 m) and iron.

Expected results

On board measurements of inorganic nutrients using a QuAAttro autoanalyser (SEAL) show typical profiles with higher nutrient concentrations at the surface (upper 50 m) close to the coast where water masses are upwelled, and lower nutrient concentrations offshore due to consumption by primary producers (See Transects 1 to 6 in plots below, Figs. 5.3.1-5.3.6). However, at the southernmost transects (14.5°S and 16°S) nutrients were depleted both on-shore and off-shore but only at the very surface (upper 20 m). Nitrite concentrations were elevated at depths (up to 8 µM) within the subsurface oxygen depleted waters. At some stations, surface dissolved silicate concentrations were <2 µM indicating potential silicate limitation for diatoms. Preliminary data indicate highest dissolved organic phosphorus and nitrogen concentrations in the upper 40 m of the water column, where inorganic nutrient concentrations were lowest.
In the first bioassay off-shore, nutrients were depleted after four days incubation in all treatments apart from the deep water additions. This probably indicates that the phytoplankton biomass was diluted too much by the deep water addition to fully utilize the additional nutrients available. All

nutrients were depleted during the on-shore bioassay in all treatments suggesting a contrasting response between plankton communities to upwelled water.

Chlorophyll a fluorescence (CTD sensor) was very variable throughout the cruise and reached the highest values at the off-shore stations during Transect 5 at the surface and Transect 6 in a thin layer just below the surface mixed layer. Interestingly, these stations coincided with red-brown colored surface waters. On board microscopy analyses revealed high abundances of large dinoflagellates, which are commonly associated with red tides. This contrasted with the more diatom-dominated communities in the transects further north.

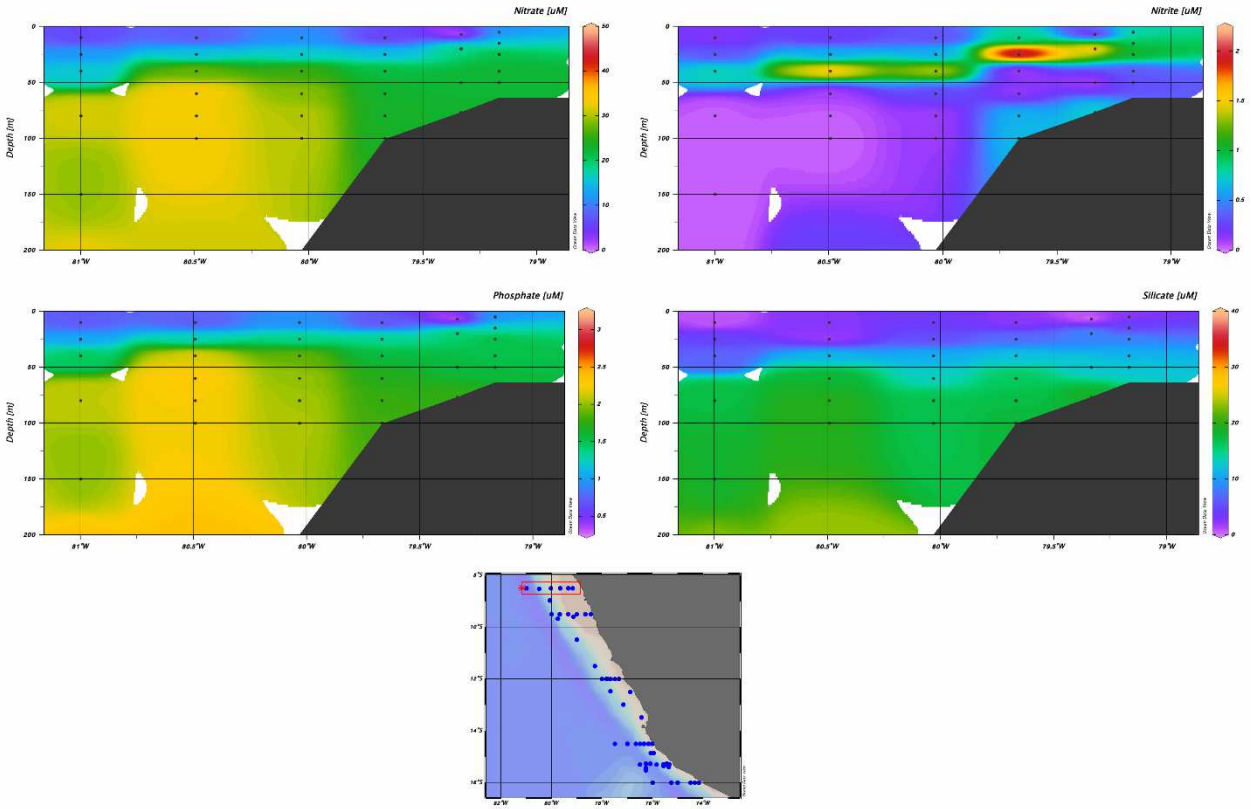

Fig. 5.3.1 Nutrient distribution for transect 1 at 8.5 °S.

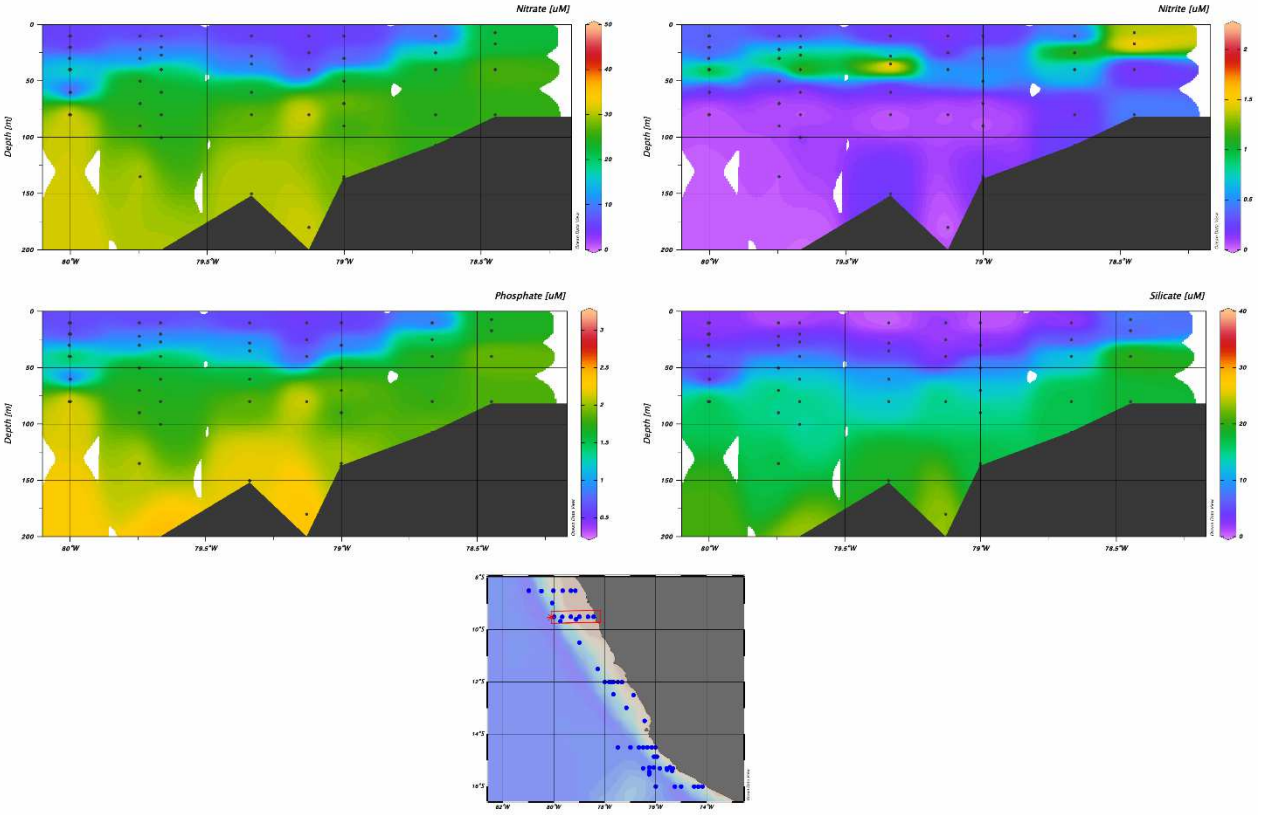

Fig. 5.3.2 Nutrient distribution for transect 2 at 9.5 °S.

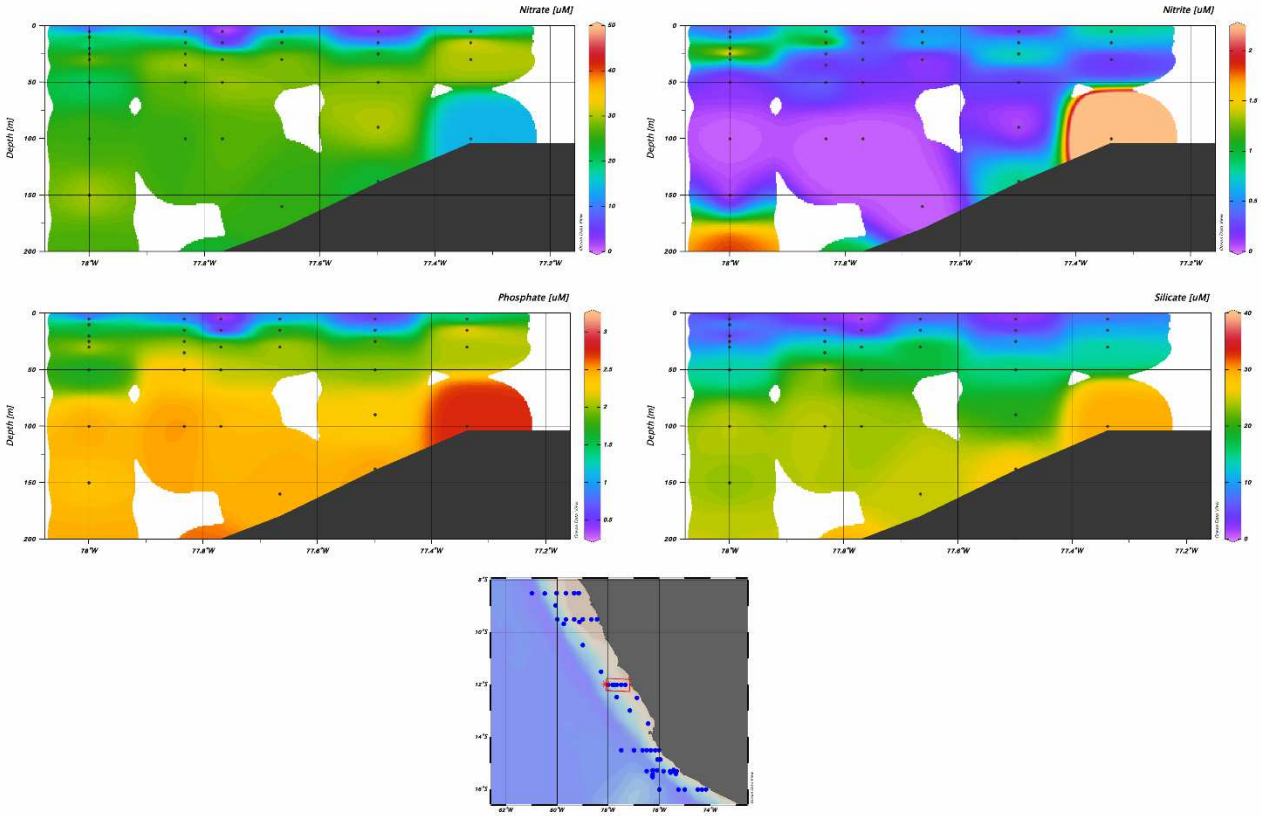

Fig. 5.3.3 Nutrient distribution for transect 3 at 12°S.

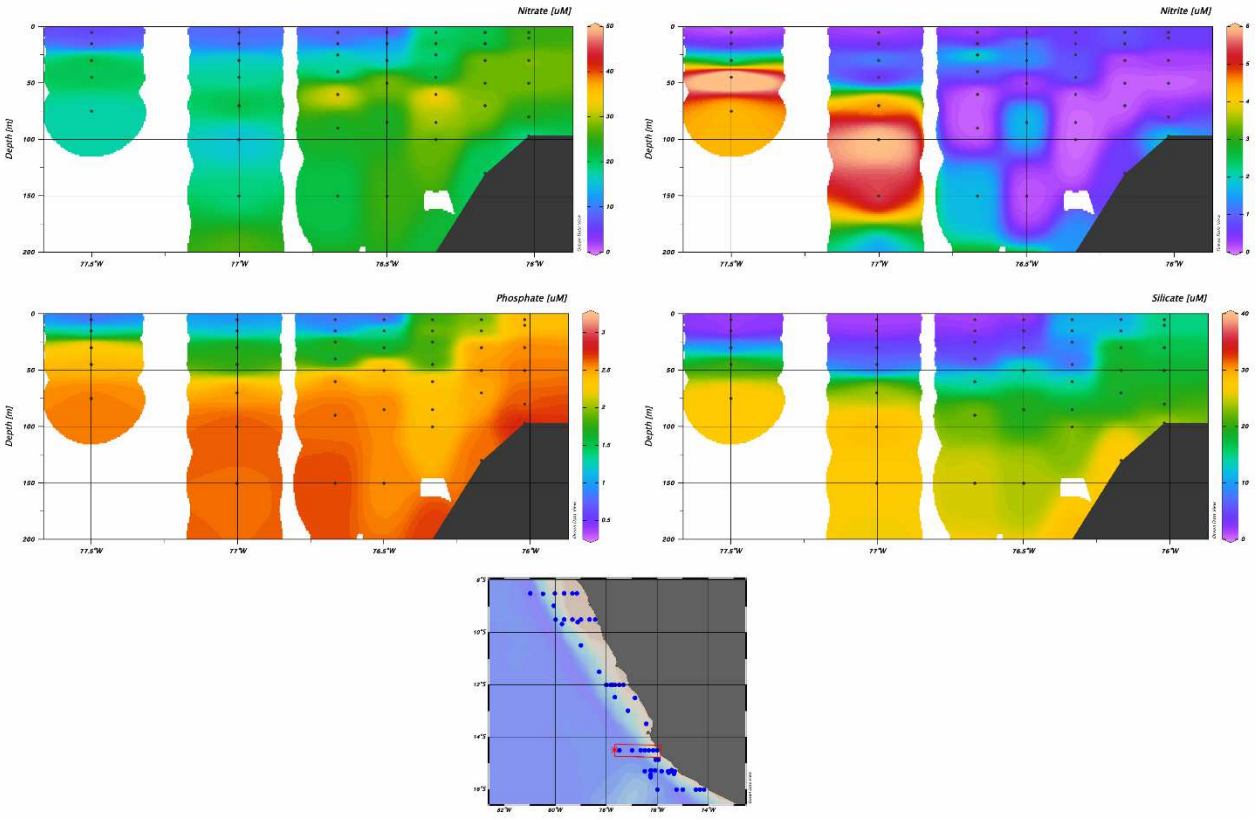

Fig. 5.3.4 Nutrient distribution for transect 4 at 14.5°S.

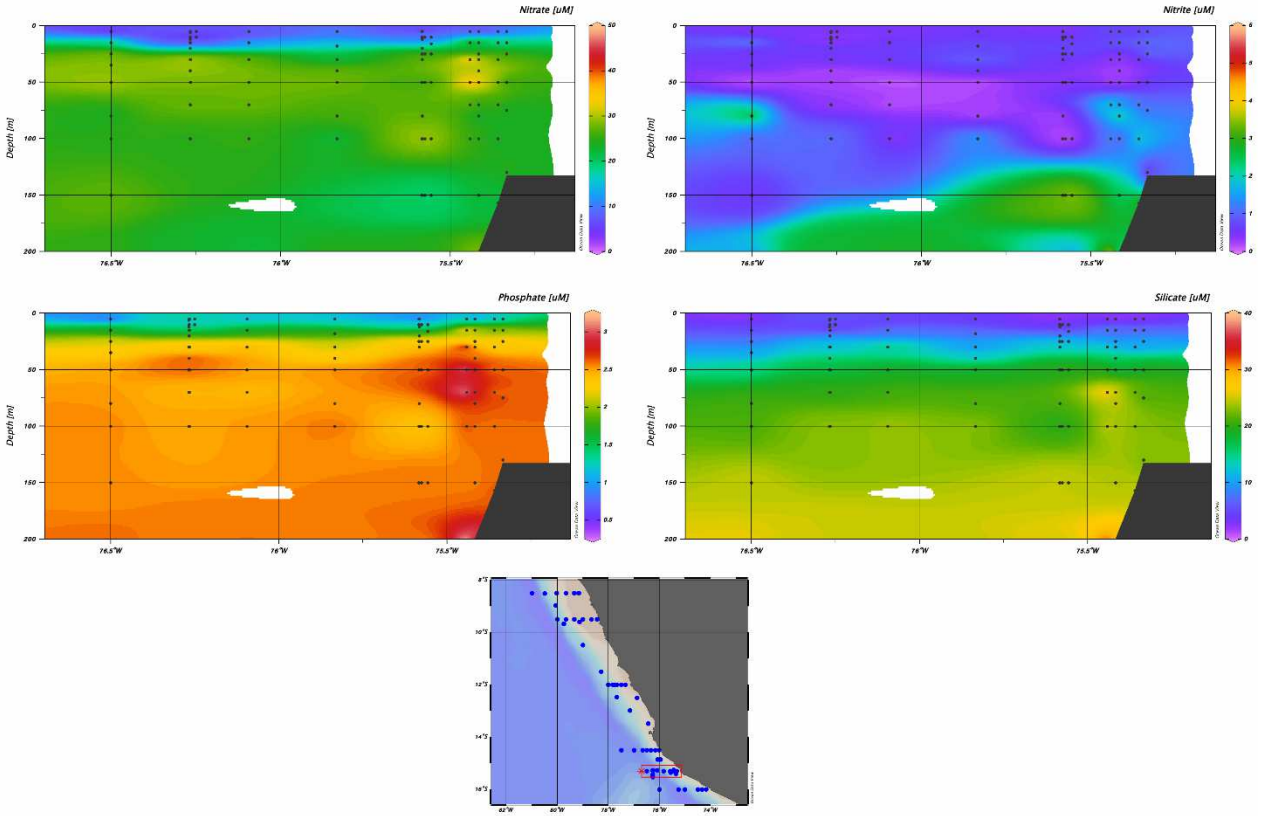

Fig. 5.3.5 Nutrient distribution for transect 5 at 15.3°S.

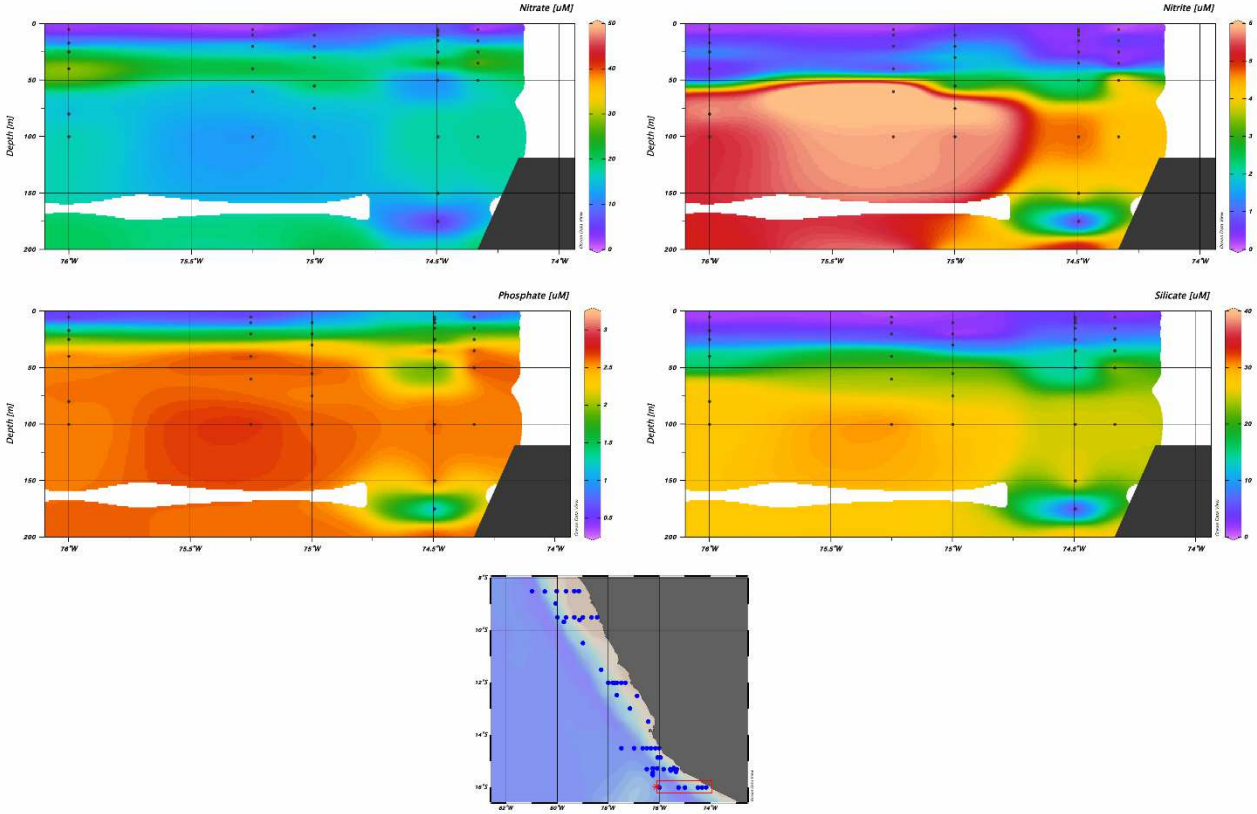

Fig. 5.3.6 Nutrient distribution for transect 6 at 16°S.

Data Repository

All datasets produced during this expedition will be made available for all CUSCO project partners in a preliminary format with the help of the Kiel Data Management Team (KDMT) in the Ocean Science Information System (OSIS-Kiel). Subsequently, the final datasets will be given a Digital Object Identifier (DOI) so that it can be identified and cited globally. These datasets will also be archived in PANGAEA and linked to the corresponding publications.

5.4 Zooplankton Ecology: Structure of the pelagic food web, trophic interactions and the role of meso- and macrozooplankton for trophic transfer efficiency in the Peruvian upwelling system

(A. Schukat[1], J. Massing[1], W. Hagen[1], H. Auel[1], E. L. Pinedo Arteaga[2])

[1]Uni HB - BreMarE

[2]IMARPE

Objectives

The major aim of this cruise was to establish, which processes and mechanisms determine the trophic transfer efficiency (TTE) of the Humboldt Upwelling System (HUS) off Peru. The Humboldt Current in the Southeast Pacific is the most productive and commercially most important upwelling system worldwide. Although the four major coastal upwelling systems have a similar primary production, the HUS provides five to ten times higher fisheries yields per unit

area than other systems. In order to elucidate the high productivity at the upper trophic levels, the BreMarE team of the University of Bremen investigates the role of meso- and macrozooplankton (especially copepods and euphausiids) in the food web. We aim at identifying and quantifying important predator-prey relationships of zooplankton taxa (e.g., as consumers of phytoplankton or prey for pelagic fish) and analyse the general structure and complexity of the pelagic food web, which greatly influences the TTE. The specific objectives of this cruise are to identify regional differences in abundance, biomass, diversity and species composition of meso- and macrozooplankton in relation to upwelling intensity and other hydrographic features. We focus on structural differences in the zooplankton community and on the length of the food chain by analysing trophic interactions and tracing carbon and energy fluxes through the marine food web, using fatty acid trophic markers and stable isotopes. These processes impact the TTE and the corresponding data will contribute to our understanding of the high productivity in terms of fisheries yields in the HUS.

Work at Sea

For the investigation of the zooplankton community, mesozooplankton was collected by stratified vertical hauls with a MULTINET MIDI (mouth opening 0.25 m^2, mesh size 200 µm, five nets). Larger crustaceans (e.g., euphausiids and decapods) were mainly collected with the MOCNESS (mouth opening 1 m^2, mesh size 330 µm, 18 nets) operated by the team of the University of Hamburg. In total, 57 stations were sampled with the MULTINET MIDI and 11 with the MOCNESS. Net samples were analysed under a dissecting microscope and live specimens of various species were sorted on board for different experiments (respiration, excretion and egg production rates) and deep-frozen at -80°C (lipids and fatty acids) or dried at 60°C (stable isotopes) for further biomarker analyses in the home labs. The remains of the net samples were preserved in a 4% formaldehyde in seawater solution for later analyses of meso- and macrozooplankton species composition, abundance, biomass and vertical distribution.

For the quantitative assessment of energy budgets of dominant zooplankton species, respiration and excretion rates were determined on board. Respiration rates of different copepod species were measured by optode respirometry with a 10-channel optode respirometer (PreSens Precision Sensing Oxy-10 Mini, Regensburg, Germany) in a temperature-controlled refrigerator. At each station, temperature profiles derived from the CTD probe were used to adjust the refrigator to the ambient temperature at sampling depth. Experiments were run in gas-tight glass bottles (~11 ml) filled with filtered seawater to avoid bias by microbial respiration. For each set of experiments, two animal-free controls were measured under exactly the same conditions to compensate for potential errors. In total, 12 respiration runs were conducted with eight calanoid copepod species, which sum up to more than 85 individual respiration measurements. After the experiments, all specimens were deep-frozen at -80°C for later dry mass determination in the home lab. Additionally, respiration rates of the most common decapod species, Pleuroncodes monodon, and the euphausiid Euphausia mucronata were determined by Winkler titration in a temperature-controlled room at 12°C. Single specimens of P. monodon and E. mucronata were incubated in 500-1000 ml gas-tight bottles for 4-6 h and 8-12 h, respectively. For each set of experiments, again two animal-free controls were measured to compensate for potential errors.

Ammonia excretion rates of copepods and euphausiids were measured by incubating the animals for several hours (6-19 h) in 50 ml (copepods) and 100 ml (euphausiids) vials. Excretion rates

were determined for the prevailing copepod and krill species, *Calanus chilensis* and *Euphausia mucronata*. Three specimens of *C. chilensis* were incubated per vial and 1 specimen of *E. mucronata*. After the incubation, animals were removed from the vial and 10 ml of the water sample was fixed with 1 ml of the work reagent containing 4% o-phthaldialdehyde/ethanol, 4% sodium borate-10-hydrate and 0.8% sodium sulfite. After fixation, samples were kept in the dark for at least 12 h before measuring ammonia concentrations with a Turner Triology, which was done by Rainer Kiko from GEOMAR/University of Kiel. For each set of incubations, a seawater and a MilliQ sample was measured as control to calculate the correct ammonia concentration of the sample. A standard stock solution was used for calibration. The removed animals were deep-frozen at -80°C. In total, 17 individual excretion measurements were performed for *C. chilensis* and 12 for *E. mucronata*.

Daily egg production rates of *C. chilensis* were measured using bottle incubation techniques, simulating ambient surface conditions of food and temperature. Single female *C. chilensis* from surface samples of the MULTINET MIDI were incubated in sealed bottles (500 ml) containing 56 µm filtered surface water and maintained at a temperature of 19°C in a temperature-controlled refrigerator. Usually, six replicate experiments were run per transect and terminated after 24 h. Eggs were then counted under a dissecting microscope and the daily egg production rate was calculated. Overall, eight replicate experiments were conducted, which sum up to 44 individual egg production measurements.

Preliminary Results

Distribution of Meso- and Macrozooplankton

Preliminary results of this cruise can only be given of the general distribution of zooplankton, especially copepods and euphausiids. Detailed analyses of the preserved samples will be done after the cruise in the home laboratories, together with dry mass determination and trophic biomarker analyses.

The coastal mesozooplankton community was dominated by small cyclopoid copepods (*Oithona* and *Oncaea*) and small calanoid copepods such as *Acartia* spp., *Paracalanus* spp. and *Centropages* spp. The bigger calanoid copepods, *Calanus chilensis* and *Eucalanus inermis*, were abundant further offshore. *C. chilensis* occurred especially in surface waters from 50 to 0 m depth, whereas Eucalanus inermis inhabited mostly low oxygen water layers between 500 and 200 m. In contrast to its congeners in other upwelling or polar regions, *C. chilensis* does not undergo diapause as copepodid 5 below 500 m, as *C. chilensis* was never found at depth below 100 m during this cruise! *C. chilensis* may follow a different life strategy and stay active year-round in surface layers.

Contrasting with the general coastal and offshore distribution pattern, *Centropages* spp. was the most abundant species at the offshore station 74 with a bottom depth of ca. 3800 m. At least three different species of *Centropages* (*C. brachiatus, chierchiae* and *gracilis*) occurred in high numbers at that station. The occurrence of these coastal species far offshore indicates that we sampled an upwelling filament or an eddy that transported coastal water masses with its plankton community offshore.

Gelatinous zooplankton, e.g. salps, was occasionally very abundant in the upper 50 m. Euphausiids were dominant at the shelf break stations and regularly showed a pronounced diel vertical migration pattern. During daytime, they inhabited water layers within the oxygen

minimum (virtually anoxic) zone between 500 and 200 m, and at night they migrated to the surface (50-0 m). The dominant krill species was *Euphausia mucronata*, which accounted for the majority of the migrating biomass. Other less abundant krill species were *Euphausia eximia*, *E. distinguenda* and *Nematocelis* sp. A major fraction of the migrating biomass was also attributed to the decapod species *Pleuroncodes monodon*. This semi-pelagic anomuran crab showed a migration pattern similar to that of *E. mucronata* and was found in high numbers at almost every transect, at the coast but also further offshore. Compared to other upwelling regions, copepods exhibiting diel vertical migration were not found in high numbers, except for a few specimens at the northernmost transect. This may be due to the pronounced oxygen minimum zone in the HUS with oxygen levels below 1 µmol l^{-1}, which generally extended from 500 to 200 m.

Data Management

All acquired data from this cruise MSM80 will be stored digitally in different archives at GEOMAR by the 'Kieler Data Management Team' (KDMT), which also takes care of long-term archiving of all these data. After publication in scientific journals, data will be made accessible for the scientific community by publishing the data in the open access data base 'PANGAEA'.

5.5 Gelatinous plankton and fish larvae communities and their trophic structure within a foodweb characterized by high trophic transfer efficiency

(B. Martin[1], S. Janßen[1], S. Kurbjuweit[1], A. Welker[1], D. Auch[1], J. A. Correa Acosta[2])

[1]Uni HH - IMF

[2]IMARPE

Objectives

Eastern boundary upwelling systems (EBUS) are among the most productive marine areas worldwide. The Humboldt Current however, provides the tenfold fisheries catches in comparison to the other EBUS, albeit they share similar quantities of phytoplankton production. The CUSCO project aims at improving knowledge on trophic transfer processes under various upwelling conditions within the Peruvian Humbuldt Upwelling system (HUS). Goal of this cruise is to assess abundance, biomass, diversity and species composition of meso- and macrozooplankton in relation to upwelling intensity and other hydrographic features. The University of Hamburg focuses on the role of fish larvae, gelatinous and semi-gelatinous plankton in the HUS food web. Variability in productivity of fish stocks is largely coherent with fluctuations in larval mortality as early life stages are particularly vulnerable and exhibit high mortality rates. Therefore, we aim at improving knowledge on how anchovy larvae conditions change with varying hydrographic conditions (such as upwelling intensity) and subsequent food web alterations. The second focus lies on the (semi-) gelatinous plankton which includes several non-crustacean components of zooplankton (Cnidaria, Ctenophora, Chaetognatha, Mollusca, Thaliacea and Appendicularia). SGP species have raised attention during the last decades of marine science since several species such as salps, cnidarians and ctenophores can form massive blooms under appropriate environmental conditions. Accordingly, they can severely affect the fish production of an ecosystem through direct predation on larvae (especially larger scyphozoans) and competition for food. Furthermore, SGP species, often considered as trophic dead ends, affect bottom-up

processes and export fluxes of organic matter. We will thus focus on trophic positions and interactions of SGP species in the HUS. Analyses of SGP and fish larvae will include biomass and abundance determinations, stable isotope and fatty acid analyses and for fish larvae RNA:DNA and Otoliths will be analysed.

Work at Sea

A Multiple Closing Net (MCN) 'Multinet Midi', equipped with five nets of different mesh sizes, was towed at 2 kn and hoistered at 0.2 ms^{-1}, down to 100 m. On the downcast two 1000 µm nets were closed (below the thermocline and at 100 m depth), whereas the remaining three nets with a mesh size of 300 µm, hieved at 0.2 ms^{-1}, were used to sample below, inside and above the thermocline. At most stations the MCN was carried out twice, one haul for studies of biomass and zooplankton composition, the samples fixed in 4 % formalin seawater solution, and the second one for taxonomic analysis and the subsequent trophic analyses. The sorted samples were either dried at 60°C or deep frozen at -80°C for biochemical analyses in the home lab (stable isotopes and fatty acids) or preserved in Ethanol (gut content and otolith analysis). In total, 78 of such oblique hauls were conducted during the cruise.

At each transect at one offshore station with water depth >1000 m a haul with a 1 m² Double-MOCNESS (Multiple Openining and Closing Net and Environmental Sensing System) was conducted to sample the mesozooplankton of different depth strata. The MOCNESS is equipped with 2 x 9 nets, mesh size 330 µm, as well as with depth, temperature and salinity sensors. The nets can be closed from the deck unit in the laboratory. The angle of the net-frame is registered and together with data from a flow-meter, the sampled water volume of each net can be calculated. Left and right sides of the nets were closed simultaneously at 1000 m, 800 m, 600 m, 400 m, 200 m, 100 m and before and after the thermocline. After recovery of the gear, one side of the nets were fixed in 4% formaline in seawater solution, the other nets were sorted and preserved for later analysis in the same way as the second MCN. At the two 24 hour stations MOCNESS hauls were conducted at day and nighttime down to 1000 m as well as at dusk horizontally in 180 m and 60 m, respectively, to study the diel vertical migration of the mesozooplankton in the Humboldt Upwelling System (HUS). An additional horizontal haul was carried out for 5 hours in a region of steep gradients from low chlorophyll to high chlorophyll level in a manner that each net was towed for 17 minutes from 0-120-0 m. See figure x for the positioning of the MOCNESS hauls.

The IKMT (Isaacs Kidd Midwater Trawl) was carried out at 26 stations during cruise MSM80. The net has a mouth opening of 10 m² and a mesh size of 4 mm in the cod end. This gear was chosen especially for catching gelatinous organisms as well as fish larvae. It was towed at 1,5 to 2 kn. At deep stations (500-1000 m catch depth) it was hoistered and hieved with 0.5 ms^{-1}, at shallower stations with 0.2 ms^{-1} to elongate the sampling time.

After recovery of the gear the fish larvae and gelatinous organisms were determined, sorted out and frozen or dried, the remaining samples were fixed in 4 % formalin for further studies in the home lab.

Microzooplankton was sampled at five stations at the 12° S transect with 2 Apstein nets, mesh size 55 and 100 µm, repectively, down to 17 m (Fig. X). These samples were fixed in 4 % formalin sewater solution for later comparison with samples with the same gear, mesh sizes and depth in the planned mesocosms at 12° S off Calao.

Preliminary results

The preliminary results will give a short introduction into fundamental findings. A more detailed taxonomic description of the gelatinous and semi-gelatinous plankton as well as fish larvae community including biomass and abundance data as well as the biochemical analyses of trophic markers remains to be continued in the laboratory back home.

In general, the main Anchovy (*Engraulis ringens*) spawning ground is supposed to be located at around 8°S in rather coastal waters. Anchovy larvae are known to dwell in cold upwelled water. Due to the prevailing low upwelling intensities and subsequently high water temperatures, especially in the North, we found relatively few anchovy larvae in this region. Fish larvae composition was, especially further offshore, dominated by *Diogenichthys laternatus* and *Vinciguerria lucetia*, both mesopelagic species. We found a higher anchovy larvae abundance in the southern part of the Peruvian shelf region, where upwelling intensities were a little higher in comparison to the North.

The gelatinous and semi-gelatinous plankton community along the Peruvian shelf was basically dominated by Thaliacea (such as *Weelia cylindrica* and *Soestia zonaria*) and siphonophores (such as *Bassia bassensis* and *Agalma* sp.). Scyphozoans and hydrozoans were found in relatively low numbers. Especially *Chrysaora plocamia*, known for its large blooms on the Peruvian shelf, was entirely lacking in the net catches. Larger quantities of *Aequorea* sp. were restricted to few stations in the northern HUS area. In general, the SGP occurrence was characterized by a high patchiness. In the North (9°S) *Pyrosoma* sp. was the most abundant taxon forming blooms of small individuals. Moreover, we found a relatively high diversity of species within this warm water region. Further south the occurrence of blooms of particular SGP species increased. At 13°S we encountered a mass occurrence of the scyphozoan *Pelagia noctiluca*. Even further south the salp *Weelia cylindrica* was highly abundant in shallow depths (above the thermocline) and large numbers of the siphonophore *Bassia bassensis* were found. One striking feature of the distribution pattern was the lack of SGP species in newly upwelled water which can be explained by the not yet evolved phytoplankton production.

Data managment

Gelatinous and semi-gelatinous animals as well as fish larvae will be stored at the Institute of Marine Ecosystem and Fishery Science of the University of Hamburg for further processing (biomass and taxonomical analyses as well as biochemical indicators like stable isotopes and fatty acids). After finishing the processing of the samples, all remaining and intact biological material will be offered to the appropriate scientific collections and museums, as indicated in the directives of the DFG. The collected data will be stored according to the guidelines of CUSCO.

7 Station List MSM80

7.1 Overall Station List

CTD: Sensor for conductivity, temperature and depth in combination with rosette water sampler and UVP underwater vision profiler; ACS: Optical profiler AC-S; MSS: Microstructure profiler; MSN: Hydro-Bios MultiNet Midi multiple opening and closing net; NET-IKMT: Isaacs Kidd Midwater Trawl; MOCNESS: double 1 m^2 Multiple Opening/Closing Net & Environmental Sensing System; SCF: ScanFish towed undulating CTD; DRIFT: Surface drifter

Station No.	Date Time [UTC]	Gear	Latitude [°S]	Longitude [°W]	Water Depth [m]	Remarks
MSM80_1-1	27.12.2018 19:19	CTD	08° 29.975' S	080° 59.999' W	6233.3	
MSM80_1-2	27.12.2018 20:06	ACS	08° 29.972' S	080° 59.990' W	6242.8	
MSM80_1-3	27.12.2018 20:50	MSS	08° 30.176' S	080° 59.859' W	6231.1	
MSM80_1-4	27.12.2018 22:13	ACS	08° 30.681' S	080° 59.704' W	6255.6	
MSM80_1-5	27.12.2018 22:42	MSN	08° 30.650' S	080° 59.609' W	6270.5	
MSM80_1-6	27.12.2018 23:39	MSN	08° 30.471' S	080° 59.266' W	6303.2	
MSM80_1-7	28.12.2018 00:43	MSN	08° 30.189' S	080° 58.526' W	6296.9	
MSM80_1-8	28.12.2018 01:17	MSN	08° 30.116' S	080° 57.827' W	6092.4	
MSM80_1-9	28.12.2018 02:38	NET-IKMT	08° 31.429' S	080° 56.341' W	5820.2	
MSM80_1-10	28.12.2018 05:28	MOCNESS	08° 35.337' S	080° 55.310' W	6077.0	
MSM80_2-1	28.12.2018 07:49	MSS	08° 29.965' S	080° 49.901' W	4327.6	
MSM80_3-1	28.12.2018 10:04	MSS	08° 29.883' S	080° 40.013' W	2770.9	
MSM80_4-1	28.12.2018 12:47	CTD	08° 29.989' S	080° 29.999' W	1326.0	
MSM80_4-2	28.12.2018 13:32	ACS	08° 29.989' S	080° 29.999' W	1325.6	
MSM80_4-3	28.12.2018 13:43	MSS	08° 30.016' S	080° 29.979' W	1329.8	
MSM80_4-4	28.12.2018 14:10	MSS	08° 30.358' S	080° 29.774' W	1330.0	
MSM80_4-5	28.12.2018 14:34	MSS	08° 30.739' S	080° 29.687' W	1328.8	
MSM80_4-6	28.12.2018 15:41	MSN	08° 31.038' S	080° 29.504' W	1342.3	
MSM80_4-7	28.12.2018 16:40	MSN	08° 31.179' S	080° 28.888' W	1304.3	
MSM80_5-1	28.12.2018 17:55	MSS	08° 29.989' S	080° 20.008' W	1138.5	
MSM80_6-1	28.12.2018 20:06	MSS	08° 30.003' S	080° 09.999' W	776.2	
MSM80_7-1	28.12.2018 22:15	CTD	08° 29.948' S	080° 01.863' W	357.1	
MSM80_7-2	28.12.2018 22:47	ACS	08° 29.947' S	080° 01.862' W	356.8	
MSM80_7-3	28.12.2018 22:57	MSS	08° 29.966' S	080° 01.860' W	357.7	
MSM80_7-4	28.12.2018 23:13	MSN	08° 29.984' S	080° 01.853' W	357.6	
MSM80_7-5	28.12.2018 23:55	MSN	08° 30.185' S	080° 01.553' W	347.0	
MSM80_7-6	29.12.2018 00:30	MSN	08° 30.627' S	080° 00.819' W	321.2	
MSM80_7-7	29.12.2018 00:46	MSS	08° 30.765' S	080° 00.567' W	312.4	
MSM80_7-8	29.12.2018 02:29	NET-IKMT	08° 33.077' S	079° 59.905' W	317.2	
MSM80_8-1	29.12.2018 03:53	MSS	08° 30.072' S	079° 52.973' W	202.8	
MSM80_9-1	29.12.2018 05:35	MSS	08° 30.011' S	079° 46.019' W	143.4	
MSM80_10-1	29.12.2018 07:20	CTD	08° 29.993' S	079° 40.034' W	102.2	
MSM80_10-2	29.12.2018 07:47	ACS	08° 29.992' S	079° 40.033' W	101.1	
MSM80_10-3	29.12.2018 07:58	MSS	08° 30.005' S	079° 40.009' W	100.4	
MSM80_10-4	29.12.2018 09:14	MSN	08° 30.530' S	079° 39.755' W	100.3	
MSM80_10-5	29.12.2018 09:32	MSN	08° 30.712' S	079° 39.536' W	98.8	
MSM80_10-6	29.12.2018 10:06	MSN	08° 31.051' S	079° 39.089' W	99.3	
MSM80_11-1	29.12.2018 10:58	MSS	08° 29.961' S	079° 33.044' W	89.8	
MSM80_12-1	29.12.2018 12:47	MSS	08° 29.875' S	079° 26.055' W	85.5	
MSM80_13-1	29.12.2018 14:51	CTD	08° 30.002' S	079° 20.106' W	77.0	
MSM80_13-2	29.12.2018 15:11	ACS	08° 30.002' S	079° 20.105' W	77.2	
MSM80_13-3	29.12.2018 15:18	MSS	08° 30.023' S	079° 20.117' W	76.9	
MSM80_13-4	29.12.2018 16:28	MSN	08° 32.191' S	079° 20.283' W	79.0	

MSM80_13-5	29.12.2018 16:44	MSN	08° 32.214' S	079° 20.202' W	80.8	
MSM80_13-6	29.12.2018 17:00	MSN	08° 31.878' S	079° 20.106' W	78.9	
MSM80_13-7	29.12.2018 17:30	NET-IKMT	08° 32.134' S	079° 19.922' W	79.1	
MSM80_14-1	29.12.2018 18:54	CTD	08° 29.980' S	079° 10.021' W	66.6	
MSM80_14-2	29.12.2018 19:14	ACS	08° 29.981' S	079° 10.021' W	65.3	
MSM80_14-3	29.12.2018 19:21	MSS	08° 29.989' S	079° 10.019' W	64.9	
MSM80_14-4	29.12.2018 20:29	MSN	08° 30.583' S	079° 09.818' W	63.9	
MSM80_14-5	29.12.2018 20:47	MSN	08° 30.642' S	079° 09.617' W		
MSM80_14-6	29.12.2018 21:12	MSN	08° 30.710' S	079° 09.316' W	64.2	
MSM80_14-7	29.12.2018 22:33	SCF	08° 30.030' S	079° 10.066' W	65.0	Start of Profile
MSM80_14-7	30.12.2018 17:03	SCF	08° 29.952' S	081° 02.517' W	5972.2	End of Profile
MSM80_15-1	30.12.2018 23:46	CTD	08° 58.148' S	080° 04.053' W	1030.8	
MSM80_15-2	31.12.2018 00:14	ACS	08° 58.147' S	080° 04.052' W	1030.7	
MSM80_15-3	31.12.2018 00:54	CTD	08° 58.148' S	080° 04.053' W	1030.9	
MSM80_15-4	31.12.2018 01:32	MSS	08° 58.218' S	080° 04.026' W	1027.5	
MSM80_15-5	31.12.2018 03:36	MSN	09° 00.397' S	080° 03.270' W	1016.3	
MSM80_15-6	31.12.2018 04:30	MSN	09° 00.489' S	080° 02.966' W	977.8	
MSM80_15-7	31.12.2018 05:00	MSN	09° 00.451' S	080° 02.197' W		
MSM80_15-8	31.12.2018 06:12	NET-IKMT	09° 01.750' S	080° 00.768' W	799.2	
MSM80_16-1	31.12.2018 13:34	CTD	09° 29.968' S	079° 00.062' W	136.3	
MSM80_16-2	31.12.2018 14:03	ACS	09° 29.967' S	079° 00.062' W	136.0	
MSM80_16-3	31.12.2018 14:14	MSS	09° 30.052' S	079° 00.023' W	135.9	
MSM80_16-4	31.12.2018 15:33	MSN	09° 30.898' S	078° 59.460' W	135.5	
MSM80_16-5	31.12.2018 16:11	DRIFT	09° 30.454' S	078° 59.295' W	134.9	Deployment
MSM80_16-5	03.01.2019 17:34	DRIFT	09° 40.048' S	079° 44.784' W	1199.6	Recovery
MSM80_17-1	31.12.2018 19:38	SCF	09° 30.029' S	078° 27.404' W	82.1	Start of Profile
MSM80_17-1	01.01.2019 11:50	SCF	09° 29.999' S	080° 05.839' W	2994.8	End of Profile
MSM80_18-1	01.01.2019 13:30	CTD	09° 29.990' S	080° 00.018' W	2424.1	
MSM80_18-2	01.01.2019 14:15	ACS	09° 29.991' S	080° 00.018' W	2424.7	
MSM80_18-3	01.01.2019 14:27	MSS	09° 30.043' S	080° 00.020' W	2409.3	
MSM80_18-4	01.01.2019 15:58	MSN	09° 30.808' S	080° 00.022' W	2406.4	
MSM80_18-5	01.01.2019 17:12	MSN	09° 30.808' S	080° 00.022' W	2407.0	
MSM80_18-6	01.01.2019 18:11	MSN	09° 30.884' S	079° 59.703' W	2575.3	
MSM80_18-7	01.01.2019 19:44	NET-IKMT	09° 33.329' S	079° 58.444' W	2209.8	
MSM80_19-1	01.01.2019 23:16	MSS	09° 30.024' S	079° 50.068' W	1454.2	
MSM80_20-1	02.01.2019 02:04	CTD	09° 29.993' S	079° 40.097' W	891.6	
MSM80_20-2	02.01.2019 02:48	ACS	09° 29.993' S	079° 40.096' W	892.1	
MSM80_20-3	02.01.2019 02:57	MSS	09° 30.042' S	079° 40.076' W	889.4	
MSM80_20-4	02.01.2019 04:45	MSN	09° 31.490' S	079° 39.741' W	835.2	
MSM80_20-5	02.01.2019 05:29	MSN	09° 31.555' S	079° 39.549' W	2781.7	
MSM80_20-6	02.01.2019 06:00	MSN	09° 31.770' S	079° 38.934' W	2338.0	
MSM80_20-7	02.01.2019 07:08	NET-IKMT	09° 33.144' S	079° 37.879' W	611.4	
MSM80_21-1	02.01.2019 09:01	MSS	09° 30.031' S	079° 30.065' W	302.5	
MSM80_22-1	02.01.2019 11:14	CTD	09° 29.993' S	079° 20.036' W	151.8	
MSM80_22-2	02.01.2019 11:43	ACS	09° 29.994' S	079° 20.034' W	152.3	
MSM80_22-3	02.01.2019 11:53	MSS	09° 30.025' S	079° 20.014' W	151.7	
MSM80_22-4	02.01.2019 13:07	MSN	09° 31.066' S	079° 19.264' W	151.9	
MSM80_22-5	02.01.2019 13:29	MSN	09° 31.097' S	079° 19.083' W	155.1	
MSM80_23-1	02.01.2019 14:33	MSS	09° 30.042' S	079° 13.069' W	153.9	
MSM80_24-1	02.01.2019 16:27	MSS	09° 30.031' S	079° 06.023' W	141.1	
MSM80_25-1	02.01.2019 18:24	CTD	09° 29.968' S	079° 00.069' W	137.5	
MSM80_25-2	02.01.2019 18:50	ACS	09° 29.968' S	079° 00.070' W	136.9	
MSM80_25-3	02.01.2019 18:58	MSS	09° 29.984' S	079° 00.066' W	137.8	
MSM80_25-4	02.01.2019 20:13	MSN	09° 30.674' S	078° 59.449' W	134.2	
MSM80_25-5	02.01.2019 20:38	MSN	09° 30.899' S	078° 59.150' W	135.3	
MSM80_25-6	02.01.2019 21:09	MSN	09° 31.207' S	078° 58.513' W	135.9	

MSM80_25-7	02.01.2019 21:47	NET-IKMT	09° 31.877' S	078° 57.964' W	137.8	
MSM80_26-1	02.01.2019 22:45	MSS	09° 29.853' S	078° 53.094' W	131.3	
MSM80_27-1	03.01.2019 00:25	MSS	09° 29.898' S	078° 46.067' W	130.7	
MSM80_28-1	03.01.2019 02:21	CTD	09° 29.952' S	078° 40.025' W	108.0	
MSM80_28-2	03.01.2019 02:48	ACS	09° 29.951' S	078° 40.024' W	106.8	
MSM80_28-3	03.01.2019 02:57	MSS	09° 29.990' S	078° 40.003' W	106.6	
MSM80_28-4	03.01.2019 04:24	MSN	09° 30.757' S	078° 39.652' W	109.8	
MSM80_28-5	03.01.2019 04:44	MSN	09° 30.772' S	078° 39.503' W	108.9	
MSM80_29-1	03.01.2019 05:43	MSS	09° 29.968' S	078° 33.032' W	96.3	
MSM80_30-1	03.01.2019 07:46	CTD	09° 29.984' S	078° 27.001' W	80.1	deployed as Jo-Jo
MSM80_30-2	03.01.2019 08:16	ACS	09° 29.984' S	078° 27.001' W	77.7	
MSM80_30-3	03.01.2019 08:27	MSS	09° 30.014' S	078° 26.966' W	79.8	
MSM80_30-4	03.01.2019 09:39	MSN	09° 30.481' S	078° 26.750' W	80.4	
MSM80_30-5	03.01.2019 09:58	MSN	09° 30.573' S	078° 26.549' W	78.4	
MSM80_30-6	03.01.2019 10:24	MSN	09° 30.747' S	078° 26.326' W	76.3	
MSM80_31-1	03.01.2019 18:12	CTD	09° 40.065' S	079° 44.780' W	1199.8	
MSM80_31-2	03.01.2019 19:00	ACS	09° 40.064' S	079° 44.778' W	1200.4	
MSM80_31-3	03.01.2019 19:09	MSS	09° 40.092' S	079° 44.758' W	1200.2	
MSM80_31-4	03.01.2019 20:58	MSN	09° 40.308' S	079° 44.060' W	1177.7	
MSM80_31-5	03.01.2019 21:47	MSN	09° 40.422' S	079° 43.886' W	1174.8	
MSM80_31-6	03.01.2019 22:14	MSN	09° 40.644' S	079° 43.590' W	1181.9	
MSM80_31-7	03.01.2019 23:59	NET-IKMT	09° 43.345' S	079° 42.076' W	1264.0	
MSM80_32-1	04.01.2019 04:09	CTD	09° 30.002' S	080° 00.035' W	2411.3	
MSM80_32-2	04.01.2019 05:56	MOCNESS	09° 32.088' S	079° 59.025' W	2301.1	
MSM80_33-1	04.01.2019 12:25	CTD	09° 57.561' S	079° 07.768' W	235.7	
MSM80_33-2	04.01.2019 12:50	ACS	09° 57.560' S	079° 07.767' W	236.0	
MSM80_33-3	04.01.2019 13:04	MSS	09° 57.644' S	079° 07.722' W	236.9	
MSM80_33-4	04.01.2019 14:19	MSN	09° 58.516' S	079° 07.257' W	239.6	
MSM80_33-5	04.01.2019 14:42	MSN	09° 58.653' S	079° 06.977' W	231.5	
MSM80_33-6	04.01.2019 15:07	MSN	09° 58.866' S	079° 06.447' W	221.7	
MSM80_33-7	04.01.2019 15:49	NET-IKMT	09° 59.591' S	079° 05.607' W	206.4	
MSM80_34-1	04.01.2019 19:20	CTD	10° 28.837' S	079° 00.188' W	998.6	
MSM80_34-2	04.01.2019 19:55	ACS	10° 28.856' S	079° 00.088' W	1001.7	
MSM80_34-3	04.01.2019 20:06	MSS	10° 28.923' S	079° 00.085' W	1010.2	
MSM80_34-4	04.01.2019 22:04	MSN	10° 29.688' S	079° 00.682' W	1098.1	
MSM80_34-5	04.01.2019 22:55	MSN	10° 29.383' S	079° 00.508' W	1061.0	
MSM80_34-6	04.01.2019 23:24	MSN	10° 28.725' S	079° 00.129' W	996.8	
MSM80_34-7	05.01.2019 00:44	NET-IKMT	10° 29.951' S	079° 00.350' W	1097.3	
MSM80_35-1	05.01.2019 07:46	CTD	11° 00.002' S	078° 02.732' W	208.6	
MSM80_35-2	05.01.2019 08:04	ACS	11° 00.001' S	078° 02.731' W	209.5	
MSM80_35-3	05.01.2019 08:14	MSS	11° 00.048' S	078° 02.722' W	212.2	
MSM80_35-4	05.01.2019 09:29	MSN	11° 00.871' S	078° 02.668' W	213.0	
MSM80_35-5	05.01.2019 09:53	MSN	11° 01.066' S	078° 02.526' W	216.1	
MSM80_35-6	05.01.2019 10:24	MSN	11° 01.605' S	078° 02.122' W	210.2	
MSM80_35-7	05.01.2019 11:00	NET-IKMT	11° 02.299' S	078° 01.871' W	209.7	
MSM80_36-1	05.01.2019 14:25	CTD	11° 29.611' S	078° 17.454' W	1023.0	
MSM80_36-2	05.01.2019 15:04	ACS	11° 29.616' S	078° 17.454' W	1024.6	
MSM80_36-3	05.01.2019 15:23	MSS	11° 29.740' S	078° 17.425' W	1041.4	
MSM80_36-4	05.01.2019 17:09	MSN	11° 30.630' S	078° 17.121' W	1060.3	
MSM80_36-5	05.01.2019 17:59	MSN	11° 30.909' S	078° 16.988' W	1118.8	
MSM80_36-6	05.01.2019 18:29	MSN	11° 31.630' S	078° 16.639' W	1090.5	
MSM80_36-7	05.01.2019 20:08	NET-IKMT	11° 34.365' S	078° 16.058' W	1160.4	
MSM80_37-1	06.01.2019 00:21	SCF	11° 59.754' S	078° 30.086' W	2842.7	Start of Profile
MSM80_37-1	06.01.2019 11:55	SCF	11° 59.696' S	077° 20.096' W	107.9	End of Profile
MSM80_38-1	06.01.2019 13:16	CTD	11° 59.780' S	077° 20.267' W	104.9	
MSM80_38-2	06.01.2019 13:07	NET-Apstein	11° 59.780' S	077° 20.266' W	105.9	

MSM80_38-3	06.01.2019 13:40	ACS	11° 59.780' S	077° 20.267' W	105.7	
MSM80_38-4	06.01.2019 13:50	MSS	11° 59.797' S	077° 20.263' W	108.2	
MSM80_38-5	06.01.2019 15:14	MSN	11° 59.656' S	077° 20.783' W	109.4	
MSM80_38-6	06.01.2019 15:35	MSN	11° 59.936' S	077° 20.660' W	107.6	
MSM80_38-7	06.01.2019 16:02	MSN	12° 00.485' S	077° 20.463' W	106.6	
MSM80_39-1	06.01.2019 16:57	MSS	11° 59.964' S	077° 25.070' W	120.4	
MSM80_40-1	06.01.2019 18:54	CTD	12° 00.006' S	077° 29.996' W	138.5	
MSM80_40-2	06.01.2019 18:46	NET-Apstein	12° 00.006' S	077° 29.994' W	139.8	
MSM80_40-3	06.01.2019 19:17	ACS	12° 00.006' S	077° 29.995' W	138.1	
MSM80_40-4	06.01.2019 19:25	MSS	12° 00.025' S	077° 29.989' W	138.6	
MSM80_40-5	06.01.2019 20:38	MSN	12° 00.824' S	077° 29.958' W	139.6	
MSM80_40-6	06.01.2019 21:01	MSN	12° 01.179' S	077° 29.765' W	141.2	
MSM80_41-1	06.01.2019 22:55	DRIFT	11° 59.907' S	077° 46.254' W	245.0	Deployment
MSM80_41-1	09.01.2019 11:00	DRIFT	12° 28.432' S	077° 40.615' W	811.3	Recovery
MSM80_41-2	06.01.2019 23:16	CTD	11° 59.823' S	077° 46.171' W	239.4	
MSM80_41-3	06.01.2019 23:49	ACS	11° 59.824' S	077° 46.169' W	239.6	
MSM80_42-1	07.01.2019 01:03	MSS	11° 59.969' S	077° 35.040' W	156.6	
MSM80_43-1	07.01.2019 03:01	CTD	11° 59.990' S	077° 39.976' W	179.2	
MSM80_43-2	07.01.2019 02:52	NET-Apstein	11° 59.991' S	077° 39.976' W	176.8	
MSM80_43-3	07.01.2019 03:24	ACS	11° 59.987' S	077° 39.971' W	179.0	
MSM80_43-4	07.01.2019 03:36	MSS	12° 00.009' S	077° 39.943' W	180.2	
MSM80_43-5	07.01.2019 04:47	MSN	12° 01.103' S	077° 39.385' W	176.6	
MSM80_43-6	07.01.2019 05:10	MSN	12° 01.408' S	077° 39.277' W	179.3	
MSM80_43-7	07.01.2019 05:40	MSN	12° 02.006' S	077° 38.938' W	179.2	
MSM80_43-8	07.01.2019 06:28	NET-IKMT	12° 02.904' S	077° 38.864' W	180.1	
MSM80_44-1	07.01.2019 07:37	MSS	12° 00.023' S	077° 44.994' W	171.6	
MSM80_45-1	07.01.2019 09:31	CTD	11° 59.968' S	077° 50.016' W	464.0	
MSM80_45-2	07.01.2019 09:27	NET-Apstein	11° 59.969' S	077° 50.015' W	467.0	
MSM80_45-3	07.01.2019 10:00	ACS	11° 59.969' S	077° 50.016' W	469.6	
MSM80_45-4	07.01.2019 10:09	MSS	11° 59.983' S	077° 50.010' W	461.1	
MSM80_45-5	07.01.2019 11:10	MSN	12° 00.588' S	077° 49.693' W	588.2	
MSM80_45-6	07.01.2019 11:48	MSN	12° 00.850' S	077° 49.632' W	644.8	
MSM80_45-7	07.01.2019 12:17	MSN	12° 01.503' S	077° 49.510' W	662.2	
MSM80_45-8	07.01.2019 12:34	MSS	12° 01.842' S	077° 49.465' W	749.3	
MSM80_45-9	07.01.2019 15:02	NET-IKMT	12° 05.898' S	077° 49.102' W	1137.4	
MSM80_45-10	07.01.2019 16:35	ACS	12° 08.579' S	077° 48.649' W	1390.3	
MSM80_45-11	07.01.2019 16:28	NET-Apstein	12° 08.578' S	077° 48.649' W	1394.6	
MSM80_46-1	07.01.2019 18:35	CTD	11° 59.988' S	078° 00.000' W	1607.3	
MSM80_46-2	07.01.2019 19:10	ACS	11° 59.988' S	078° 00.000' W	1607.3	
MSM80_46-3	07.01.2019 19:18	MSS	12° 00.029' S	078° 00.004' W	1614.3	
MSM80_46-4	07.01.2019 22:44	MOCNESS	12° 00.300' S	077° 59.906' W	1625.6	
MSM80_46-5	08.01.2019 01:35	CTD	11° 59.952' S	077° 59.989' W	1606.0	
MSM80_46-6	08.01.2019 02:26	MSN	11° 59.951' S	077° 59.990' W	1607.7	
MSM80_46-7	08.01.2019 02:50	MSS	12° 00.016' S	077° 59.973' W	1607.4	
MSM80_46-8	08.01.2019 04:01	MOCNESS	12° 01.373' S	077° 59.895' W	1762.1	
MSM80_46-9	08.01.2019 04:54	MSN	12° 02.654' S	077° 59.457' W	1747.4	
MSM80_46-10	08.01.2019 07:28	CTD	11° 59.985' S	078° 00.022' W	1612.0	
MSM80_46-11	08.01.2019 08:15	MSN	11° 59.998' S	078° 00.019' W	1612.0	
MSM80_46-12	08.01.2019 08:51	ACS	11° 59.998' S	078° 00.019' W	1611.9	
MSM80_46-13	08.01.2019 09:43	CTD	11° 59.998' S	078° 00.019' W	1612.0	deployed as Jo-Jo
MSM80_46-14	08.01.2019 14:03	CTD	12° 00.001' S	078° 00.029' W	1613.0	
MSM80_46-15	08.01.2019 14:45	MSN	12° 00.002' S	078° 00.029' W	1610.9	
MSM80_46-16	08.01.2019 16:02	MSN	12° 01.022' S	077° 59.202' W	1692.6	
MSM80_46-17	08.01.2019 17:17	MSN	12° 02.632' S	077° 57.923' W	1580.6	
MSM80_46-18	08.01.2019 18:41	ACS	12° 00.001' S	078° 00.044' W	1617.1	
MSM80_46-19	08.01.2019 19:15	CTD	12° 00.001' S	078° 00.045' W	1617.1	

MSM80_46-20	08.01.2019 20:24	MSN	12° 00.000' S	078° 00.043' W	1617.4	
MSM80_46-21	08.01.2019 22:12	MOCNESS	12° 02.330' S	077° 59.879' W	1755.9	
MSM80_46-22	09.01.2019 00:08	CTD	12° 00.005' S	078° 00.032' W	1618.4	
MSM80_46-23	09.01.2019 00:41	ACS	12° 00.004' S	078° 00.031' W	1616.2	
MSM80_46-24	09.01.2019 00:45	MSS	12° 00.018' S	078° 00.033' W	1617.3	
MSM80_46-25	09.01.2019 02:25	MSN	12° 02.097' S	078° 00.452' W	1800.8	
MSM80_47-1	09.01.2019 04:48	MSN	12° 10.147' S	077° 55.230' W	1885.3	
MSM80_48-1	09.01.2019 11:33	CTD	12° 28.435' S	077° 40.577' W	810.9	
MSM80_48-2	09.01.2019 12:11	ACS	12° 28.437' S	077° 40.435' W	811.6	
MSM80_48-3	09.01.2019 12:19	MSS	12° 28.448' S	077° 40.413' W	812.4	
MSM80_48-4	09.01.2019 14:07	MSN	12° 29.811' S	077° 40.065' W	829.4	
MSM80_48-5	09.01.2019 14:45	MSN	12° 29.986' S	077° 39.868' W	834.2	
MSM80_48-6	09.01.2019 15:11	MSN	12° 30.395' S	077° 39.481' W	850.2	
MSM80_48-7	09.01.2019 16:37	NET-IKMT	12° 32.990' S	077° 39.256' W	926.5	
MSM80_49-1	09.01.2019 22:04	CTD	12° 30.031' S	076° 52.988' W	104.2	
MSM80_49-2	09.01.2019 22:27	ACS	12° 30.030' S	076° 52.986' W	105.3	
MSM80_49-3	09.01.2019 22:35	MSS	12° 30.050' S	076° 52.979' W	105.7	
MSM80_49-4	09.01.2019 23:40	MSN	12° 30.999' S	076° 52.801' W	108.3	
MSM80_49-5	10.01.2019 00:08	MSN	12° 31.372' S	076° 52.524' W	108.6	
MSM80_49-6	10.01.2019 00:42	NET-IKMT	12° 31.973' S	076° 52.271' W	112.4	
MSM80_50-1	10.01.2019 04:23	CTD	12° 59.542' S	077° 09.740' W	1021.1	
MSM80_50-2	10.01.2019 05:04	ACS	12° 59.543' S	077° 09.741' W	1024.8	
MSM80_50-3	10.01.2019 05:13	MSS	12° 59.561' S	077° 09.733' W	1022.1	
MSM80_50-4	10.01.2019 06:59	MSN	13° 00.291' S	077° 09.331' W	1010.3	
MSM80_50-5	10.01.2019 07:49	MSN	13° 00.521' S	077° 09.132' W	1031.8	
MSM80_50-6	10.01.2019 08:24	MSN	13° 00.909' S	077° 08.709' W	1065.6	
MSM80_50-7	10.01.2019 09:50	NET-IKMT	13° 02.593' S	077° 08.074' W	1121.2	
MSM80_51-1	10.01.2019 15:28	CTD	13° 29.365' S	076° 26.263' W	101.9	
MSM80_51-2	10.01.2019 15:53	ACS	13° 29.365' S	076° 26.262' W	102.8	
MSM80_51-3	10.01.2019 16:16	CTD	13° 29.366' S	076° 26.262' W	102.1	
MSM80_51-4	10.01.2019 16:35	MSS	13° 29.450' S	076° 26.300' W	102.6	
MSM80_51-5	10.01.2019 17:41	MSN	13° 30.856' S	076° 26.348' W	103.4	
MSM80_51-6	10.01.2019 18:06	MSN	13° 31.284' S	076° 26.276' W	104.5	
MSM80_51-7	10.01.2019 18:35	MSN	13° 31.911' S	076° 26.137' W	101.7	
MSM80_51-8	10.01.2019 19:10	NET-IKMT	13° 32.677' S	076° 26.281' W	104.3	
MSM80_52-1	11.01.2019 03:04	SCF	14° 29.986' S	076° 01.894' W	105.6	Start of Profile
MSM80_52-1	11.01.2019 17:31	SCF	14° 30.002' S	077° 30.545' W	4549.2	End of Profile
MSM80_53-1	11.01.2019 19:10	CTD	14° 29.987' S	077° 30.026' W	4563.6	
MSM80_53-2	11.01.2019 20:08	ACS	14° 29.985' S	077° 30.024' W	4561.7	
MSM80_53-3	11.01.2019 20:15	MSS	14° 29.996' S	077° 30.019' W	4556.4	
MSM80_53-4	11.01.2019 22:37	MSN	14° 30.820' S	077° 29.901' W	4538.4	
MSM80_53-5	11.01.2019 23:57	MSN	14° 30.935' S	077° 29.778' W	4565.0	
MSM80_53-6	12.01.2019 01:12	NET-IKMT	14° 32.275' S	077° 29.019' W	4447.7	
MSM80_54-1	12.01.2019 03:14	MSS	14° 29.974' S	077° 20.092' W	4669.0	
MSM80_55-1	12.01.2019 05:35	MSS	14° 30.019' S	077° 10.020' W	5027.9	
MSM80_56-1	12.01.2019 07:50	MSS	14° 28.510' S	077° 00.661' W	4990.5	
MSM80_56-2	12.01.2019 09:31	CTD	14° 29.772' S	077° 00.127' W	4942.7	deployed as Jo-Jo
MSM80_56-3	12.01.2019 12:48	ACS	14° 29.773' S	077° 00.127' W	5989.3	
MSM80_56-4	12.01.2019 13:35	CTD	14° 29.773' S	077° 00.127' W	0.0	
MSM80_56-5	12.01.2019 14:50	MSN	14° 29.773' S	077° 00.126' W	4960.1	
MSM80_56-6	12.01.2019 15:42	MSN	14° 29.989' S	076° 59.940' W	4946.3	
MSM80_57-1	12.01.2019 16:57	MSS	14° 29.999' S	076° 50.063' W	4071.5	
MSM80_58-1	12.01.2019 19:32	CTD	14° 29.977' S	076° 40.032' W	2651.1	
MSM80_58-2	12.01.2019 20:16	ACS	14° 29.977' S	076° 40.031' W	2650.6	
MSM80_58-3	12.01.2019 20:26	MSS	14° 30.001' S	076° 40.022' W	2639.7	
MSM80_58-4	12.01.2019 22:10	MSN	14° 30.821' S	076° 39.812' W	2599.3	

MSM80_58-5	12.01.2019 22:59	MSN	14° 31.046' S	076° 39.654' W	2608.7	
MSM80_58-6	12.01.2019 23:31	MSN	14° 31.629' S	076° 39.240' W	3896.1	
MSM80_58-7	13.01.2019 01:05	NET-IKMT	14° 34.024' S	076° 38.539' W	2609.3	
MSM80_59-1	13.01.2019 03:07	MSS	14° 30.009' S	076° 35.041' W	1764.0	
MSM80_60-1	13.01.2019 05:19	CTD	14° 29.927' S	076° 30.038' W	1418.5	
MSM80_60-2	13.01.2019 06:02	ACS	14° 29.927' S	076° 30.039' W	1423.4	
MSM80_60-3	13.01.2019 06:09	MSS	14° 29.943' S	076° 30.029' W	1419.2	
MSM80_60-4	13.01.2019 07:55	MSN	14° 30.957' S	076° 29.617' W	1522.8	
MSM80_61-1	13.01.2019 09:09	MSS	14° 29.984' S	076° 24.992' W	467.5	
MSM80_62-1	13.01.2019 11:13	MSS	14° 29.871' S	076° 15.078' W	145.7	
MSM80_63-1	13.01.2019 13:06	CTD	14° 29.971' S	076° 10.019' W	131.2	
MSM80_63-2	13.01.2019 13:21	ACS	14° 29.972' S	076° 10.019' W	132.1	
MSM80_63-3	13.01.2019 13:43	MSS	14° 30.026' S	076° 10.034' W	129.9	
MSM80_63-4	13.01.2019 14:58	MSN	14° 31.369' S	076° 09.933' W	126.9	
MSM80_63-5	13.01.2019 15:14	MSN	14° 31.465' S	076° 09.870' W	126.5	
MSM80_63-6	13.01.2019 15:33	MSN	14° 31.766' S	076° 09.669' W	129.7	
MSM80_63-7	13.01.2019 16:01	NET-IKMT	14° 32.378' S	076° 09.435' W	129.3	
MSM80_64-1	13.01.2019 16:54	MSS	14° 29.985' S	076° 04.994' W	124.6	
MSM80_65-1	13.01.2019 18:38	CTD	14° 29.976' S	076° 01.119' W	96.2	
MSM80_65-2	13.01.2019 18:36	NET-Apstein	14° 29.976' S	076° 01.119' W	94.3	
MSM80_65-3	13.01.2019 19:00	ACS	14° 29.976' S	076° 01.119' W	98.8	
MSM80_65-4	13.01.2019 19:08	MSS	14° 29.994' S	076° 01.113' W	97.2	
MSM80_65-5	13.01.2019 20:19	MSN	14° 30.786' S	076° 00.887' W	97.6	
MSM80_65-6	13.01.2019 20:37	MSN	14° 30.991' S	076° 00.717' W	92.7	
MSM80_66-1	13.01.2019 22:48	CTD	14° 29.958' S	076° 20.022' W	222.4	
MSM80_66-2	13.01.2019 23:19	ACS	14° 29.957' S	076° 20.022' W	228.5	
MSM80_66-3	13.01.2019 23:26	MSS	14° 29.973' S	076° 20.015' W	223.4	
MSM80_66-4	14.01.2019 00:41	MSN	14° 31.025' S	076° 19.586' W	206.3	
MSM80_66-5	14.01.2019 01:04	MSN	14° 31.231' S	076° 19.429' W	201.6	
MSM80_66-6	14.01.2019 02:01	SCF	14° 30.283' S	076° 19.663' W	218.3	Start of Profile
MSM80_66-6	14.01.2019 14:36	SCF	15° 18.099' S	075° 19.700' W	123.2	End of Profile
MSM80_67-1	14.01.2019 15:41	CTD	15° 17.918' S	075° 20.015' W	133.2	
MSM80_67-2	14.01.2019 16:09	ACS	15° 17.918' S	075° 20.015' W	132.6	
MSM80_67-3	14.01.2019 16:21	MSS	15° 17.948' S	075° 19.987' W	130.8	
MSM80_67-4	14.01.2019 17:39	MSN	15° 19.123' S	075° 19.613' W	134.2	
MSM80_67-5	14.01.2019 18:01	MSN	15° 19.449' S	075° 19.408' W	136.4	
MSM80_67-6	14.01.2019 18:28	MSN	15° 19.949' S	075° 18.990' W	135.9	
MSM80_67-7	14.01.2019 19:09	NET-IKMT	15° 20.820' S	075° 18.631' W	138.1	
MSM80_68-1	14.01.2019 20:38	DRIFT	15° 17.953' S	075° 25.030' W	526.7	Deployment
MSM80_68-1	20.01.2019 03:54	DRIFT	15° 15.219' S	075° 26.519' W	233.9	Recovery
MSM80_68-2	14.01.2019 21:16	CTD	15° 17.808' S	075° 25.068' W	515.3	
MSM80_68-3	14.01.2019 21:53	ACS	15° 17.808' S	075° 25.067' W	517.3	
MSM80_68-4	14.01.2019 22:10	MSS	15° 18.276' S	075° 24.796' W	535.7	
MSM80_68-5	14.01.2019 23:46	MSN	15° 19.462' S	075° 23.999' W	478.5	
MSM80_68-6	15.01.2019 00:40	NET-IKMT	15° 20.293' S	075° 23.827' W	444.9	
MSM80_68-7	15.01.2019 01:24	MSN	15° 21.193' S	075° 23.554' W	417.2	
MSM80_68-8	15.01.2019 01:47	MSN	15° 21.588' S	075° 23.374' W	400.8	
MSM80_69-1	15.01.2019 06:40	CTD	14° 51.008' S	076° 04.706' W	412.2	
MSM80_69-2	15.01.2019 07:05	ACS	14° 51.008' S	076° 04.705' W	414.7	
MSM80_69-3	15.01.2019 10:25	MSS	14° 51.007' S	076° 01.087' W	276.6	
MSM80_70-1	15.01.2019 13:00	CTD	14° 51.027' S	075° 57.508' W	202.5	
MSM80_70-2	15.01.2019 13:27	ACS	14° 51.027' S	075° 57.508' W	200.4	
MSM80_70-3	15.01.2019 13:42	MSN	14° 51.028' S	075° 57.508' W	201.4	
MSM80_70-4	15.01.2019 14:07	MSN	14° 51.159' S	075° 57.269' W	199.1	
MSM80_70-5	15.01.2019 14:45	MSN	14° 51.503' S	075° 56.782' W	194.5	
MSM80_70-6	15.01.2019 15:34	NET-IKMT	14° 52.326' S	075° 56.057' W	198.2	

MSM80_71-1	15.01.2019 20:42	SCF	15° 18.015' S	075° 20.012' W	133.0	Start of Profile
MSM80_71-1	16.01.2019 11:14	SCF	15° 17.997' S	076° 50.086' W	3381.9	End of Profile
MSM80_72-1	16.01.2019 11:46	MSS	15° 19.813' S	076° 49.481' W	3197.7	
MSM80_73-1	16.01.2019 14:14	MSS	15° 17.979' S	076° 40.031' W	3507.3	
MSM80_74-1	16.01.2019 17:11	CTD	15° 18.017' S	076° 30.039' W	3837.5	
MSM80_74-2	16.01.2019 17:59	ACS	15° 18.017' S	076° 30.039' W	3830.2	
MSM80_74-3	16.01.2019 18:07	MSS	15° 18.026' S	076° 30.029' W	3840.0	
MSM80_74-4	16.01.2019 19:58	MSN	15° 18.747' S	076° 29.612' W	3802.5	
MSM80_75-1	16.01.2019 21:39	MSS	15° 17.998' S	076° 20.015' W	5060.8	
MSM80_76-1	16.01.2019 23:44	MSS	15° 17.922' S	076° 10.060' W	4124.1	
MSM80_77-1	17.01.2019 01:46	MSS	15° 18.068' S	075° 59.987' W	3260.9	
MSM80_78-1	17.01.2019 04:14	CTD	15° 17.984' S	075° 50.045' W	2301.1	
MSM80_78-2	17.01.2019 04:59	ACS	15° 17.987' S	075° 50.046' W	2297.1	
MSM80_78-3	17.01.2019 05:07	MSS	15° 18.000' S	075° 50.038' W	2297.6	
MSM80_78-4	17.01.2019 07:03	MSN	15° 19.107' S	075° 49.481' W	2324.3	
MSM80_78-5	17.01.2019 07:54	MSN	15° 19.246' S	075° 49.181' W	3898.8	
MSM80_78-6	17.01.2019 09:30	MOCNESS	15° 21.355' S	075° 47.378' W	2347.8	
MSM80_79-1	17.01.2019 11:33	MSS	15° 17.900' S	075° 39.998' W	1404.2	
MSM80_80-1	17.01.2019 13:45	CTD	15° 17.966' S	075° 35.013' W	1168.9	
MSM80_80-2	17.01.2019 14:19	ACS	15° 17.966' S	075° 35.013' W	1170.2	
MSM80_80-3	17.01.2019 15:32	MOCNESS	15° 19.219' S	075° 34.151' W	1148.7	
MSM80_80-4	17.01.2019 16:59	MSS	15° 17.811' S	075° 35.048' W	1165.5	
MSM80_80-5	17.01.2019 19:22	CTD	15° 17.990' S	075° 34.996' W	1171.0	
MSM80_80-6	17.01.2019 20:23	MSN	15° 17.983' S	075° 34.985' W	1165.8	
MSM80_80-7	17.01.2019 20:56	MSS	15° 17.988' S	075° 34.971' W	1171.7	
MSM80_80-8	17.01.2019 22:35	MOCNESS	15° 18.969' S	075° 34.450' W	1165.5	
MSM80_80-9	18.01.2019 01:54	CTD	15° 18.462' S	075° 35.086' W	1185.6	
MSM80_80-10	18.01.2019 02:43	MSN	15° 18.435' S	075° 35.040' W	1185.2	
MSM80_80-11	18.01.2019 04:53	MOCNESS	15° 19.709' S	075° 34.364' W	1201.4	
MSM80_80-12	18.01.2019 07:19	CTD	15° 17.977' S	075° 35.014' W	1173.4	
MSM80_80-13	18.01.2019 08:16	MSN	15° 17.968' S	075° 35.003' W	1168.8	
MSM80_80-14	18.01.2019 09:25	CTD	15° 17.982' S	075° 35.005' W	1167.2	deployed as Jo-Jo
MSM80_80-15	18.01.2019 12:46	ACS	15° 17.692' S	075° 34.646' W	1139.3	
MSM80_80-16	18.01.2019 13:26	CTD	15° 17.651' S	075° 34.596' W	1134.4	
MSM80_80-17	18.01.2019 14:21	MSN	15° 17.628' S	075° 34.567' W	1131.4	
MSM80_80-18	18.01.2019 15:10	CTD	15° 17.627' S	075° 34.562' W	1131.1	
MSM80_80-19	18.01.2019 15:32	ACS	15° 17.627' S	075° 34.561' W	1134.9	
MSM80_80-20	18.01.2019 15:42	MSS	15° 17.643' S	075° 34.550' W	1131.2	
MSM80_81-1	18.01.2019 17:55	MSS	15° 17.984' S	075° 29.990' W		
MSM80_82-1	18.01.2019 20:06	CTD	15° 17.974' S	075° 25.006' W	547.0	
MSM80_82-2	18.01.2019 20:36	ACS	15° 17.975' S	075° 25.007' W	532.8	
MSM80_83-1	18.01.2019 21:55	CTD	15° 24.239' S	075° 21.555' W	156.1	
MSM80_83-2	18.01.2019 22:24	ACS	15° 24.239' S	075° 21.555' W	161.5	
MSM80_83-3	18.01.2019 22:42	MSN	15° 24.238' S	075° 21.555' W	156.2	
MSM80_83-4	18.01.2019 22:55	MSS	15° 24.223' S	075° 21.569' W	155.6	
MSM80_83-5	19.01.2019 00:15	MSN	15° 22.266' S	075° 22.724' W	282.2	
MSM80_83-6	19.01.2019 00:44	MSN	15° 22.129' S	075° 22.666' W	274.6	
MSM80_83-7	19.01.2019 02:01	NET-IKMT	15° 23.899' S	075° 23.563' W	467.0	
MSM80_84-1	19.01.2019 04:18	SCF	15° 25.284' S	075° 12.449' W	129.8	Start of Profile
MSM80_84-1	19.01.2019 23:30	SCF	15° 27.581' S	076° 13.242' W	4905.5	End of Profile
MSM80_85-1	20.01.2019 04:17	CTD	15° 15.223' S	075° 26.524' W	234.1	
MSM80_85-2	20.01.2019 04:44	ACS	15° 15.215' S	075° 26.517' W	233.6	
MSM80_85-3	20.01.2019 04:52	MSS	15° 15.238' S	075° 26.514' W	236.2	
MSM80_86-1	20.01.2019 06:59	SCF	15° 12.001' S	075° 30.072' W	142.7	Start of Profile
MSM80_86-1	20.01.2019 17:40	SCF	15° 11.997' S	076° 36.060' W	3915.9	End of Profile
MSM80_87-1	20.01.2019 18:58	CTD	15° 11.983' S	076° 36.005' W	3925.2	

MSM80_87-2	20.01.2019 19:32	ACS	15° 11.983' S	076° 36.004' W	4166.5	
MSM80_88-1	20.01.2019 21:59	CTD	15° 15.942' S	076° 15.013' W	4262.4	
MSM80_88-2	20.01.2019 22:34	ACS	15° 15.942' S	076° 15.013' W	4259.4	
MSM80_89-1	21.01.2019 00:05	CTD	15° 16.249' S	076° 05.716' W	4001.7	
MSM80_89-2	21.01.2019 01:01	ACS	15° 16.254' S	076° 05.996' W	3991.5	
MSM80_89-3	21.01.2019 01:33	MSS	15° 17.120' S	076° 05.800' W	4165.1	
MSM80_89-4	21.01.2019 03:03	MSN	15° 15.986' S	076° 06.006' W	3988.6	
MSM80_89-5	21.01.2019 03:39	MOCNESS	15° 15.997' S	076° 06.468' W	3975.0	
MSM80_90-1	21.01.2019 08:44	CTD	15° 15.990' S	076° 16.091' W	4290.6	
MSM80_90-2	21.01.2019 09:36	ACS	15° 15.990' S	076° 16.091' W	4312.3	
MSM80_90-3	21.01.2019 09:45	MSS	15° 15.997' S	076° 16.087' W	4307.6	
MSM80_90-4	21.01.2019 10:52	MSN	15° 17.026' S	076° 15.596' W	4490.3	
MSM80_90-5	21.01.2019 11:31	SCF	15° 15.995' S	076° 15.973' W	4292.5	Start of Profile
MSM80_90-5	21.01.2019 14:48	SCF	15° 35.385' S	076° 15.979' W	3992.9	End of Profile
MSM80_91-1	21.01.2019 16:19	CTD	15° 31.830' S	076° 16.035' W	4035.6	
MSM80_91-2	21.01.2019 17:05	ACS	15° 31.830' S	076° 16.035' W	4022.5	
MSM80_91-3	21.01.2019 17:12	MSS	15° 31.847' S	076° 16.017' W	4024.9	
MSM80_92-1	21.01.2019 19:21	CTD	15° 28.798' S	076° 16.023' W	4393.6	
MSM80_92-2	21.01.2019 19:58	ACS	15° 28.799' S	076° 16.023' W	4406.8	
MSM80_92-3	21.01.2019 20:08	MSS	15° 28.846' S	076° 15.969' W	4392.7	
MSM80_93-1	21.01.2019 22:02	CTD	15° 25.709' S	076° 15.966' W	4651.8	
MSM80_93-2	21.01.2019 22:45	ACS	15° 25.709' S	076° 15.966' W	4614.4	
MSM80_93-3	21.01.2019 22:53	MSS	15° 25.726' S	076° 15.957' W	4617.1	
MSM80_94-1	22.01.2019 07:37	ACS	15° 59.990' S	075° 00.050' W	2815.0	
MSM80_94-2	22.01.2019 07:45	MSS	16° 00.003' S	075° 00.033' W	2820.1	
MSM80_94-3	22.01.2019 09:20	CTD	16° 00.347' S	074° 59.759' W	2876.0	deployed as Jo-Jo
MSM80_94-4	22.01.2019 12:34	DRIFT	16° 00.007' S	075° 00.133' W	2862.1	Deployment
MSM80_94-4	25.01.2019 22:43	DRIFT	16° 23.870' S	076° 02.553' W	3712.8	Recovery
MSM80_94-5	22.01.2019 13:18	MSN	15° 59.986' S	075° 00.122' W	2849.5	
MSM80_94-6	22.01.2019 14:24	CTD	15° 59.987' S	075° 00.121' W	2850.0	
MSM80_95-1	22.01.2019 19:37	CTD	16° 00.001' S	074° 09.998' W	122.9	
MSM80_95-2	22.01.2019 19:59	ACS	16° 00.001' S	074° 09.999' W	115.4	
MSM80_95-3	22.01.2019 20:07	MSS	16° 00.029' S	074° 09.979' W	114.7	
MSM80_95-4	22.01.2019 21:18	MSN	16° 00.808' S	074° 09.551' W	124.5	
MSM80_95-5	22.01.2019 21:38	MSN	16° 00.941' S	074° 09.311' W	128.1	
MSM80_95-6	22.01.2019 22:03	MSN	16° 01.156' S	074° 08.924' W	130.6	
MSM80_95-7	22.01.2019 22:39	NET-IKMT	16° 01.673' S	074° 08.451' W	130.9	
MSM80_95-8	22.01.2019 23:48	SCF	16° 00.025' S	074° 10.099' W	118.0	Start of Profile
MSM80_95-8	23.01.2019 17:20	SCF	16° 00.006' S	076° 00.006' W	3727.6	End of Profile
MSM80_96-1	23.01.2019 18:32	CTD	15° 59.983' S	076° 00.015' W	3725.9	
MSM80_96-2	23.01.2019 19:10	ACS	15° 59.983' S	076° 00.015' W	3734.9	
MSM80_96-3	23.01.2019 19:20	MSS	16° 00.004' S	076° 00.007' W	3730.9	
MSM80_96-4	23.01.2019 21:11	MSN	16° 00.813' S	075° 59.410' W	3766.1	
MSM80_97-1	23.01.2019 23:09	MSS	16° 00.030' S	075° 45.005' W	4877.6	
MSM80_98-1	24.01.2019 01:37	MSS	16° 00.072' S	075° 30.038' W	5587.0	
MSM80_99-1	24.01.2019 04:50	CTD	15° 59.996' S	075° 15.039' W	4509.6	
MSM80_99-2	24.01.2019 05:33	ACS	15° 59.993' S	075° 15.038' W	4499.2	
MSM80_99-3	24.01.2019 05:42	MSS	16° 00.017' S	075° 15.020' W	4509.3	
MSM80_99-4	24.01.2019 08:06	MOCNESS	16° 02.067' S	075° 12.419' W	4533.7	
MSM80_99-5	24.01.2019 09:34	MSN	16° 03.119' S	075° 10.372' W	5952.5	
MSM80_99-6	24.01.2019 11:09	MSN	15° 59.995' S	075° 15.028' W	4507.3	
MSM80_100-1	24.01.2019 14:04	MSS	16° 00.020' S	074° 50.042' W	2298.6	
MSM80_101-1	24.01.2019 16:10	MSS	16° 00.019' S	074° 40.004' W	1796.3	
MSM80_102-1	24.01.2019 18:40	CTD	15° 59.990' S	074° 30.029' W	965.5	
MSM80_102-2	24.01.2019 19:17	ACS	15° 59.989' S	074° 30.027' W	963.5	
MSM80_102-3	24.01.2019 19:26	MSS	16° 00.011' S	074° 30.017' W	961.9	

MSM80_102-4	24.01.2019 21:09	MSN	16° 00.910' S	074° 29.241' W	912.3	
MSM80_102-5	24.01.2019 21:53	MSN	16° 01.013' S	074° 29.014' W	916.9	
MSM80_102-6	24.01.2019 23:16	NET-IKMT	16° 02.368' S	074° 27.603' W	923.2	
MSM80_102-7	25.01.2019 01:04	MSN	16° 00.155' S	074° 29.849' W	951.5	
MSM80_102-8	25.01.2019 01:43	CTD	16° 00.329' S	074° 29.703' W	933.3	
MSM80_103-1	25.01.2019 03:01	MSS	16° 00.047' S	074° 24.924' W	929.4	
MSM80_104-1	25.01.2019 04:44	CTD	15° 59.980' S	074° 19.985' W	615.4	
MSM80_104-2	25.01.2019 05:19	ACS	15° 59.980' S	074° 19.983' W	618.2	
MSM80_104-3	25.01.2019 05:27	MSS	16° 00.019' S	074° 19.980' W	622.0	
MSM80_104-4	25.01.2019 06:52	MSN	16° 01.659' S	074° 19.250' W	693.4	
MSM80_104-5	25.01.2019 07:25	MSN	16° 02.154' S	074° 18.643' W	546.2	
MSM80_104-6	25.01.2019 08:00	MSN	16° 02.319' S	074° 18.409' W	514.7	
MSM80_104-7	25.01.2019 09:13	CTD	15° 59.978' S	074° 20.015' W	625.3	deployed as Jo-Jo
MSM80_105-1	25.01.2019 13:00	MSS	15° 59.927' S	074° 15.002' W	285.3	
MSM80_106-1	25.01.2019 23:44	CTD	16° 23.850' S	076° 02.604' W	3835.9	
MSM80_106-2	26.01.2019 00:49	ACS	16° 23.849' S	076° 02.603' W	3842.5	
MSM80_106-3	26.01.2019 01:00	MSS	16° 23.982' S	076° 02.618' W	3847.3	
MSM80_106-4	26.01.2019 02:25	MSS	16° 25.505' S	076° 03.077' W	4194.0	Equipment Test
MSM80_106-5	26.01.2019 02:46	MSS	16° 25.942' S	076° 03.124' W	4004.9	Untwisting of Cable
MSM80_106-6	26.01.2019 04:25	MSN	16° 26.779' S	076° 03.001' W	4038.3	
MSM80_106-7	26.01.2019 05:45	MSN	16° 26.990' S	076° 02.729' W	4028.8	

8 Data and Sample Storage and Availability

The CUSCO data management is located at the GEOMAR in Kiel. All metadata of the onboard DSHIP-System is publicly available through the information and data archival system of the "Kiel Data Management Team (KDMT)". The "Ocean Scientific Information System (OSIS-Kiel)" is accessible for all project partners and will be used to share expedition information and data from ongoing research projects. For non-authorized users, OSIS provides the relevant information about expeditions and publications available in reviewed articles or data publications. The submission status of data files, including the responsible researcher, as a contact person will be made visible. The data will then be transferred to a World Data Center (PANGEA) for long-term archiving. The data publishing process is based on the available files in OSIS and is therefore globally accessible to anyone interested. Links to data publishers and/or project leaders provide contact information for external researchers. It is expected that most of the relevant results will be published by the cruise participants, CUSCO project scientists and collaborating researchers within three years after the end of the cruise.

9 Acknowledgements

We are very grateful to Capitain Björn Maaß and the entire crew of R/V Maria S. Merian for their excellent, very professional, creative and extremely friendly support during the research cruise MSM80. Their tireless efforts were essential for the scientific success of the expedition. Scientists' participation and cruise logistics, including i.a. container transports, shipment of frozen samples and the participation of Peruvian colleagues from the partner institution IMARPE, were funded by the German Federal Ministry for Education and Research (BMBF) in the framework of the joint research project CUSCO - Coastal Upwelling System in a Changing Ocean as part of the MARE:N programme for coastal, marine and polar research and the FONA^3 strategy for research for sustainability (03F0813C).